IAEA-TECDOC-1629

World Distribution of Uranium Deposits (UDEPO) with Uranium Deposit Classification

2009 Edition

IAEA
International Atomic Energy Agency

IAEA-TECDOC-1629

World Distribution of Uranium Deposits (UDEPO) with Uranium Deposit Classification

2009 Edition

IAEA
International Atomic Energy Agency

The originating Section of this publication in the IAEA was:

Nuclear Fuel Cycle and Materials Section
International Atomic Energy Agency
Vienna International Centre
P.O. Box 100
1400 Vienna, Austria

WORLD DISTRIBUTION OF URANIUM DEPOSITS (UDEPO)
WITH URANIUM DEPOSIT CLASSIFICATION

IAEA, VIENNA, 2009
IAEA-TECDOC-1629
ISBN 978–92–0–110509–7
ISSN 1011-4289

Printed by the IAEA in Austria
October 2009

FOREWORD

Having comprehensive information on the worldwide uranium deposits is crucial for implementation of significant nuclear power programmes in the world, especially with the increasing interest in nuclear power and concerns about the supply of energy resources.

Starting from the early years of the development of nuclear energy for peaceful uses, the International Atomic Energy Agency has published numerous reports on different types of uranium deposits, their geological characteristics and geographical distribution.

With the increased amount of information available on uranium deposits throughout the world, the IAEA was able to establish an electronic database and publish it in the form of an Atlas in 1995. The atlas later was supported with a World Guidebook to Accompany IAEA Map: World Distribution of Uranium Deposits, in the form of a databook in 1996. The name of the database was World Distribution of Uranium Deposits (UDEPO).

The UDEPO database was revised and expanded in 2004 to store to provide more detailed information on uranium geology and technical characteristics of the deposits. The revised database has been published on the internet since 2004. The database and its web site are being updated continuously.

This report and its attached CD-ROM contain information on 878 uranium deposits worldwide and reflect a snapshot of the database as of end of 2008. The database itself is being updated continuously. The reader can access the most up to date information at www-nfcis.iaea.org.

The IAEA wishes to thank the consultants who took part in the preparation of the UDEPO database. The IAEA is also grateful to the Member States and individual organizations for their generous support in providing experts and data to make this database more complete. The IAEA officer responsible for this publication was M. Ceyhan of the Division of Nuclear Fuel Cycle.

EDITORIAL NOTE

The use of particular designations of countries or territories does not imply any judgement by the publisher, the IAEA, as to the legal status of such countries or territories, of their authorities and institutions or of the delimitation of their boundaries.

The mention of names of specific companies or products (whether or not indicated as registered) does not imply any intention to infringe proprietary rights, nor should it be construed as an endorsement or recommendation on the part of the IAEA.

CONTENTS

1. INTRODUCTION

1.1. Background

In 1996, the IAEA published the Guidebook to Accompany IAEA Map: World distribution of Uranium Deposits (the 'Guidebook'). This publication, which was the culmination of a process that began in 1990, introduced a descriptive deposit classification that expanded upon the classification used in the OECD/NEA-IAEA Red Book. Experts from six countries and from the IAEA collaborated on establishing the deposit classification. They also contributed information on a total of 582 deposits worldwide, and provided summary information on these deposits that became part of the Guidebook including their location, status (operating, dormant, depleted, etc.), resources (within a specific resource range — e.g. 1 500 to 5 000 t U), average grade (within a grade range — e.g. 0.03–0.10% U), geologic age, host rocks and tectonic setting.

Provision is also made in the database to record references relating to the deposits and to include maps and photos of deposits. To have been included in the database, a deposit must have minimum resources of >500 t U at an average of 0.03% U or greater (note: exceptions to these guidelines have been allowed in a small number of cases where small deposits occur near operating or proposed production centres).

The deposit-specific information, a map showing deposit locations [1] and a discussion of the new deposit classification were published in the 1996 Guidebook [2]. The Guidebook and the database on which it is based have come to be known collectively as UDEPO. The database was created on a computer based system to allow publishing above mentioned product easily.

Major modification has been implemented on UDEPO database in 2004. The database has been moved to MS SQL relational database server to allow building client/server architecture applications so that multiple users are able to access to the database at the same time. Another advantage of having database on the server is ability to update continuously. This has also allowed publishing the database through the internet. A web application has been developed and made available to the public access in 2004 (http://www-nfcis.iaea.org/) [3]. The UDEPO database and its web site have been continuously updated and improved since then. As of end of 2008 there are 873 deposits recorded in the database.

1.2. Purpose and Scope of UDEPO

In 2002, the IAEA began an effort to integrate all nuclear fuel cycle related databases and computer simulations to make them more readily accessible to the Member States. A consultants meeting was held in 2003 to establish guidelines for restructuring UDEPO to ensure that it would be compatible with the integrated database approach. Assembling UDEPO data into a new structure began in 2003. A website, which was developed to publish the database, became available to the public in February 2004. The site has been periodically revised based on feedback from users and recommendations from consultants.

A consultants meeting was held in 2005 to establish guidelines for a publication that would update and expand upon the original Guidebook. In addition to becoming part of the IAEA integrated database approach and thus readily available to Member States, the update was considered to be very timely, because since the inception of the UDEPO process in 1990 and publication of the Guidebook in 1996, the uranium industry has undergone significant changes. Nowhere are industry changes more apparent than in the recent history of the uranium market price, which as shown in Fig. 1, reached a historical peak of US$ 112/kg U in

current dollars in 1978–1979 (US$ 240/kg U in constant 2003 dollars). Since the price peak in 1979, the market began a precipitous decline, finally bottoming out at about US$ 20/kg U in 1994. Beginning in 2000, however, the market price, in response to concerns about the adequacy of uranium supply began to steadily increase, having reached US$ 220/kg U in early 2007.

Figure 2 shows the historical relationship between uranium requirements (demand) and uranium production (supply). As shown in figure, supply exceeded demand until 1990 when that relationship was reversed. The gap between newly mined and processed uranium (primary supply) and uranium requirements that developed after 1990 was filled by secondary supply including highly enriched uranium (HEU) from military stockpiles and inventory drawdown. In 2003, total demand was covered about equally by primary and secondary supply.

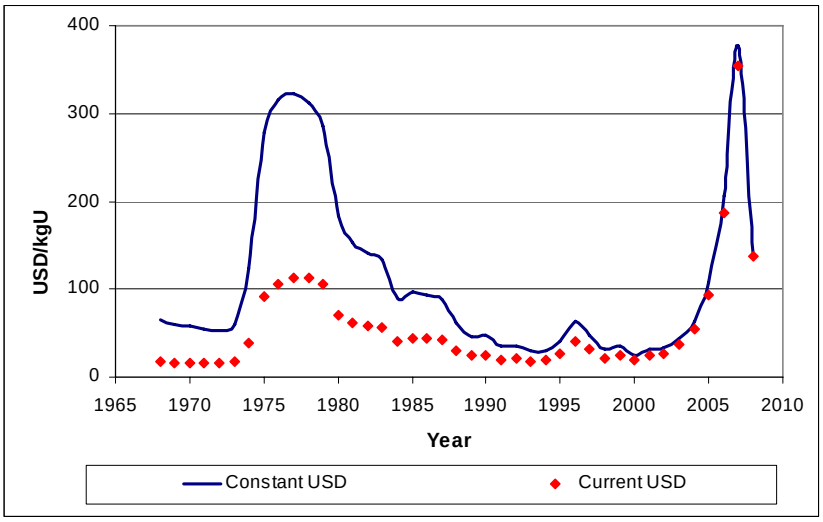

Fig. 1. Historical uranium market prices [4] and[5].

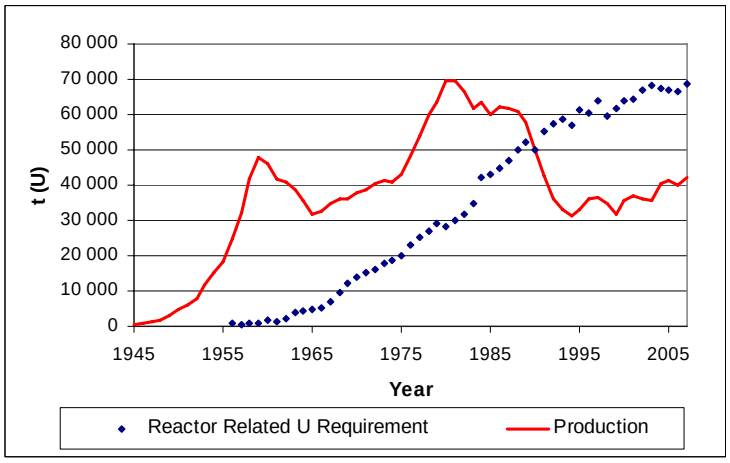

Fig. 2. Worldwide annual production and reactor related requirements (1945–2005) [6].

The depressed uranium market prices, which prevailed during the 1980s and 1990s, were partly the result of drawing down of inventory that was built up during the period of excess capacity and production prior to 1990. Inventory drawdown, in combination with availability of other secondary supply sources, displaced demand for primary supply, driving down prices and forcing consolidation within the uranium production industry. Beginning in early 2000, however, inventories had been largely drawn down to strategic levels and the potential to expand other secondary supply sources is limited. Therefore, if as expected nuclear power continues to grow, uranium requirements will increase proportionately and newly mined and processed uranium will once again be the dominant supply source.

Concerns about the adequacy of production capacity to meet near-term requirements and the adequacy of high-confidence resources to meet longer term requirements have contributed to the rapid increase in uranium prices starting in 2001. Worldwide uranium exploration expenditures between 1945 and 2003 are estimated to have totaled approximately US$ 13.7 billion. Figure 3 shows annual distribution of historical exploration expenditures, which collectively resulted in discovery of the resources on which past uranium production was based (estimated 2 287 380 t U) and the resources on which the near-term future of the nuclear fuel cycle depends.

Many if not most of the deposits that resulted from past exploration are included in the expanded UDEPO database. The resources for many of these deposits will, however, require additional exploration before they are sufficiently well defined to be reliable as future exploitation candidates. As shown in Fig. 3, exploration expenditures worldwide have been at relatively low levels since the early 1990s, though they have begun to increase in response to increases in market price and increasing demand for primary supply. The UDEPO database identifies undeveloped deposits that could be candidates for future exploration and/or development and provides information on their geology and resource potential.

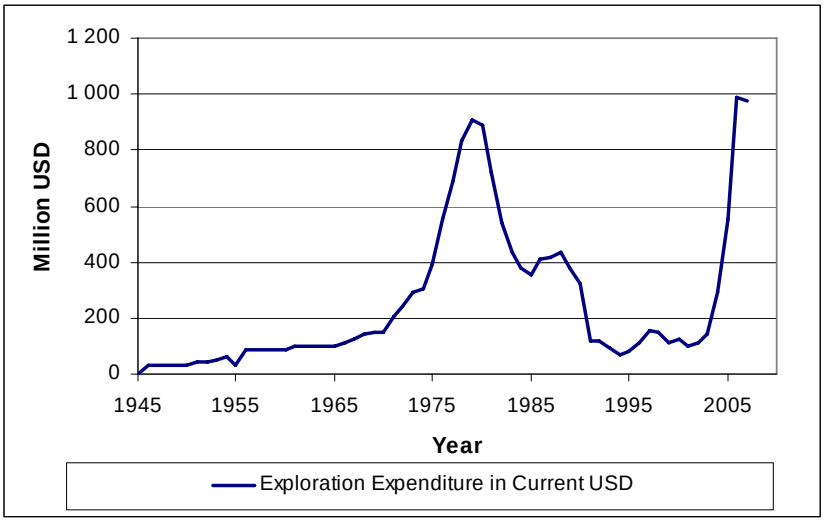

Fig. 3. Historical exploration expenditures in current USD [6].

1.3. Definitions

Uranium occurrence: A naturally occurring, anomalous concentration of uranium.

Uranium deposit: A mass of naturally occurring mineral from which uranium could be exploited at present or in the future.

Initial (Global) Resource: The total amount of uranium which exists in the deposit before any production occurred.

1.3.1. Resource categories

- **Reasonably assured resources (RAR).** RAR include uranium that occurs in known mineral deposits of delineated size, grade and configuration such that the quantities which could be recovered within the given production cost ranges with currently proven mining and processing technology, can be specified. Estimates of tonnage and grade are based on specific sample data and measurements of the deposits and on knowledge of deposit characteristics. Reasonably assured resources have a high assurance of existence. Unless otherwise noted RAR are expressed in terms of quantities of uranium recoverable from mineable ore.

- **Inferred resources** (formerly estimated additional resources [EAR-I]). Uranium in addition to RAR that is inferred to occur based on direct geological evidence, in extensions of well-explored deposits, or in deposits in which geological continuity has been established but where specific data, including measurements of the deposits, and knowledge of the deposit's characteristics are considered to be adequate to classify the resource as RAR. Estimates of tonnage, grade and cost of further of further delineation and recovery are based on such sampling as is available and on knowledge of the deposit characteristics as determined in the best known parts of the deposit or in similar deposits. Less reliance can be placed on the estimates in this category than on those for RAR. Unless otherwise noted, EAR-I are expressed in terms of quantities of uranium recoverable from mineable ore.

- **Identified resources** (formerly known resources). reasonably assured resources plus inferred resources.

- **Prognosticated resources** refers to uranium, in addition to inferred resources, that is expected to occur in deposits for which the evidence is mainly indirect and which are believed to exist in well-defined geological trends or areas of mineralization with known deposits.

- **Speculative resources (SR)** refers to uranium, in addition to prognosticated resources, that is thought to exist, mostly on the basis of indirect evidence and geological extrapolations, in deposits discoverable with existing exploration techniques.

1.3.2. Deposit types

Uranium resources can be assigned on the basis of their geological setting to the following categories of uranium ore deposit types (arranged according to their approximate economic significance): [7]

1. Unconformity related deposits: Unconformity related deposits are associated with and occur immediately below and above an unconformable contact that separates a crystalline basement intensively altered from overlying clastic sediments of Proterozoic age.

Two sub-types of unconformity related deposits have been recognized reflecting both stratigraphic and structural control [8][9][10] :

- ***Fracture controlled***, dominantly basement hosted (McArthur River, Rabbit Lake, Eagle Point, McClean Lake, Dominique-Peter in Canada; Jabiluka, Ranger, Nabarlek, Koongarra in Australia),
- ***Clay bounded***, massive ore developed along and just above or immediately below the unconformity in the overlying cover sandstones (Cigar Lake, Key Lake, Collins Bay A, B and D zones, Midwest, McClean, Cluff Lake D in Canada).

2. Sandstone deposits: Sandstone uranium deposits occur in medium to coarse-grained sandstones deposited in a continental fluvial or marginal marine sedimentary environment. Uranium is precipitated under reducing conditions caused by a variety of reducing agents within the sandstone, for example, carbonaceous material, sulphides (pyrite), hydrocarbons and ferro-magnesium minerals (chlorite), etc. Sandstone uranium deposits can be divided into four main sub-types:

- *Roll-front deposits*: The mineralised zones are convex down the hydrologic gradient. They display diffuse boundaries with reduced sandstone on the down-gradient side and sharp contacts with oxidised sandstone on the up-gradient side. The mineralised zones are elongate and sinuous approximately parallel to the strike, and perpendicular to the direction of deposition and groundwater flow. Resources can range from a few hundred tonnes to several thousands of tonnes of uranium, at grades averaging 0.05% to 0.25%. Examples are Moynkum, Inkay and Mynkuduk (Kazakhstan); Crow Butte and Smith Ranch (USA) and Bukinay, Sugraly and Uchkuduk (Uzbekistan).

- *Tabular deposits:* They consist of uranium matrix impregnations that form irregularly shaped lenticular masses within reduced sediments. The mineralised zones are largely oriented parallel to the depositional trend. Individual deposits can contain several hundreds of tonnes up to 150 000 tonnes of uranium, at average grades ranging from 0.05% to 0.5%, occasionally up to 1%. Examples of deposits include Westmoreland (Australia), Nuhetting (China), Hamr-Stráz (Czech Republic), Akouta, Arlit, Imouraren (Niger) and Colorado Plateau (USA).
- *Basal channel deposits*: Paleodrainage systems consist of several hundred metres wide channels filled with thick permeable alluvial-fluvial sediments. Here, the uranium is predominantly associated with detrital plant debris in ore bodies that display, in a planview, an elongated lens or ribbon-like configuration and, in a section view, a lenticular or, more rarely, a roll shape. Individual deposits can range from several hundreds to 20 000 tonnes uranium, at grades ranging from 0.01% to 3%. Examples are the deposits of Dalmatovskoye (Transural Region), Malinovskoye (West Siberia), Khiagdinskoye (Vitim district) in Russian Federation and Beverley in Australia.
- *Tectonic/lithologic deposits* occur in sandstone related to a permeable zone. Uranium is precipitated in open zones related to tectonic extension. Individual deposits contain a few hundred tonnes up to 5 000 tonnes of uranium at average grades ranging from 0.1% to 0.5%. Examples include the deposits of Mas Laveyre (France) and Mikouloungou (Gabon).

3. Hematite breccia complex deposits: Deposits of this group occur in hematite-rich breccias and contain uranium in association with copper, gold, silver and rare earths. The main representative is the Olympic Dam deposit in South Australia. Significant deposits and prospects of this type include Prominent Hill, Ernest Henry, Starra, Osborne in Australia; Candelaria, Salobo and Sossego in South America; Michelin and Sue-Dianne in Canada.

4. Quartzpebble conglomerate deposits: Detrital uranium oxide ores are found in quartzpebble conglomerates deposited as basal units in fluvial to lacustrine braided stream systems older than 2.3–2.4 Ga. The conglomerate matrix is pyritiferous, and gold, as well as other oxide and sulphide detrital minerals are often present in minor amounts. Examples include deposits found in the Witwatersrand Basin where uranium is mined as a by-product of gold. Uranium deposits of this type were mined in the Blind River/Elliot Lake area of Canada.

5. Vein deposits (granite related deposits): In vein deposits, the major part of the mineralisation fills fractures with highly variable thickness, and generally important extension along strike. The veins consist mainly of gangue material (e.g. carbonates, quartz) and ore material, mainly pitchblende. Typical examples range from the thick and massive pitchblende veins of Pribram (Czech Republic), Schlema-Alberoda (Germany) and Shinkolobwe (Democratic Republic of the Congo), to the stockworks and episyenite columns of Bernardan (France) and Gunnar (Canada), to the narrow cracks in granite or metamorphic rocks, also filled with pitchblende of Mina Fe (Spain) and Singhbhum (India).

6. Intrusive deposits: Deposits included in this type are those associated with intrusive or anatectic rocks of different chemical composition (alaskite, granite, monzonite, peralkaline syenite, carbonatite and pegmatite). Examples include the Rossing and Trekkopje deposits (Namibia), the uranium occurrences in the porphyry copper deposits such as Bingham Canyon and Twin Butte (USA), the Ilimaussaq deposit (Greenland), Palabora (South Africa), as well as the deposits in the Bancroft area (Canada).

7. Volcanic and caldera related deposits: Uranium deposits of this type are located within and nearby volcanic caldera filled by mafic to felsic volcanic complexes and intercalated clastic sediments. Mineralisation is largely controlled by structures (minor stratabound), occurs at several stratigraphic levels of the volcanic and sedimentary units and extends into the basement where it is found in fractured granite and in metamorphites. Uranium minerals are commonly associated with molybdenum, other sulphides, violet fluorine and quartz. Most significant commercial deposits are located within Streltsovsk caldera in the Russian Federation. Examples are known in China (Gan-Hang volcanic belt), Mongolia (Dornot deposit), and Mexico (Nopal deposit).

8. Metasomatite deposits: Deposits of this type are confined to the areas of tectono-magmatic activity of the Precambrian shields and are related to near-fault alkali metasomatites, developed upon different basement rocks: granites, migmatites, gneisses and ferruginous quartzites with production of albitites, aegirinites, alkali-amphibolic and carbonaceous-ferruginous rocks. Ore lenses and stocks are a few metres to tens of metres thick and a few hundred metres long. Vertical extent of ore mineralisation can be up to 1.5 km. Ores are uraninite-brannerite by composition and belong to ordinary grade. The reserves are usually medium scale or large. Examples include Michurinskoye, Vatutinskoye, Severinskoye, Zheltorechenskoye and Pervomayskoye deposits (Ukraine), Lagoa Real, Itataia and Espinharas (Brazil).

9. Surficial deposits: Surficial uranium deposits are broadly defined as young (Tertiary to Recent) near–surface uranium concentrations in sediments and soils. The largest of the

surficial uranium deposits are in calcrete (calcium and magnesium carbonates), and they have been found in Australia (Yeelirrie deposit), Namibia (Langer Heinrich deposit) and Somalia. These calcrete-hosted deposits are associated with deeply weathered uranium-rich granites. They also can occur in valley-fill sediments along Tertiary drainage channels and in playa lake sediments (e.g. Lake Maitland, Australia). Surficial deposits also can occur in peat bogs and soils.

10. Collapse breccia pipe deposits: Deposits in this group occur in circular, vertical pipes filled with down-dropped fragments. The uranium is concentrated as primary uranium ore, generally uraninite, in the permeable breccia matrix, and in the arcuate, ring-fracture zone surrounding the pipe. They are only known in the USA. Type examples are the deposits in the Arizona Strip north of the Grand Canyon and those immediately south of the Grand Canyon.

11. Phosphorite deposits: Phosphorite deposits consist of marine phosphorite of continental-shelf origin containing syn-sedimentary stratiform, disseminated uranium in fine-grained apatite. Phosphorite deposits constitute large uranium resources, but at a very low grade. Uranium can be recovered as a by-product of phosphate production. Examples include New Wales Florida (pebble phosphate) and Uncle Sam (USA), Gantour (Morocco) and Al-Abiad (Jordan). Other type of phosphorite deposits consists of organic phosphate, including argillaceous marine sediments enriched in fish remains that are uraniferous (Melovoe deposit, Kazakhstan).

12. Other deposits

- **Metamorphic deposits:** In metamorphic uranium deposits, the uranium concentration directly results from metamorphic processes. The temperature and pressure conditions, and age of the uranium deposition have to be similar to those of the metamorphism of the enclosing rocks. Examples include the Forstau deposit (Austria) and Mary Kathleen (Australia).
- **Limestone and paleokarst deposits:** This includes uranium mineralisation in the Jurassic Todilto Limestone in the Grants district (USA) where uraninite occurs in intra-formational folds and fractures as introduced mineralization.
- **Uranium coal deposits:** Elevated uranium contents occur in lignite/coal, and in clay and sandstone immediately adjacent to lignite. Examples are uranium in the Serres Basin (Greece), in North and South Dakota (USA), Koldjat and Nizhne Iliyskoe (Kazakhstan) and Freital (Germany). Uranium grades are very low and average less than 50 ppm U.

13. Rock types with elevated uranium contents: Elevated uranium contents have been observed in different rock types such as pegmatite, granites and black shale. In the past no economic deposits have been mined commercially in these types of rocks. Their grades are very low, and it is unlikely that they will be economic in the foreseeable future.

- *Rare metal pegmatites*: These pegmatites contain Sn, Ta, Nb and Li mineralisation. They have variable U, Th and rare earth elements contents. Examples include Greenbushes and Wodgina pegmatites (Western Australia). The Greenbushes pegmatites commonly have 6–20 ppm U and 3–25 ppm Th.
- *Black Shale*: Black shale related uranium mineralisation consists of marine organic-rich shale or coal-rich pyritic shale, containing syn-sedimentary disseminated uranium adsorbed onto organic material. Examples include the uraniferous alum shale in Sweden

and Estonia, the Chatanooga shale (USA), the Chanziping deposit (China), and the Gera-Ronneburg deposit (Germany).

1.3.3. Deposit status

1. **Closed**: A deposit where production has taken place in the past, but where no further production activities are anticipated.
2. **Depleted***:* Refers to a deposit from which economic resources have been depleted or mined out.
3. **Development**: Refers to a deposit for which project licensing has been largely completed and construction is underway. Development activities include drilling and coring to complete final mine plans and establish final processing flowsheets, construction of support infrastructure and surface facilities, shaft sinking and underground development in the case of an underground mine or overburden stripping in the case of an open pit mine, mill construction, tailings management construction, etc.
4. **Dormant**: Refers to a deposit on which there is no current activity and for which no activity is known to be planned.
5. **Exploration**: Refers to a deposit that requires further exploration to fully define its resource potential. 'Exploration' does not, however, necessarily mean that there is an active exploration programme currently underway at a given deposit, just that additional exploration is warranted. The status of future exploration planning is unknown.
6. **Fully explored**: Refers to a deposit where exploration has proceeded to a point where there is sufficient information on which to base a preliminary feasibility study. Further activities on a fully explored deposit will generally fall under the pre-development/development category.
7. **Operating***:* Refers to a deposit on which mining and processing are currently underway.
8. **Partially explored**: Refers to a deposit on which exploration has been initiated but where additional exploration is required to determine resource potential. This category does not suggest what the current status of exploration planning is.
9. **Permitted**: Project permits and licenses are typically issued in a series. For example, a project can receive a license for underground test mining and then subsequent licenses for construction and finally mining and milling. Issuance of each successive permit/license is predicated on satisfying conditions of preceding permits/licenses. When a project has all permits and licenses in hand to begin production it is referred to as being 'permitted'.
10. **Reclamation**: Refers to a project that has terminated production and is in the process of rehabilitating mining and processing sites.
11. **Reclaimed**: Refers to a project in which rehabilitation has been completed and approved by regulatory authorities.
12. **Standby**: Refers to a project that has produced in the past and is capable of producing in the future. Standby status implies that operating licenses remain in force or can be reinstated and that equipment is either operational or can be restored to operational condition.
13. **Unknown**: Status not known

1.4. UDEPO database structure

The World Distribution of Uranium Deposits **(UDEPO)** is a database on the technical and geological characteristics of uranium deposits worldwide. The UDEPO web site is designed to allow users to retrieve data sets on a variety of deposit related topics ranging from specific information on individual uranium deposits to statistical information on uranium deposits worldwide. Data can be searched by deposit type and operational status and by country, using filter options provided.

The basic building blocks for the UDEPO database are the more than 900 individual deposits for which information is available in the database. The database is arranged in a relational database format which has one main table and a number of associated tables. Structured nature of the database allows filtering and querying the database in more systematic way.

1.4.1. Data included

UDEPO database contains information mainly on technical and geological characteristics of the uranium deposits in addition to the general information about the deposits. Below Table shows the complete list of the data fields which are included in the database. Some of the fields are restricted for internal use and not published to the external parties. Publicly available data fields are marked with asterisk.

Most of the topics in the preceding list are self explanatory. There are, however, certain data fields that require further discussion. TABLE 2 gives some of the data fields of UDEPO which have predefined values as lookup list and the predefined values. Data entry to those fields has to be one of the predefined values.

TABLE 1. LIST OF UDEPO DATA FIELDS

General Information	**Technical Information**	**Geological Information**
Deposit Name*	Resource Range (t U) *	Deposit Type*
Geological District*	Grade Range (% U) *	Lithology*
Geological Region*	Deposit Status*	Tectonics*
Political/Geographical Provice*	Current Processing Plant*	Alteration*
Country*	Cumulative Production*	Host Rock Age*
Ownership*	Production Period*	Age of Mineralization*
Operator*	Produced Grade*	Ore Mineralization*
Coordinate*	Initial (Global) Resources (t U)	Mineralization Description*
Other/Synonym Names	Initial Grade (% U)	Ore Controls*
Information Sources	Remaining Resources (t U)	Metallogenic Aspects*
References*	Remaining Grade (% U)	Deposit Shape, Width, Length, Thickness and Depth*
	Cost Category	
	Mining Methods	
	Milling Processes	
	Commodities	

* Data fields which are publicly available on the UDEPO internet site.

TABLE 2. SOME OF THE UDEPO DATA FIELDS AND THEIR PREDEFINED VALUES

Deposit Types	Deposit Status	Resource Ranges (t U)	Grade Ranges (%U)	Mining Methods
• Unconformity-Proterozoic Fracture bound • Unconformity-Proterozoic Clay bound • Unconformity-Phanerozoic • Sandstone–Roll Type • Sandstone–Tabular • Sandstone–Basal Channel • Sandstone–Tectonic/Lithologic • Hematite Breccia Complex • Quartz-pebble Conglomerate • Vein • Intrusive • Volcanic • Metasomatite • Surficial • Collapse Breccia Pipe • Metamorphic • Phosphorite • Lignite/Coal • Black Shales • Other • Unknown	• Closed • Depleted • Development • Dormant • Exploration • Fully explored • Operating • Partially explored • Permitted • Reclamation • Reclaimed • Standby • Unknown	• < 500 • 500–1 000 • 1 000–2 500 • 2 500–5 000 • 5 000 –10 000 • 10 000 –25 000 • 25 000 –50 000 • 50 000–100 000 • > 100 000 • Unknown	• < 0.03 • 0.03–0.05 • 0.05–0.10 • 0.10–0.20 • 0.20–0.50 • 0.50–1.00 • 1.00–5.00 • > 5.00 • Unknown	• Open Pit • Underground • In Situ Leaching • In Place Leaching • Other • Unknown

Resource range refers to the original 'identified resources' of a deposit. 'identified resources' include reasonably assured resources plus inferred resources. Each of these resource categories is defined in the Glossary. Resources for individual deposits are listed in TABLE 2 (numbers of deposits included in the database that fall within each range are shown in parentheses).

Resources are reported within ranges because more definitive resource totals are not available for a portion of the deposits in the database. In addition, quoting exact resource totals would necessitate acknowledging the source of the information, which may not always be known or may be proprietary. Finally, details regarding the parameters used to calculate published resource totals such as economic ore cutoff grade are usually not available.

Original resources are listed rather than remaining resources to reflect the original potential of the deposit and the potential of given geological district or region to host deposits of a certain size. For deposits that have been or are currently in production, remaining resources can be determined by subtracting cumulative production from original resources.

Grade range refers to the ore grade of the original resources. The reasons for using a range instead of specific grade values are the same as those listed above for resources. The grade ranges utilized in UDEPO are presented in TABLE 2:

Deposit status defines the current status of each deposit. The deposit statuses which are available in the UDEPO database are given in TABLE 2.

1.5. Overview of Uranium Resources, Production and Demand

Information given in this section is taken from Red Book 2007 [6] if not otherwise stated.

TABLE 3. URANIUM RESOURCES BY COUNTRY

	Uranium Resources (t U) (below US$ 130 /kg U)			
Country	**RAR**	**Inferred**	**Total**	**%**
Australia	725 000	518 000	1 243 000	22.7
Kazakhstan	378 000	439 200	817 200	14.9
Canada	329 200	121 000	450 200	8.2
USA	339 000		339 000	6.2
South Africa	284 400	150 700	435 100	8.0
Namibia	176 400	30 900	207 300	3.8
Brazil	157 400	121 000	278 400	5.1
Niger	243 100	30 900	274 000	5.0
Russian Federation	172 400	373 300	545 700	10.0
Uzbekistan	72 400	38 600	111 000	2.0
India	48 900	24 000	72 900	1.3
China	48 800	19 100	67 900	1.2
Others	363 300	263 900	627 200	11.5
Total	**3 338 300**	**2 130 600**	**5 468 900**	**100.0**

TABLE 4. URANIUM RESOURCES BY DEPOSIT TYPE

	Uranium Resources (t U) (below US$ 130 /kg U)			
Deposit Type	**RAR**	**Inferred**	**Total**	**%**
Unconformity related	491.6	158.1	649.7	11.9
Sandstone	999.5	524.4	1523.9	27.9
Hematite breccia complex	499.4	401.5	900.9	16.5
Quartz-pebble conglomerate	163.6	138.3	301.9	5.5
Vein	156.8	167.7	324.5	5.9
Intrusive	183.7	104.2	287.9	5.3
Volcanic and caldera related	157.8	53.5	211.3	3.9
Metasomatite	304.9	368.8	673.7	12.3
Others	284.3	154.4	438.7	8.0
Unspecified	96.7	59.7	156.7	2.9
Total	**3338.3**	**2130.6**	**5468.9**	**100.00**

TABLE 5. 2006 AND 2007 URANIUM PRODUCTION BY COUNTRY

	Uranium Production (t U)		
Country	**2004**	**2005**	**% in 2005**
Canada	9 862	9 850	22.7
Australia	7 593	7 600	17.5
Kazakhstan	5 281	7 245	16.7
Niger	3 443	3 633	8.4
Russian Federation	3 190	3 381	7.8
Namibia	3 067	3 800	8.8
Uzbekistan	2 260	2 300	5.3
South Africa	534	750	1.7
USA	1 805	2 000	4.6
Others	2 568	2 769	6.4
Total	**39 603**	**43 328**	**100**

TABLE 6. 2006 AND 2007 URANIUM PRODUCTION BY PRODUCTION METHOD

	Uranium Production (%)	
Uranium Production Method	**2006**	**2007**
Underground Mining	39.9	37.7
Open Pit	24.2	23.7
In Situ Leaching	24.9	27.7
Co-product/by-product	8.6	8.4
Others	2.4	2.5
Total	**100.0**	**100.0**

TABLE 7. 2004 URANIUM PRODUCTION AND NO. OF ACTIVE PRODUCTION CENTERS BY DEPOSIT TYPE (REFERENCE IS IAEA INTERNAL COMMUNICATION)

Deposit Type	**% of 2004 Production**	**No of Production Centers**
Unconformity related	39.3	4
Sandstone	28.6	20
Metasomatic	10.2	3
Hematite breccia complex	9.0	1
Volcanic	8.0	2
Quartz pebble conglomerate	1.8	1
Vein	1.6	6
Intrusive	<1	3
Surficial	0	
Collapse breccia	0	
Phosphorite	0	
Others[*]	0	
Total[†]	**98.5**	**40**

[*] Metamorphic, Limestone and Uraniferous coal
[†] 0.5% of 2004 production from environmental cleanup projects; the balance is for in internal rounding.

The above table shows worldwide uranium output by deposit type in 2004. Production is shown as a percentage of 2004 production; the number of production centers that produced from each deposit type is also shown.

TABLE 8. 2007 URANIUM PRODUCTION BY DEPOSIT

Deposit	**Country**	**2006 Production (t U)**
McArthur River-Key Lake	Canada	7 200
Ranger	Australia	4 029
Rossing	Namibia	3 067
Priargunsky	Russian Federation	3 190
Olympic Dam	Australia	2 868
Rabbit Lake	Canada	1 972
Akouta	Niger	1 866
Arlit	Niger	1 565
Akdala	Kazakhstan	1 000
Highland-Smith Ranch	USA	786
Others		12 060
Total		**39 603**

TABLE 9. URANIUM DEMAND BY COUNTRY FOR 2007

Country	**Nat. Uranium Demand (t U, 2007)**
USA	22 890
Japan	8 790
France	9 000
Russian Federation	4 100
Korea, Republic of	3 420
Germany	3 490
Ukraine	2 480
Canada	1 900
China	1 500
UK	1 500
Belgium	1 065
Others	12 465
Total	**69 110**

2. URANIUM DEPOSIT TYPES

2.1. Unconformity related deposits

2.1.1. Definition

Unconformity related deposits comprise massive pods, veins and/or disseminations of uraninite spatially associated with major unconformities that separate Paleoproterozoic metamorphic basement from overlying Paleoproterozoic-Mesoproterozoic siliciclastic basins. The basement has been altered to varying depths by lateritic weathering. Basement and post-unconformity rocks show strong alteration effects associated with mineralized zones. The overlying basin sediments are usually flat-lying, un-metamorphosed, fluvial red-bed strata. Uraninite (commonly in the form of pitchblende) is the dominant uranium mineral in the monometallic (or 'simple') deposit and the main mineral in the polymetallic (or 'complex') deposit that includes variable amounts of Ni, Co, As, Pb and traces of Au, Pt, Cu and other elements. Some deposits include both ore types and transitional types. Monometallic ores are hosted by basement metasediments, while polymetallic ores are generally hosted by sandstones and paleo-weathered basement at the unconformity.

Two sub-types of unconformity related deposits have been recognized reflecting both stratigraphic and structural control [8][9][10]:

- ***Fracture controlled***, dominantly basement hosted (McArthur River, Rabbit Lake, Eagle Point, McClean Lake, Dominique-Peter in Canada; Jabiluka, Ranger, Nabarlek, Koongarra in Australia),

- ***Clay bounded***, massive ore developed along and just above or immediately below the unconformity in the overlying cover sandstones (Cigar Lake, Key Lake, Collins Bay A, B and D zones, Midwest, McClean, Cluff Lake D in Canada).

The fracture controlled mineralization typically occurs along steeply to moderately dipping shears, fractures and breccias, which may extend more than 400 m into basement rocks below the unconformity. The main structures are commonly reverse faults (McArthur River, Koongarra, Ranger 3). Mineralization occurs as disseminated and massive uraninite/pitchblende in the fractures and breccia matrix. In contrast, clay bounded mineralization is developed along the basement-sandstone unconformity and forms linear, pipe and cigar shaped orebodies typically characterized by a high grade core (1–15% U) and surrounded by a lower grade halo. Mineralization may extend into the overlying sandstone cover, along cataclastic breccia and fracture zones, forming 'perched' mineralization such as at Cigar Lake. Most of the orebodies have root-like extensions in the basement.

Examples of the two sub-types are included in this discussion as important representatives of the broader classification 'unconformity related deposits'. Both subtypes can, however, occur together in the same deposit and they may in fact be part of the same basic deposit model with clay bounded and fracture controlled subtypes as end members of a series. For example, ore grade mineralization at McArthur River, the largest and highest grade unconformity related deposit, straddles the unconformity.

2.1.2. Geologic setting of Jabiluka, Australia and Cigar Lake, Canada

Though Proterozoic unconformity related deposits are geologically diverse in their details, they share some unifying characteristics. In Australia, the basement rocks are

Paleoproterozoic metasediments mantling Archaean granito-gneissic domes. The overlying sandstones of the Kombolgie Subgroup in the Alligator Rivers region are of Late Palaeoproterozoic age as shown by radiometric ages of the underlying Plum Tree Creek Volcanics at 1822 Ma [11] and intrusion of the Jimbu Microgranite into the top of the Kombolgie at 1720 Ma [12]. In the Rudall region, Western Australia, these sediments (Coolbro Sandstone of the Throssell Group) are Meso- and Neoproterozoic and have been folded.

In the Athabasca Basin, Canada, deposition of the overlying sandstones commenced before 1644 Ma, age of internal tuffaceous units [13]. The authors estimate that sedimentation began at about 1740–1730 Ma considering metamorphic ages on titanites as young as 1750 Ma in basement rocks. Similarly, basal units of the Thelon Basin have a maximum age of 1750–1720 Ma [14].

The style of high-grade unconformity related deposits at the unconformity, as seen at McArthur River and Cigar Lake, has not been found to date in the Pine Creek Inlier in northern Australia. Most Australian unconformity related uranium deposits in the Alligator Rivers, Rum Jungle and South Alligator Valley fields are strata bound, and are hosted by breccia zones, faults and shear structures.

The high- to very high-grade deposits (5–15% U) occur in clay-altered sandstones immediately above the unconformity (Cigar Lake) and in faulted sandstones (McArthur River) at and below the unconformity. Mineralisation commonly extends into the altered basement rocks and can be either 'monometallic' (uranium) or 'polymetallic' (U+Ni+Co+As+Mo+Pb and/or traces of Au-Pt-Pd). Bitumen ('thucholites') often occurs in the mineralised zone.

Deposits immediately below the unconformity are usually medium- to high-grade (0.3–2.0% U) and are dominantly monometallic (Eagle Point, Jabiluka). The uranium mineralisation occurs in faults and fracture zones of altered metasediments that contain graphitic rocks.

The host rocks are pelitic, arkosic and carbonate sediments which have been metamorphosed to amphibolite grade facies in the Athabasca Basin and the Alligator River field, but only to greenschist grade at Rum Jungle and the South Alligator River field. Retrograde metamorphism (greenschist facies) has been superimposed on these metasediments. Palaeoweathering of the crystalline basement rocks is recorded in the basement of the Athabasca Basin. Similarly, in the Alligator Rivers region a regionally extensive palaeo-saprolitic profile, commonly over 50 m thick, is recorded in the basement.

Intensive alteration of the host rocks (mainly chloritic, but also sericitic, argillic, and carbonate alterations) surrounds the mineralisation. Some of these deposits (Jabiluka, Koongarra and Ranger 1) contain gold mineralisation and minor Pt-Pd mineralisation. Some smaller deposits are polymetallic, such as those in Rum Jungle that contain copper, lead, cobalt and nickel.

Uranium U-Pb isotope age dating studies have indicated a 1737 Ma age [15] for mineralization at Ranger. Recent age dating shows that for the Jabiluka deposit massive uraninite first precipitated at about 1680 Ma [16]. The Sm-Nd ages for mineralization at the Nabarlek and Koongarra deposits are all in the range of 1 600–1 650 Ma [17]. More recent regional mapping and age-dating constrains the age of the Kombolgie Subgroup to 1 822–1 720 Ma, bracketing it with the U-Pb age of the pitchblende at Ranger and the intrusion of

the Jimbu Microgranite (1 720 Ma). The main mineralization at Jabiluka, Koongarra and Nabarlek formed after deposition of the Kombolgie Subgroup.

Athabasca Basin uranium deposits records one or two main hydrothermal oer related events at circa 1550–1500 Ma and 1350–1300 Ma that were overprinted by further alteration and uranium remobilization events at approximately 1200–1150 Ma, 900 Ma and 300–200 Ma.

2.1.2.1. Fracture controlled type example: Jabiluka deposits, Australia

The three Jabiluka deposits occur within the Alligator Rivers Uranium Field along the northwest margin of the McArthur Basin. They are in the lower member of the Cahill Formation, along the north-eastern flank of the Archean granitic Nanambu Complex.

Jabiluka 1 lies 300 m west of Jabiluka 2.Jabiluka 3 is located down dip and to the south from Jabiluka 1 [18]. The Jabiluka 1 deposit measures about 400m in a north-westerly direction and 200m in a north-easterly direction and dips south at 15–30º. In the Main Mine Series the ore zone is up to 35m thick. Jabiluka 2 deposit extends for at least 1000m in a west-north-west direction and at least 400m north–south. The deposit is still open to the south and east at depth. In the Main Mine Series the ore zones are up to 135m thick.

The metasedimentary sequence at Jabiluka consists of alternating quartz–muscovite–chlorite schist, quartz–chlorite schist, quartz–graphite schist and magnesite–dolomite. Some units are feldspathic, locally containing garnet, sillimanite and zircon. Hancock et al., [19]consider that the sequence is overturned and the ore bodies occur along the lower limb of a recumbent fold. In the vicinity of the deposits, retrograde metamorphism has resulted in chloritisation of biotite and garnet, together with sericitisation of feldspar, sillimanite and cordierite.

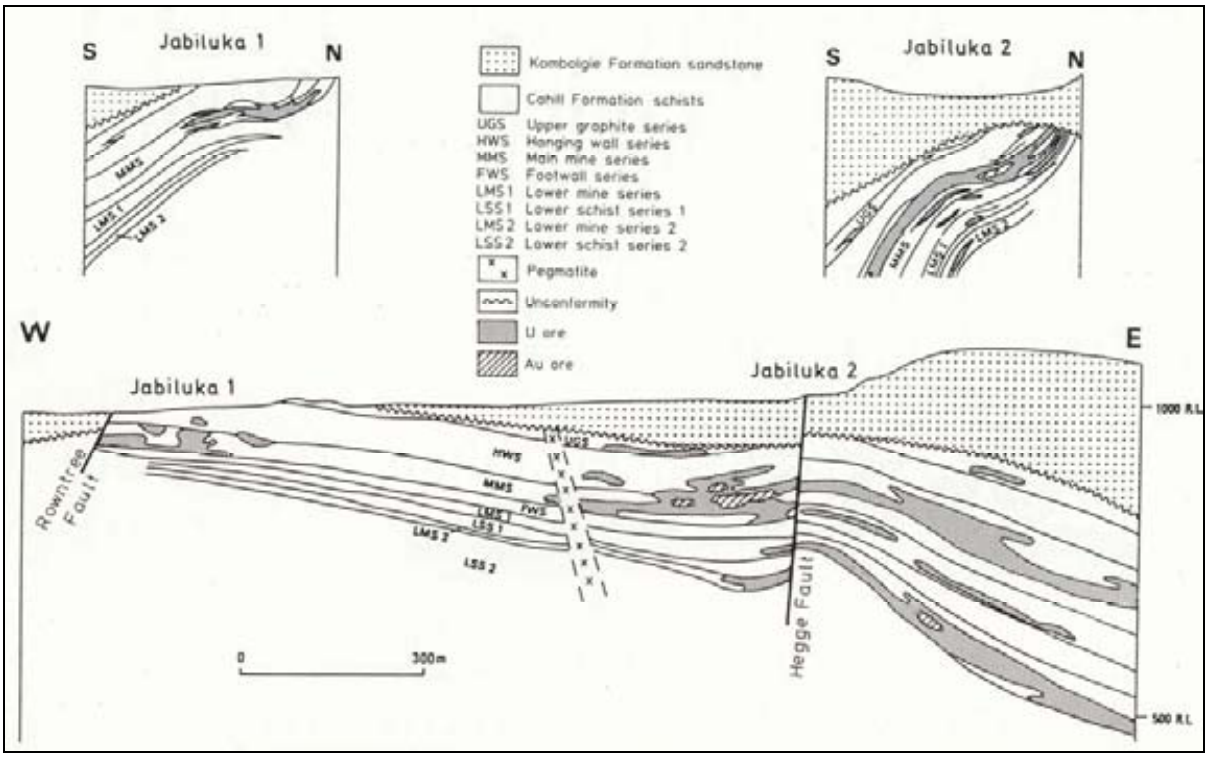

Fig. 4. Jabiluka, generalized S-N cross-sections and W-E longitudinal section of Jabiluka I and II [23].

Mineralization is structurally controlled and is within breccia zones that are subconformable to the layering of the Cahill Formation, and breccias that are developed within the hinge zone of fault related folds.

Primary mineralisation in the Jabiluka deposit complex is uraninite with minor coffinite, brannerite and organo–uranium minerals [20]. Mineralisation occurs in three main forms: breccias; veins adjacent to breccias; and as disseminations within the schists. The bulk of the economic mineralisation occurs in breccia zones [19].

Hancock et al [19] showed that chloritic alteration associated with mineralisation is extensive parallel to the unconformity, but appears to decrease with depth below the unconformity. In places, the basal sandstone above the unconformity has been intensely replaced by chlorite.

Sulphides include pyrite with lesser chalcopyrite and galena. Major gangue minerals are chlorite, quartz, sericite and graphite.

Gold mineralisation occurs in graphite horizons in the western part of the Jabiluka 2 ore body. The gold is mainly in breccia zones of the Main Mine Series; the ore averages 2m in thickness [21]. The gold zone contains 2.392 Mt ore averaging 3.7 g/t Au and 0.40% U [22].

2.1.2.2. Clay bounded Type Example: Cigar Lake deposit, Canada

The Cigar Lake deposit is located near the eastern rim of the Athabasca sedimentary basin. The deposit lies at a depth of 410–450 m below surface. It was discovered by the drilling of an electromagnetic conductor [24][25][26].

The geological environment of the deposit is comparable to that of the other major uranium deposits of the basin. It is situated at the unconformity between Aphebian and Archean metasediments of the Wollaston Group and detrital units of the unmetamorphosed Helikian Athabasca Group. It occurs in the sandstones, immediately above the unconformity, although minor mineralization is present up to 300m above the unconformity (perched mineralization), and in rare veins in the underlying basement. The Athabasca Group, consists of predominant quartz sandstones with conglomerate layers particularly at the base of the group. However, the basal conglomerate is absent at the deposit, wedging out against an east-west, up to 30m high, pre-Athabasca basement ridge, on top of which is located the orebody [25][26].

The basement rocks comprise graphitic, biotite-cordierite-pyrite pelitic gneisses, diopsidic calcsilicate gneisses and granitoid segregations derived from anatexis of the surrounding rocks. The pelitic gneisses, where they underlie the orebody, are augen textured (cordierite voids). The mineralogy and geochemistry of the graphitic metapelitic gneisses suggest that they where originally shales. The abundance of magnesium in the intercalated carbonate layers indicates an evaporitic origin [26]. The metapelitic rocks reached the upper amphibolite grade during Hudsonian regional metamorphism.

Alteration of the crystalline basement rocks is of three distinct types 1) retrograde alteration, which is associated with the late stages of the Hudsonian orogeny, 2) alteration associated with the development of a pre-Athabasca paleo-weathering profile, and 3) hydrothermal alteration, which is restricted to the uranium mineralization and extends up into the Athabasca sandstone, above the deposit.

Intense lateritic paleo-weathering has altered the crystalline basement to depths in excess of 50 m below the unconformity. Post-sandstone, early diagenetic and later ore related

diagenetic hydrothermal processes have altered the cover sediments and crystalline rocks near the paleo-surface. Ore related hydrothermal activity overprinted the former alteration zones by illitization, chloritization, carbonatization, tourmalinization (dravite), silicification, sulfidization, destruction of graphite, and corrosion of quartz. This alteration is intensely developed within the deposit and extends from the unconformity to about 100m into the basement and 200m into the overlying Athabasca sandstone [26].

Uranium minerals occur in the clay body as disseminated to often massive, continuous mineralization forming a linear, cigar-shaped, flat-lying lens, 2 200 m in length, 10–105 m in width, and 5–30 m in thickness. The lens comprises a high grade core (>50% U, 1–12 m thick) surrounded by a lower grade halo. The ore-wall rock boundary is rather sharp. Minor mineralization extends along cataclastic zones higher up into sandstone (‘perched mineralization’) and downward into the basement. Perched mineralization (pitchblende and coffinite with minor pyrite and marcassite, and commonly microscopic hydrocarbon matter) possibly results from remobilization of unconformity mineralization along steeply dipping faults. Basement mineralization is of limited importance and comprises rare, thin, locally brecciated mineralized intervals.

In the main mineralization, uranium minerals include uraninite, pitchblende, coffinite, and secondary uranium minerals. Associated metallic minerals are Ni-Co arsenides, sulfo-arsenides and sulfides, and sulfides of Fe, Cu, Pb and minor Zn and Mo. The average grade for various elements is as follow: Pb 1.77%, As 2.29%, Ni 1.38%, Co 0.21%, Cu 0.96%, Mo 0.21% and Zn 0.06% [25]. Gangue minerals include illite, kaolinite, chlorite, siderite, and calcite. Some carbonaceous material (bitumen) is also present.

In situ U-Pb results from three stages of uraninite and coffinite [27]display ages of 1 461, 1 176 and 876 Ma. These ages correspond with the age of the clay mineral alteration (1 477 Ma) associated with unconformity-type uranium deposits, ages of magnetization events (1600–1450 and 900 Ma) from the Athabasca Basin, and the Grenvillian Orogeny (1 100 Ma).

2.1.3. Ore geometry and metallogenesis

Conventional models for unconformity-associated uranium deposits invoke late diagenetic to hydrothermal processes. There is sufficient diversity in unconformity-associated deposits to require multiple models or variants of a main model [28]. These models [29][30][31][32][33] propose that oxidizing uranium-transporting basin fluids, heated by geothermal gradient, attained 200°C (5–6 km) at the unconformity and reacted with basement graphite causing uranium precipitation due to mixing of reduced and oxidized fluids [29]. Precipitation was primarily focused by structural and physiochemical traps [10]. These traps operated in fixed locations for very long periods of time [34], perhaps hundred of millions of years. Zones of fluid mixing are characterized by alteration haloes that contain illite, kaolinite, dravite, chlorite, euhedral quartz and locally Ni-Co-As-Cu sulfides [31].

Deposits where formed after at least the deposition of basal sandstone formations, because the extent of uranium and alteration minerals is throughout the local stratigraphic columns.

The fragmentation of the supercontinent Columbia, associated with the development of anorogenic magmatism and continental rifting, which began at 1.6 Ga and continued until its final breakup at about 1.2 Ga, represents a major geodynamic event that may have been responsible for a critical change in fluid regime in the Athabasca basin, linked to the formation of uranium mineralization [35].

In Canada, fluid circulation associated with emplacement of later Mackenzie dikes (1 267 Ma [36]), initiated partial recrystallization of uraninite. Stable isotope compositions of the alteration minerals (illite, chlorites and kaolinite) in conjunction with their paragenesis indicate that oxidized basinal fluids were derived primarily from evolved seawater and leached uranium from the overlying sandstones of the Athabasca Formation and transported it into the basement via infiltration along fracture zones associated with reverse faults. Graphitic units in the basement and pre-ore alteration served as physical (fractured zones) and chemical (reductants) traps for the uranium mineralization.

The various conventional models all try to account for the combined efficiency of source, transport and deposition of uranium, as summarized by Cuney et al [37].

Primary sources in the basement include radiogenic S-type granites and pegmatites, metasedimentary terrains with abundant pelite whose uranium content is well above Clarke values, pegmatites and previous uranium concentrations. Regions relatively well endowed with uranium, such as the Wollaston and Mudjatik domains of the Trans Hudson orogen in Canada, or the Pine Creek geosyncline in Australia, have a much better chance of generating world-class deposits given favourable subsequent conditions. Intermediate stage reservoirs of uranium were the fluids and the sediments that came from the above ultimate sources. A number of workers have held that the sediments were the main reservoir for the metals. Some models reject the basin-filling strata as a significant source of uranium, noting that minerals capable of yielding uranium are absent, or focus on the relatively high uranium content in unaltered basement rocks. For Jefferson et al. [28], there is no doubt that hydrothermal alteration of basement rocks preferentially released uranium.

2.1.4. Uranium resources and production in unconformity related deposits

Initial resources for the major unconformity related deposits in Australia and Canada are given in TABLE 10.

TABLE 10. INITIAL RESOURCES OF THE MAJOR UNCONFORMITY RELATED DEPOSITS IN AUSTRALIA AND CANADA[28][38][39]

Deposit	**Country**	**Ore Resources (Mt)**	**Average grade (% U)**	**Contained U (Tonnes)**
Ranger 1 Orebody	Australia	22.16	0.22	48 668
Ranger 3 Orebody	Australia	95.93	0.13	119 484
Jabiluka 2 Orebody	Australia	52.31	0.33	172 992
Nabarlek	Australia	0.59	1.54	9 208
Koongarra 1 orebody	Australia	1.81	0.68	12 296
McArthur River	Canada	1.34	17.8	239 106
Cigar Lake	Canada	0.89	15.3	135 500
Key Lake	Canada	3.70	2.0	73 900
Eagle Point	Canada	3.32	1.54	51 150

A large proportion of Australia's uranium production since 1980 has been from two unconformity related deposits–Ranger (No. 1 and No. 3 Orebodies) and Nabarlek. Production from Ranger No. 1 Orebody was 41 003 t U, Ranger No. 3 Orebody 35 509 t U (1998 to Dec. 2006) and Nabarlek 9208 t U. Between 1954 and 1971, small unconformity related deposits were mined in the Rum Jungle uranium field (Dyson's, White's, Mount Burton and Rum Jungle Creek South) (total production 1 255 t U) and in the South Alligator Valley uranium field (total production 541 t U).

Uranium production in the Athabasca Basin started in 1976 with the Rabbit Lake operation, followed by Cluff Lake (1980), Key Lake (1983) and McClean Lake (1999). Since, several deposits have been mined-out (Rabbit Lake, 17 769 t; Collins Bay A-B-D, 24 400 t; Eagle Point, 51 150; Key Lake, 73 900 t; McClean deposits, 19 327 t; Cluff Lake deposits, 20 608 t). Cumulative production from the most recent McArthur River mine between 1999 and 2006 totalled 45 000 t U. Annual capacity of the McArthur River mine-mill complex, which is owned by Cameco (69.8%) and AREVA) (30.2%) is 8 460 t U.

2.2. Sandstone deposits

2.2.1. Definition

Sandstone uranium deposits occur in carbon and/or pyrite-bearing fluvial (less commonly marine), arkosic, medium to coarse-grained sandstones that contain, are interbedded with, and are bounded by less permeable horizons. Primary uranium minerals are predominantly pitchblende, coffinite, and to a lesser extent vanadates and phosphates [40][41][42]. Uranium is precipitated under reducing conditions caused by a variety of reducing agents within the sandstones (for example, carbonaceous material, sulphides, hydrocarbons and iron-magnesium minerals as chlorite). Major known sandstone deposits range in age from Palaeozoic to Tertiary. There are also small Precambrian sandstone deposits associated with carbonaceous matter of probable algal origin. Sandstone uranium deposits can be divided into four main types [43], which are listed below along with representative examples.

- ***Roll front type*** — Moinkum, Inkai and Mynkuduk (Kazakhstan), Crow Butte and Smith Ranch (USA) and Bukinay, Sugraly and Uchkuduk (Uzbekistan).
- ***Tectonic-lithologic type*** — Mikouloungou (Gabon) and Mas Lavayre, Lodève district (France).
- ***Basal channel type*** — Dalmatovskoye, Transural region and Khiagdinskoye, Vitim district (Russian Federation) and Beverley (South Australia).
- ***Tabular type*** — Ambrosia Lake, Grants Mineral Belt, New Mexico (USA): Westmoreland (Australia), Akouta, Imouraren and Arlit (Niger), Coutras (France) and Colorado Plateau (USA).

With few exceptions, sandstone uranium deposits are of diagenetic-epigenetic, low-temperature origin. Groundwater chemistry and migration are instrumental in leaching uranium from source rocks and transporting it in low concentrations to a chemical interface commonly provided by reducing or complexing agents where it is deposited. Essential parameters that control these processes include depositional environment, host rock lithology and permeability, adsorptive/reducing agents, groundwater chemistry amenable to leaching and transporting uranium, a uranium source and apparently an arid to semi-arid climate.

Fluvial, first cycle feldspathic or arkosic sandstones (weakly mature) of limited thickness (<10 m) interbedded with layers of fine-grained, low permeability clastic sediments deposited in intracratonic basins provide the most favourable host rocks for large, relatively high-grade sandstone uranium deposits. Marginal marine environments are also prospective, but to a lesser degree. The presence of uraniferous tuffaceous material either as a constituent of the host sandstone or in overlying strata may enhance the favourability of a fluvial system, due to its potential as a uranium source rock. Acidic volcanic and crystalline terrains are also considered to be potential uranium source rocks for sandstone uranium deposits.

The feldspar component of the host rocks, though probably of no direct importance in the mineralizing process, indicates a granitic source from which the uranium may have originated and an environment of rapid erosion and sedimentation providing the required hydro-physical conditions, particularly permeability for adequate groundwater migration. Impermeable or less permeable strata or other barriers may be instrumental in vertically and laterally channelling uraniferous fluids to favourable sites of uranium deposition, while at the same time prohibiting widespread flushing and dilution of fluids.

Uranium is soluble in large quantities only in its hexavalent state (+6 valence). Therefore, uranium-transporting fluids have to be sufficiently oxygenated to keep uranium in solution for transport, but at the same time limited in oxidizing potential so that reduction and precipitation of uranium can take place in sufficient ore grades and quantities to be commercially important. Complexing agents such as carbonate ions are important for enhancing the solubility and mobility of the uranyl ion in the form of carbonate or other complexes in neutral or alkaline groundwater that may be oxidizing or reducing [44].

Hexavalent uranium in solution must be reduced to the tetravalent state (+4 valence) to form commercially important concentrations of pitchblende or coffinite, the principal uranium minerals in most reduced sandstone deposits. Under certain conditions uranium minerals may also crystallize in an oxidizing environment when complexing agents such as vanadium compounds are present to fix the uranyl-ion in the form of uranyl vanadates which are fairly stable in oxidized rocks. A reductant is required to convert (reduce) hexavalent uranium to tetravalent uranium. Many substances have been invoked as uranyl reductants including $\pm$ coalified vegetal matter, woody fragments (coalification not higher than sub-bituminous) , structureless organic matter (humate), petroleum, ‘dead oil’, ‘sour’ natural gas, hydrogen sulfide and pyrite or other sulfides. Bacterial activity is considered by some authors to be an important factor in producing a reducing environment.

Sandstone uranium deposits are amenable to conventional open-pit and underground mining methods (for example the Arlit district, Niger) or by in-situ leaching and heap leaching (Australia, China, Kazakhstan, Russian Federation, the USA and Uzbekistan).

2.2.2. Roll front type deposits

2.2.2.1. Definition

Roll front deposits are zones of uranium-matrix impregnations that crosscut sandstone bedding and extend vertically between overlying and underlying less-permeable horizons. In cross section, roll front deposits are crecent-shaped and are convex in a down-gradient direction. The Moinkum deposit in Kazakhstan is described in the following sections as a representative example of roll front deposits.

2.2.2.2. Geological setting of Moinkum Deposit

The Moinkum deposit complex in Kazakhstan, which was discovered in 1973, as an extension of the Kanjugan deposit (same mineralized sand layers), is divided into three areas: Moinkum South, Moinkum Center and Tortkuduk (Moinkum North).

The Moinkum deposit complex is located in the southern part of the Chu-Sarysu basin, immediately north of the Karatau hills (Kazakhstan, N44°15'–E69°00'). The Chu-Sarysu basin is located within the Kendyktas-Tchou-Ili-Betpak-Dala U-Cu province, which is limited by alpine regional faults. Tectonically, Moinkum is located in the regional Souzak depression, which is limited by the Souzak and Juantobé faults to the south and to the north, respectively. Between these two faults, there are several parallel, north-south trending domal features, which are related to an Upper Paleogene monoclinal flexure (Ojiraï-Tobin). Dip orientation within the southern part of this flexure zone is related to a unique folded structure formed by NW and NE trending anticlines and synclines.

Three structurally related levels are distinguished in the basin: (a) the lower level lies within the folded Caledonian basement and is represented by epizonal schists and Cambrian-Ordovician limestones (Karatau anticline); (b) the intermediate level is represented by platform sediments, which were weakly metamorphosed and faulted at the end of Palaeozoic time (Souzak-Baykadam depression, Talas-Tasty uplift and 'Petit Karatou' tilting); and (c) the upper level, which is represented by Meso-Cenozoic platform sedimentary cover. Late tectonic structures have induced important folding in the platform cover, playing a major role in the location of uranium deposits (e.g. the Pechanoye and Tortkuduk deposits are linked to sub-meridian structures issued from Itmouroun fault reactivation). The most intense tectonic activity in immediate proximity to the Moinkum deposit complex is related to the Karatau uplift (Pliocene-Quaternary). This tectonic activity, however, had minimal influence on formation of the Moinkum deposits.

Three main deformational phases affected the Kendyktas structural-metallogenic province:

- ductile and brittle deformation of the basement before sedimentary cover emplacement,
- brittle deformation related to alpine orogeny,
- ductile deformation affecting Palaeogene and Cretaceous sediments.

The Kendyktas structural-metallogenic province is divided into two sedimentary zones: (a) the Kenze- metallogenic zone with four major deposits (Mynkuduk, Inkai; Boudenovskoye and Jalpak) hosted in Cretaceous sandstones (Mynkuduk and Inkuduk horizons) and (b) the Uvanas-Kanjugan metallogenic zone with three major deposits (Uvanas, Kanjugan and Moinkum) hosted in Palaeocene/Eocene sandstones (Kanjugan and Uyuk horizons).

The Paleocene/Eocene host sandstones of the Moinkum deposit complex were deposited by north-northwest flowing river systems that originated in the Tian-Shan Mountains, 500 km to the south.

2.2.2.3. Ore geometry and metallogenesis of the Moinkum deposit

Roll front systems develop at the interface between oxidized and reduced sandstones. In the upgradient direction, roll front systems are characterized by thin anomalous concentrations of uranium at the top and base of oxidized host sandstones, which are referred to as the 'wings' or 'tails' of the roll front. The wings represent remnant mineralization associated with lower

permeability sandstone or with shales or claystones, which was preserved as the roll front system migrated down gradient.

At the oxidation-reduction interface (redox or O/R), the wings converge into a crecent-shaped roll front, which is convex down hydrologic gradient. The roll front is characterized by sharp contacts with hematite and/or limonite–bearing sandstone on the up-gradient side (except in re-reduced deposits) and diffuse contacts with carbon and/or pyrite-bearing sandstone on the down gradient side [45][46]. Perpendicular to the hydrologic gradient, roll front deposits are elongate and sinuous. Mineralization related to the wings is typically less than one metre in thickness, but can attain thicknesses in excess of 10 metres; mineralized zones within the roll front range from less than one to several tens of metres.

Uranium mineralization was introduced into the roll front system by the same laterally circulating groundwater that oxidized the host sandstones. The source of the uranium is generally thought to have been de-vitrification of volcanic tuff, which was either admixed in the host sands or in overlying beds, or was leached from highlands underlain by acidic volcanic or crystalline terrains. As roll front systems migrate down hydrologic gradient, oxidizing groundwater remobilizes uranium along the up gradient side of the roll front and redeposits it down gradient at the redox boundary. As this process progresses down gradient, +6 valence uranium dissolved in the groundwater in small concentrations (2–4 ppb) is also being continually added to the roll front system at the redox boundary.

The Moinkum deposit complex lies within a regional oxidation system that extends from the Tian-Shan Mountains north-west for a distance of 500km. The nearby Karatau Mountains had little if any influence on the position of the redox front or the formation of the Moinkum ore bodies. The Moinkum deposits are comprised of several north-south trending mineralized bands. The ore displays typical roll front morphologies with top and bottom wings (or tails) converging into roll fronts. The wings are irregularly developed: the upper wing is rarely present, while the lower wing can be followed continuously for several hundred metres. The greater continuity of the lower wing is due to higher content of reduced material in the lower sand horizons.

The lower wings contain the most significant mineralization in the up-gradient part of the Moinkum roll front system. There are, however several mineralized lenses of commercial significance in the middle of sandstone units and in the upper wings. Ore thickness in the wings varies from 10 cm to12 m. The main roll front, which is located at the redox contact, can reach widths of 200–300 m and thicknesses of up to 25 metres along selected profiles.

Individual roll fronts in the Moinkum deposit complex range in length from 300 to 15 000m and in width between between 50 and 1 600 m. Roll fronts are developed on at least three levels ranging in depth between 220 and 520 m. These levels correspond to three Upper Paleocene to Middle Eocene sandstone horizons: Kanjugan, Uyuk and Ikan, each of which hosts a separate aquifer system. In the Moinkum deposit complex, 31 mineralized occurrences have been discovered. Uyuk is the main mineralized level. The mineralized sand thickness (per single roll) ranges between 2 and 25 m, with grades varying from 0.016 to 0.785%U. The average ore grade of the Moinkum deposit complex is 0.06%U.

The ore in the Moinkum deposit complex is hosted in gray, fine to medium-grained, loosely cemented arkosic sands. The detrital component of the sands includes sub-rounded grains of quartz, feldspar, mica, clay and accessory minerals (pyrite, marcasite, goethite, hydro-goethite, calcite, collophane, ferrosilite, native selenium and ilsemannite pebbles). Most of the

uranium ore occurs as coating on detrital grains, as veinlets inside organic lithoclasts, as disseminated minerals or in the silty-clayey cement.

The ore minerals are mainly coffinite (93–100%), less often carbono-coffinite, and very rarely nasturane (0–7%). Associated ore compounds include iron and sulphur-rich organic matter (organic carbon C = 10ppm–0.05%; CO_2 = 0.04–0.13%; Fe = 0.42–2.75%; S = 0.09–0.71%; P= 0–0.13%) and traces of Se, Rh, Mo, Sc, Co and Ni.

2.2.2.4. Uranium resources and production in Moinkum and Tortkuduk deposits

Initial resources (B+C1+C2 Russian categories) totaled about 42 250 t U with an average grade at 0.061% U, including the Moinkum and Tortkuduk areas. Production using ISL technology has been ongoing since 1982 in the Central Moinkum deposit, which is 100%-owned by Kazatomprom. ISL pilot tests were performed between 1998 and 2004 in the South Moinkum and Tortkuduk deposits; commercial-scale production began at South Moinkum in late 2005. The owner of the South Moinkum and Tortkuduk deposits is KATCO, a joint venture shared by COGEMA (51%) and Kazatomprom (49%); COGEMA is the operator of the KATCO project.

2.2.3. Tectonic-lithologic type deposits

2.2.3.1. Definition

Tectonic-lithologic deposits are discordant to the surrounding strata. They occur along permeable fault zones with linguiform impregnation of the adjacent clastic sediments (i.e. tongue-like impregnations extending away from faults into the surrounding country rock). Thick, steeply dipping ore bodies referred to as ‘stack’ deposits can result from redistribution of primary uranium into permissive hosts such as fault zones or permeable sedimentary units by younger processes, such as is found in the Grants Uranium Belt. They may also have originated by the introduction of primary uranium as interpreted for some deposits in Gabon (Mikouloungou). Tectonic-lithologic deposits range up to 100 m long and 40 m wide and contain up to 5 100 t U at a grade of 0.15 to 0.5%U. The Mikouloungou deposit in Gabon is described in the following sections as a representative example of tectonic-lithologic deposits.

2.2.3.2. Geological setting of the Mikouloungou deposit

The Mikouloungou deposit is located in the Franceville basin (Haut Ogooué district, Gabon) (S1°37'–E13°26'). The Early Proterozoic Francevillian sedimentary series, which hosts the ore in the Franceville Basin, unconformably overlies Archean crystalline basement. The Francevillian series consists of a 1–4 km thick, un-metamorphosed, sedimentary sequence comprising five major formations labelled sequentially FA to FE from bottom to top [47]. The basal sequence of the Franceville series, the FA Formation (500–1000 m thick) is mainly composed of conglomerates and fine- to coarse-grained, fluvial to deltaic sandstones [47]. During the first stage of diagenesis of the FA Formation, quartz overgrowths developed around detrital quartz grains and illite and chlorite formed in the matrix [48]. Depth of burial reached during the first stage of diagenesis was about 4 km [48], [49]. The age of siliceous diagenesis was estimated from Sm-Nd isochrones on authigenic illites at 2.03±0.08 Ga [50]. The overlying FB Formation mainly consists of highly organic marine shales, which are more or less calcareous at the base, changing to pure sandstones at the top of the formation. The FC formation is composed of massive dolomite and chert interbedded with black shales, whereas the FD and FE Formations are mainly composed of ignimbrites and epiclastic sandstones with interbedded shales.

All uranium ore deposits within the Franceville Basin are located in the upper part of the FA Formation, immediately below the redox boundary represented by the black shales of the overlying FB Formation.

2.2.3.3. Ore geometry and metallogenesis of the Mikouloungou deposit

The Mikouloungou mineralization extends for more than 1500 m along an east-west-striking overthrust that dips 45°N and persists for more than 250 m vertically. N-dipping FB 1 pelites in the upper block of the thrust overlie horizontal to gently SW-dipping FA sandstones in the lower block.

Mineralization occurs (a) along the footwall of the thrust zone independent of the lithology and (b) extending as tongue-like projections for 5 to 20 m from the thrust into the coarse-grained sandstone horizons. In plan view, the ore tongues show irregular, amoeboid shapes.

The ore controls within the Mikouloungou deposit are both structural and lithologic. Mineralization is sharply separated from the adjacent pelites by the overthrust. It occurs only on the footwall side of the fault and within coarse-grained kaolinized sandstones where joints with gouge partly control the mineralization. A change in alteration is observed within the host rocks from barren, fresh feldspathic sandstone to sandstone impregnated with pitchblende and clay minerals close to the fault. A lithochemical control was possibly provided by the overthrusted pelites. Their organic material may have produced a reducing environment increasing the precipitation of uranium. Silicification also appears to have influenced the distribution of the uranium. Uranium is concentrated predominantly in fluvial sands in the form of microcrystalline pitchblende within the organic matrix and occurs preferentially on the flanks or rims of paleochannels or where an intermediate thickness of sandstone is combined with high concentrations of organics. Tectonic-lithologic type mineralization occurs in rock units deposited in an organic-rich sedimentological environment and displays a strong affinity to cataclastic zones adjacent to uplifted crystalline basement (Mounana) or to overthrusted carbonaceous shales (Mikouloungou).

Ore minerals in the Mikouloungou deposit include pitchblende and coffinite in reduced zones, and uranyl vanadates and phosphates in oxidized zones. Associated minerals include karelianite, montroseite and roscoelite in reduced mineralization, and minor amounts of pyrite, marcasite, melnicovite, galena, sphalerite, chalcopyrite, barite and calcite as fissure fillings.

Uranium deposition has been dated by U-Pb discordia as 2.05±0.03 Ga [51]. High-grade pods of uranium mineralization reached criticality at 1.97±0.06 Ga [52] shortly after or during the mineralizing event and at maximum burial depths.

Two genetic models have been used to describe the ‘Francevillian deposits’ [48][53][54][55][56][57], the second improving upon the first by including more consistent fluid data and more comprehensive geological synthesis. All data obtained by these authors confirm that the FB black shales are source rocks for petroleum trapped within the uranium deposits. The earlier model concluded that all of the uranium deposits are in tectonic structures that served as traps for both petroleum and uranium. Uranium mineralization occurs in this setting when an oxidized uranium-bearing fluid has mixed with a reduced petroleum-bearing fluid [48]. The uranium ores are affected by hydro-fracturing which formed a pathway for the oxidized uranium-bearing fluids and the reduced fluids. Hydrofracturing may have been initiated by over-pressured fluids coming from under-compacted zones in the FB

black shales. The second model provides detailed processes for each fluid involved in the first model. Low temperature diagenetic brines are responsible for U-Zr-P-Pb-REE leaching by the dissolution of accessory minerals (zircon and monazite) in FA sandstones [54][57]. The Th/U ratio increase from monazite (Th/U=18.6) to the Th-silicate alteration phase (Th/U=88.7) is interpreted to be a result of alteration by oxidising brines with leaching of U together with LREE and P. During the ore-stage in the extensional regime, fracturing allowed mixing of meteoric recharge introduced into the basin and deep basinal brines. The resulting mixture was expelled laterally due to compaction of sandstones, and upwards along sub-vertical N-S basement rooted fractures. Due to the rapid burial of the FB pelites, overpressured fluids (hydrocarbons C_9 and C_{10}-rich fluids) occurred in the black shales during this stage. The extensional phase allowed the transmission of these overpressured fluids into the FA sandstone reservoir. Mixing of the expelled mineralizing fluid and hydrocarbon-rich fluid resulted in precipitation of uranium mineralization at the redox boundary that developed during diagenesis of FA sandstones with oxidising conditions and hydrocarbon-generating pelites.

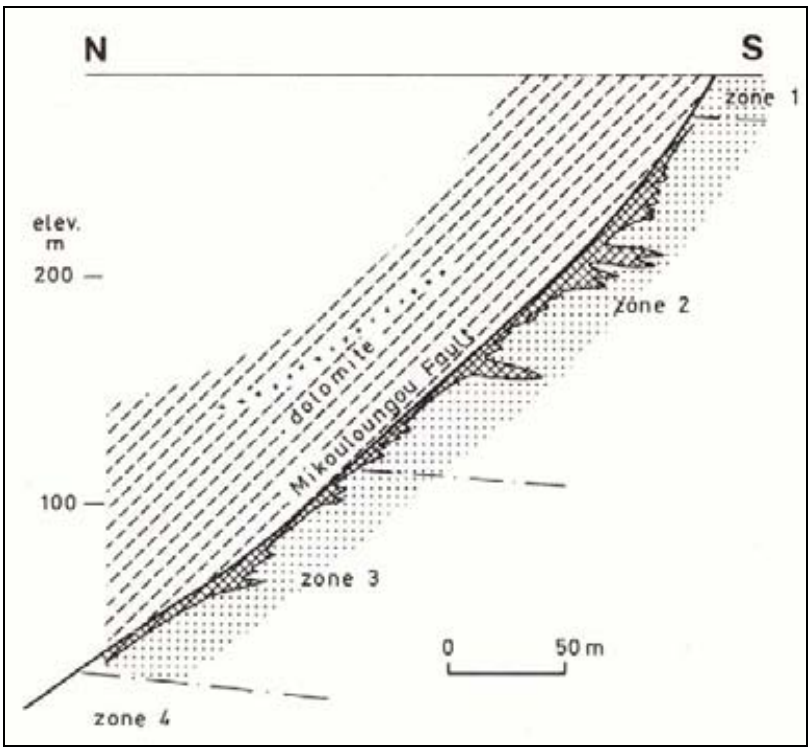

Fig. 5. Mikouloungou deposit, schematic S-N cross-section displaying the tectonic-lithologic control of the uranium mineralization [58]).

2.2.3.4. Uranium resources and production in the Franceville basin

Initial resources for the Mikouloungou deposit totalled about 9 951 t U with an average grade of 0.336% U. Total initial resources for the Franceville district, totalled approximately 21 150 t U. Uranium production in the Franceville district was controlled by Compagnie des Mines d'Uranium de Franceville (COMUF), which is owned by COGEMA (68%), Gabon government (25%), S.G.C.F. (6%) and others (1%). The operator was COGEMA. The mill, which has now been decommissioned, was located at Mounana (the first deposit discovered in the Franceville district). Cumulative production from the Franceville district totalled 26 610.

Production from the Mikouloungou deposit between 1997 and 1999 totalled about 1 134 t U at an average production grade of 0.28%; the Mikouloungou deposit is now depleted.

2.2.4. Basal channel type deposits

2.2.4.1. Definition

The paleodrainage systems that host basal channel deposits consist of several hundred meter-wide channels filled with thick permeable alluvial-fluvial sediments. The uranium mineralization is predominantly associated with detrital plant debris in ore bodies that display, in a plan view, an elongated lens or ribbon-like configuration and, in cross section view, a lenticular or, more rarely, a roll shape. Individual deposits range from several hundreds to 20 000 t U, at grades ranging from 0.01% to 0.10% U. Typical examples of basal channel deposits include the Dalmatovskoye deposit, Transural region and Khiagdinskoye, Vitim district (Russian Federation) and Beverley (South Australia). The Dalmatovskoye deposit is described in the following sections as a representative example of basal channel type deposits.

2.2.4.2. Geological setting of the Dalmatovskoye deposit

The Dalmatovskoye deposit is located in the Transural uranium district in the southwestern part of the West-Siberian Platform. The district is characterized by Middle to Upper Jurassic paleochannel systems which occupied the southwestern alluvial coastal plain of the Jurassic sea in the eastern foreland of the Caledonian Ural Mountains. The channels were incised into a basement of Devonian felsic volcanics and continental and marine sediments.

The paleodrainage systems that host the Dalmatovskoye deposit consist of 1 to 5 km wide channels filled with 30 to 120 m thick, permeable alluvial-fluvial sediments of middle to late Jurassic age. Lithologies include beach gravel, conglomerate, sand, silt and mud containing large amounts of plant debris (average 0.5 to 3% C_{org}). Three sedimentary cycles are distinguished, which are attributed to attenuating movement during the final folding and uplift phase in the Ural Mountains. Subsequent to the end of orogenic activity, the river valleys degraded to chains of drainage lakes into which proluvial and lacustrine sediments were deposited during Late Jurassic–Early Cretaceous time. These sediments consist of 30 to 150 m-thick impermeable, pink, carbonaceous silt, clay and sand which contain 100 to 300 ppm U in the form of syngenetic uranium associated with dispersed plant remains. Cretaceous and Tertiary sediments ranging between 300 and 700 m thick rest on the Jurassic rocks.

The northern limit of the uranium district is conterminous with the northern boundary of Late Jurassic–Early Cretaceous pink sediments, which in turn coincides with the boundary between the late Jurassic semi-arid and humid climate zones to the south and north, respectively.

2.2.4.3. Ore geometry and metallogenesis of the Dalmatovskoye deposit

The uranium deposits in the Transural district of Russian Federation range from less than 1 to as much as 25 km long, 50 to 1 500 m wide and up to 50 m thick and occur at depths in excess of 300 m. Individual ore bodies have dimensions of <1 to 7 km long, 50 to 700 m wide and 1.5 to 20 m thick. In plan view the ore bodies display an elongated lens or ribbon-like configuration and in cross section are predominantly lenticular and more rarely roll shape. Lenses occur singularly or en echelon, stacked at several levels separated by aquicludes. Some of the ore bodies trend along and others are oblique to channel axes.

Mineralization within the Transural district is lithologically and geochemically controlled. The uranium deposits of the district are of epigenetic origin with uranium having been introduced into the deposits by laterally circulating oxygenated meteoric waters. The solutions probably entered the permeable gray alluvial-fluvial horizon at valley heads in the western uplands of the Ural foreland. Rocks in this region include rhyolites with 4 to 5 times background uranium values. The oxygenated solutions oxidized the originally reduced gray facies and established redox fronts along which uranium and associated elements (Mo, V, Se and Re) were fixed in a zonal distribution typical for these deposits. Ore concentration was restricted to lithological intervals containing 1.5–2.5% C_{org}. The main stage of uranium mobilization is attributed to an early weathering period under semiarid conditions affecting the peneplain formed during the waning stage of tectonism in the Ural region. Overlying impermeable sediments of the pink proluvial-lacustrine facies prohibited downward percolation of mineralizing solutions and provided protection against erosion of ore host rocks.

A redox interface developed in the paleo-drainage system from downstream influx of oxygenated waters. Re-reduction, which is documented by bleaching, is assumed to post date deposition of the overlying, impermeable pink facies. The reducing agent was plant debris originally present in high amounts of up to 3% C. Oxidation and re-reduction altered the uranium-bearing gray alluvial–fluvial sediments. Neither alteration facies contains Fe-oxides or carbonaceous matter.

The principal uranium minerals in the Transural district are uranium oxides (sooty pitchblende) and coffinite. Associated minerals include marcasite, pyrite, jordisite, sphalerite, chalcopyrite, ferriselite, native selenium and rhenium and vanadium oxides. The uranium and associated minerals occur in disseminated form along redox interfaces. Isotope dating of uranium minerals yields an age of 135±7 m.y.

The Dalmatovskoye deposit consists of a number of ore bodies, which occur at depths of 360 to 500 m in a main 11-km long paleovalley and a tributary 8-km long paleovalley. Both paleovalleys are up to 1.5 km wide. Single ore bodies within the Dalmatovskoye deposit are 400 to 4 500 m long, 50 to 700 m wide and 2 to 12 m thick. Thickness of the ore in roll fronts can reach 20m. Host rock channel facies are Middle-Upper Jurassic alluvial sediments composed of pink oxidized and gray reduced sandy gravel, sandstone and conglomerate interbedded with silty mudstone. The channels are incised about 100 m deep into schists and towards the headwaters to the southwest into Devonian rhyolite and rhyolite-porphyry. Faults in the area of the Dalmatovskoye deposit trend east-west, northwest-southeast and northeast-southwest.

Uranium is present at Dalmatovskoye as coffinite and pitchblende, in grades varying from 0.01 to 3%; the average grade is 0.04% U. High-grade uranium sections may contain Sc, Re, Mo and REE minerals. Uranium distribution is controlled by redox boundaries in sand-gravel aquifers. In plan view, most ore bodies are lenticular in shape and are markedly elongated along the valley axis. In cross-section, the mineralization occurs in single rolls or lenses or stacked lenses at several levels separated by argillaceous aquicludes.

2.2.4.4. Uranium Resources and Production in Transural district

Three deposits and a number of ‘occurrences’ of basal channel sandstone deposits are reported in the Transural district, including Dalmatovskoye (10 200 t U RAR), Dobrovolnoye (RAR+EAR1 7 400 t U) and Khokhlovskoye (Speculatively Resources 10 000 t U). Ore grades range from 0.01 to 0.05 % U. The prognosticated resources of the district are estimated

as 115 000 t U recoverable at <US$ 80/kg U, 40 000 of which are projected to be recoverable at <US$ 40/kg U.

Mining operations at the Dalmatovskoye deposit are currently underway using sulfuric acid-based ISL technology. The other two deposits require further investigation and ISL testing. Planned annual maximum production in the Transural district is 1000 t U to be achieved in 2010. JSC 'Dalur', which is owned 75% percent by TVEL – the Russian state owned nuclear fuel producing company, is the operator at the Dalmatovskoye mine. Commercial ISL mining began at Dalmatovskoye in 2002. In 2006 the main processing plant came into operation; annual production will gradually increase from the 200 t U in 2005 to 500 t U in 2008.

2.2.5. Tabular sandstone type deposits

2.2.5.1. Definition

Tabular uranium deposits 'consist of uranium matrix impregnations that form irregularly shaped lenticular masses within reduced sediments. The mineralized zones are largely oriented parallel to the depositional trend' [43]. Examples of tabular sandstone deposits include, Hamr-Stráz (Czech Republic), Akouta and Arlit (Niger) and the deposits of the Colorado Plateau, (USA).

2.2.5.2. Geologic settings

Tabular sandstone deposits occur in several broadly similar geologic settings. For purposes of this discussion, tabular deposits are subdivided into the intrinsic and extrinsic carbon subtypes and the vanadium-uranium deposit subtypes. The source of the uranium reductant and associated minerals provides the main basis on which the subtypes are defined.

Subtype 1: Intrinsic carbon related deposits

The uranium mineralization in intrinsic carbon related deposits is associated with detrital carbonaceous debris that was deposited contemporaneously with the host sandstone. Examples of this deposit type include Arlit and Akouta (Niger) and Coutras (France). These deposits typically occur in reduced continental sandstones. The uranium, which was introduced into the host sandstones by laterally circulating groundwater, is closely associated with detrital plant debris, which acted as a reductant.

Subtype 2: Extrinsic carbon related deposits ('Grants type')

The uranium mineralization in extrinsic carbon related deposits is associated with redistributed carbonaceous matter (e.g. humate), which post-dates deposition of the host sandstones. The uranium deposits of the Ambrosia Lake district in New Mexico, USA are the best examples of extrinsic carbon related tabular uranium deposits. The host sandstones in the Ambrosia Lake district were deposited by west to east flowing fluvial systems that deposited a broad alluvial fan that extends across a large part of northwestern New Mexico. Major ore bodies in Ambrosia Lake are restricted to the braided, straight and sinuous channel facies within the fan complex.

The uranium mineralization in Ambrosia Lake, which resulted from a chemical reaction between uranium-bearing groundwater and elongate humate masses, consists of submicroscopic coffinite with minor amounts of amorphous urano-organic clay complexes in a matrix of dark-colored, apparently structureless carbonaceous matter that impregnates and

partially replaces the sandstone. The carbonaceous matrix of the ore has been identified as degraded humate — humic acids derived from decaying plant debris that were introduced into the host sandstones by laterally migrating groundwater. As the humic acids migrated they began to condense or polymerize and form into gel-like substances that adhered to the host sand grains [59].

The approximate chemical composition of humate is $(C_{15}H_{16}O_8NS)_n$. [59]. The humate material resembles amorphous carbon, having lost most of its hydrogen and oxygen.The humate masses were shaped by groundwater flow, streamlining them to minimize flow resistance. As the humate masses took form, lack of circulation and the concentration of organic content increased the reducing environment in their interiors. The humate was able to capture uranyl cations by ion exchange. The adsorbed organically bound uranium was reduced and fixed within the humate masses. Within the Ambrosia Lake district, there are also abundant examples of uranium ore associated with plumes of humic material directly associated with carbonized logs or organic trash accumulations (intrinsic carbon). However, the extent of locally derived humic material is minimal in the Ambrosia Lake district; conversely, the regional scale of the humate masses in the Ambrosia Lake district makes them unique among worldwide sandstone deposits.

The uranium in the Ambrosia Lake district was probably sourced from de-vitrification of volcanic ash in overlying sediments. The uranium ore bodies are typically elongate, paralleling the original transport direction of the host sands and the shape of the humate masses.

Subtype 3: Vanadium-uranium deposits (‘saltwash type’)

‘Saltwash type’ uranium deposits are unique among sandstone uranium deposits in that either vanadium or uranium can be the dominant commercial commodity, depending on fluxuations in commodity prices. The main examples of this deposit subtype are the deposits of the Henry Basin and Uravan Mineral Belt districts, Colorado and Utah, USA. The host rocks for the vanadium-uranium deposits are continental fluvial sandstones. The host sands are reduced and contain carbonaceous plant debris similar to intrinsic carbon related deposits.

The source of the uranium for the Uravan deposits was probably de-vitrification of tuffaceous sediments overlying the host sandstone units. The source of the vanadium is more problematic. Three sources of vanadium have been proposed: 1) alteration of ilmenite and magnetite within the host sands and/or adjoining crystalline highlands; 2) diagenesis of overlying sediments; and 3) leaching from distant sedimentary and/or crystalline terrains [60].

2.2.5.3. Ore geometry and metallogenesis of tabular deposits

Regardless of which subtype they belong to, tabular uranium deposits have many characteristics in common: they typically parallel bedding; their overall shape is controlled by the shape/distribution of reductant — intrinsic or extrinsic carbon; and they are frequently elongated in the direction of host sediment transport. Tabular deposits also have similar metallogenetic histories regardless of subtype. The uranium was sourced from de-vitrification of volcanic tuff, which was either admixed in the host sands or in overlying beds, or was leached from highlands underlain by acidic volcanic or crystalline terrains. Uranium was introduced into the host sands by laterally circulating oxidized groundwater and was precipitated by reducing conditions associated with carbonaceous material.

The source of the vanadium in the vanadium-uranium deposits is more problematic. One of the more widely held hypotheses suggests that the association of vanadium and uranium resulted from mixing of two ground waters with different chemistry — one containing organic complexes and vanadium derived from alteration of ilmenite and magnetite, the other containing +6 valence uranium [61]. The uranium was reduced by +3 vanadium resulting in +4 valence uranium and +3 valence vanadium.

Individual extrinsic carbon ore bodies range between 500 m to 4 km long, 50 to 300 m wide and up to 20 m thick. Individual vanadium-uranium deposits of the Saltwash type are typically relative small, ranging from 100 to 500 m long, 10 to 50 m wide and 1 to 10 m thick.

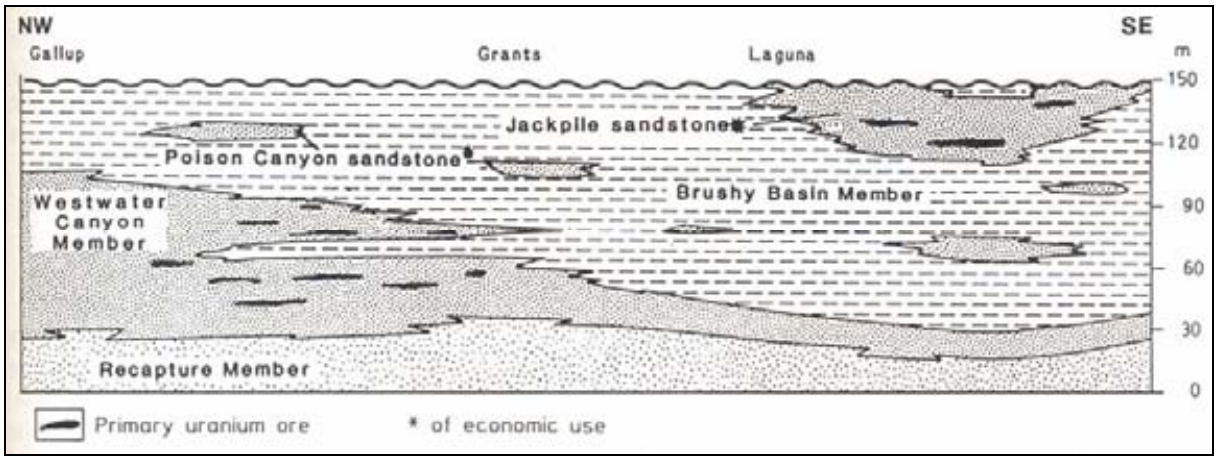

Fig. 6. Grants uranium region, schematic NW-SE stratigraphic section of the Morrison Formation along the southern part of the mineral belt [47].

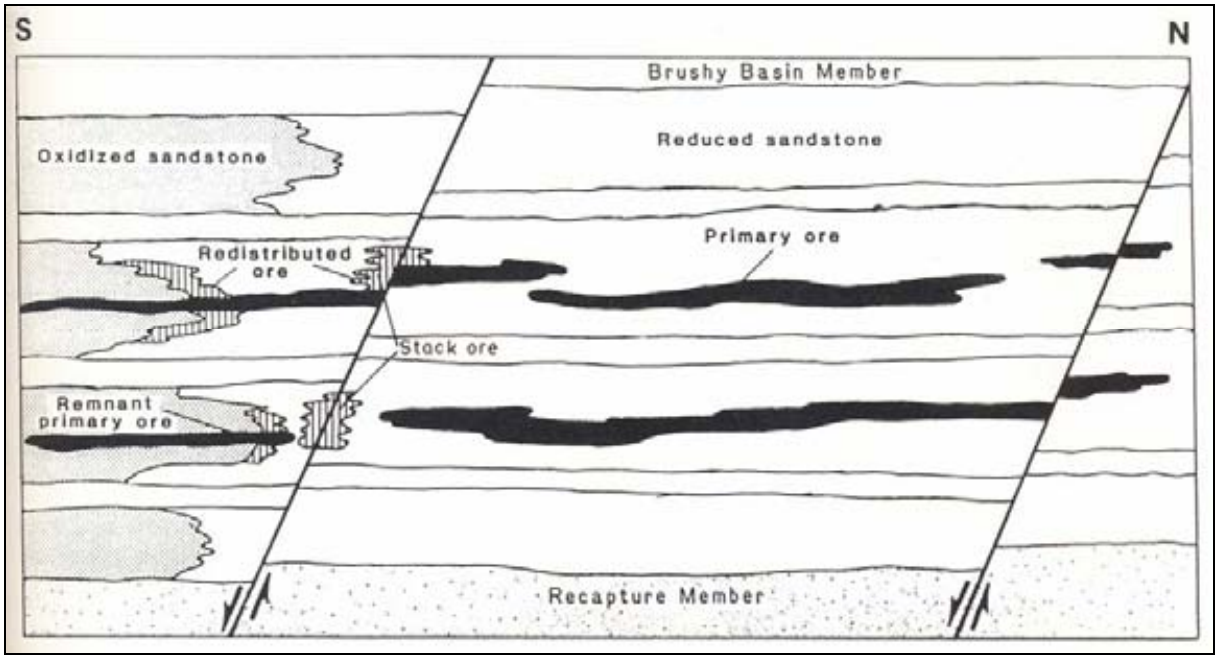

Fig. 7. Grants uranium region, diagrammatic S-N section illustrating the structural position and configuration of primary and redistributed U mineralization in Morrison Formation [47].

2.2.5.4. Uranium resources and production in sandstone deposits

The resources of individual tabular uranium deposits vary widely, ranging from clusters of relatively small deposits in the 300 to 1 500 t U range, which is typical of the Saltwash vanadium-uranium deposits to intrinsic and extrinsic carbon related deposits that exceed 50 000 t U. Original resources at Arlit and Akouta in Niger, the two largest known intrinsic carbon related deposits, exceeded 50 000 t U each, with average grades of 0.35% and 0.50%, respectively. Cumulative production through 2005 from the Akouta underground mine (mill capacity 2 300 t U) and the Arlit open pit mine (mill capacity 1500 t U), totaled approximately 98 000 t U. COGEMA is the operator of both operations in Niger.

Uranium production from extrinsic carbon related deposits in New Mexico is estimated to have totaled approximately 124 200 t U. Mt Taylor, the largest single known deposit in the Ambrosia Lake district, has resources totaling 16 150 t U, with an average grade of 0.42% U. Mining at Mt Taylor was suspended in 1990. Most of the mining in the Ambrosia Lake district was by underground methods.

2.3. Hematite Breccia Complex deposits

2.3.1. Definition

Deposits of this group occur in hematite-rich breccias and contain uranium in association with copper, gold, silver and rare earths. The main representative of this deposit type, Olympic Dam, has been assigned to a broad suite of loosely related iron oxide–copper–gold deposits ranging in age from ~2 570 to 1 000 Ma that include Prominent Hill, Ernest Henry (~1 480 Ma), Starra (~1 500 Ma), Osborne (1 540 Ma) in Australia; Candelaria (~1 100 Ma), Salobo (2 570–1 880 Ma?) and Sossego in South America, Michelin and Sue-Dianne in Canada [62]. Although some of these iron-rich deposits contain uranium in trace to minor amounts, Olympic Dam (formed at ~ 1 596 Ma) is the only known large Proterozoic iron-rich deposit that contains uranium in economic quantities. They are found in a number of different tectonic settings (rift, subduction zones, basin collapse).

2.3.2. Geologic setting of Olympic Dam Deposit, Australia

The Olympic Dam deposit occurs in a hematite-rich granite breccia complex in the Gawler Craton, South Australia. It is overlain by approximately 300m of flat-lying sedimentary rocks of the Pandurra Formation. The breccia complex is associated with a Mesoproterozoic plutonic intrusion and co-magmatic continental felsic volcanics. The intrusion, volcanics and breccia complex developed in a post-orogenic tectonic setting.

The Olympic Dam Breccia Complex (ODBC) occurs entirely within the Mesoproterozoic Roxby Downs granitic intrusion, and includes a complete gradation from granite breccias through hematite–granite breccias to hematite-rich breccias. 1) **Granite-rich breccias** vary from fractured granite, through breccias with altered granite-derived matrix, to highly altered, matrix-rich breccias with relict granite fragments. The matrix of these granite-rich breccias consists of fine granitic material together with sericite, chlorite, hematite and variable amounts of barite, fluorite, sulphides and uranium minerals. 2) The **hematite-rich breccias** have been subdivided into three general groups [63]: hematite–quartz breccias, hematite breccias, and heterolithic hematitic breccias.

Hematite–quartz breccias comprise fragments of hematite and quartz in a matrix of microgranular hematite and quartz. This breccia type is essentially devoid of copper and

uranium mineralisation. Locally this type of breccia contains abundant barite veins and vein fragments.

Hematite breccias contain clasts and matrix composed mainly of hematite. Hematite breccias are the least abundant of the three main types of hematite-rich breccias, but they host a significant proportion of the ore mineralisation. These breccias are typically steely grey to black in colour. Minor components include quartz, fluorite, barite and altered granite-derived mineral fragments.

Heterolithic hematitic breccias include intermediate members of the range from granitic to hematite breccias. This category is the most abundant of the hematite-rich breccias and it hosts most of the copper–uranium–gold–silver ore. Hematite clasts range from dark red–brown through steel grey to jet-black in colour. Other clasts include altered granite fragments, highly altered ultramafic, mafic and felsic intrusives, finely laminated hematitic siltstone and sandstone, and massive to poorly layered arkose-like rocks. These breccias also include variable proportions of sericite, chlorite, quartz, barite, siderite and fluorite.

Within the ODBC there is a broad zonal distribution of the major rock types. The central core of the complex is barren hematite–quartz breccias, with several localised diatreme structures. The hematite–quartz core is flanked to the east and west by zones of intermingled hematite-rich breccias and altered granitic breccias. These zones are approximately 1km wide and extend almost 5km in a north-west–south-east direction. Virtually all the economic copper–uranium mineralisation is hosted by hematite-rich breccias (heterolithic hematitic breccias and hematite breccias) within this broad zone. Heterolithic hematitic breccias form a large number of discrete irregular, elongate or lenticular bodies within this zone. Hematite breccias form relatively small irregular bodies either within or on the margins of larger heterolithic hematitic breccia bodies.

The zone of hematite-rich breccias is surrounded by granitic breccias extending up to 3km beyond the outer limits of the hematite-rich breccias. The outer limits of the ODBC are gradational with the Roxby Downs Granite.

Dykes and intrusive tuffs of ultramafic, mafic and felsic rock types intrude into the ODBC, particularly the eastern and southern parts of the complex. These intrusive rocks are closely associated with volcanic diatreme structures [63][64]. The diatremes contain ‘subsided subaerial tuffs and conglomerates which pass laterally and downwards into phreatomagmatic breccias’ [64].

Localised zones of volcaniclastics broaden upwards, and near the unconformity they include: surficial volcaniclastic rocks, mainly laminated ash and conglomerate (containing fragments of Gawler Range Volcanics), and reworked hydrothermal breccias. These volcaniclastic rocks appear to have accumulated in maar craters produced by phreatomagmatic eruptions [63][65].

Three key hydrothermal alteration and ore mineral assemblages are recognised in the Olymic Dam metallogenic province: CAM: calcsilicate-alkali feldspar ± magnetite ± Fe-Cu sulfides (generally minor); MB: magnetite-biotite ± Fe-Cu sulfides, and HSCC: hematite-sericite-chlorite-carbonate ± Fe-Cu sulfides ± U, REE minerals.

Ore grade Cu-U-Au mineralisation is generally associated with the HSCC assemblage, which is paragenetically later than the CAM and MB assemblages in most deposits and prospects [66].

2.3.3. Ore geometry and metallogenesis of Olympic Dam Deposit, Australia

The Olympic Dam deposit contains iron, copper, uranium, gold, silver and rare earth elements (mainly cerium and lanthanum). Only copper, uranium, gold and silver are currently being recovered. Ore grade copper–uranium–gold–silver mineralisation forms a large number of ore zones mostly within heterolithic breccias and hematite breccias. The central core and mineralised breccias are approximately 3 km by 3.5 km (in plan view) with a north-westerly arm 3 km long and 300–500 m wide.

Uranium mineralisation at Olympic Dam occurs within heterolithic hematitic breccias and hematite breccias as disseminations, microveinlets and aggregates of fine-grained pitchblende intergrown with copper sulphides. Pitchblende also forms small aggregates which are intergrown with or replace breccia material. Small amounts of coffinite and brannerite are closely associated with pitchblende. Narrow, higher-grade uranium zones often occur in the bornite–chalcocite zones, especially with hematite breccias [65]. Some high-grade zones of uranium mineralisation transgress the bornite–chalcopyrite interface.

The principal copper sulphide minerals are chalcopyrite, bornite and chalcocite. Throughout the deposit there is a well-developed zonal distribution of the principal copper sulphide minerals. Chalcopyrite (and pyrite) occur in the deeper and outer parts of the orebody whereas bornite and chalcocite occur in the upper and more central parts. The boundary between bornite–chalcocite mineralisation and chalcopyrite mineralisation (the bornite–chalcopyrite interface) is usually sharp [63]. This boundary forms a convoluted surface which generally dips downwards towards the boundary of the central hematite–quartz breccia. Grades of 4% to 6% Cu are common in the bornite–chalcocite zones, whereas the chalcopyrite zones are usually less than 3% Cu [63]. Ore textures show that much of the copper sulphide mineralisation either post-dates or is coeval with the hematite [65].

Gold and silver mineralisation occurs mostly as fine-grained disseminations either within, or closely associated with copper sulphide minerals. The mineralised hematite breccias commonly contain approximately 0.2% La and 0.3% Ce. The most abundant rare earth element minerals are bastnaesite and florencite, which are fine-grained and commonly intergrown with hematite and sericite [67].

The breccias and mineralisation at Olympic Dam were formed by hydrothermal processes. Much of the brecciation occurred in the near surface eruptive environment of a crater complex during eruptions caused by boiling and explosive interaction of water (from lake, sea or groundwater) with magma [63].

On the basis of geological evidence, [63]argue that the hydrothermal activity which formed the breccia complex occurred in the time between intrusion of the Roxby Downs Granite (~1 590 Ma) and cessation of Gawler Range Volcanic activity (~1575 Ma). The results of U–Pb isotopic age dating [68][69] together with geological evidence [63]suggest that introduction and deposition of ore metals occurred at the same time as the formation of the hematite breccias. For rocks within the breccia complex and the diatreme, U–Pb zircon dates indicate that the breccia complex formed at ~1 596 Ma, and that brecciation closely followed emplacement and cooling of the Roxby Downs Granite [69][70].

Uranium mineralisaton was formed from relatively low-tempertaure, saline and highly oxidized fluids. These fluid either mixed with hot, saline and reduced fluids carrying copper and gold [67][71] or reacted with magnetite bearing calc-silicate altered rocks enriched in copper and gold [72]

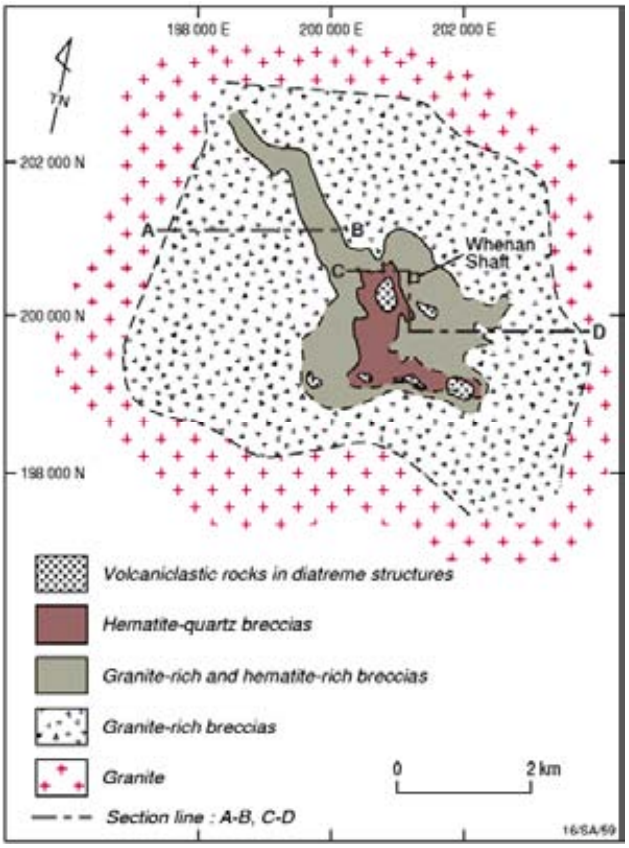

Fig. 8. Simplified geological plan of the Olympic Dam Breccia Complex [63].

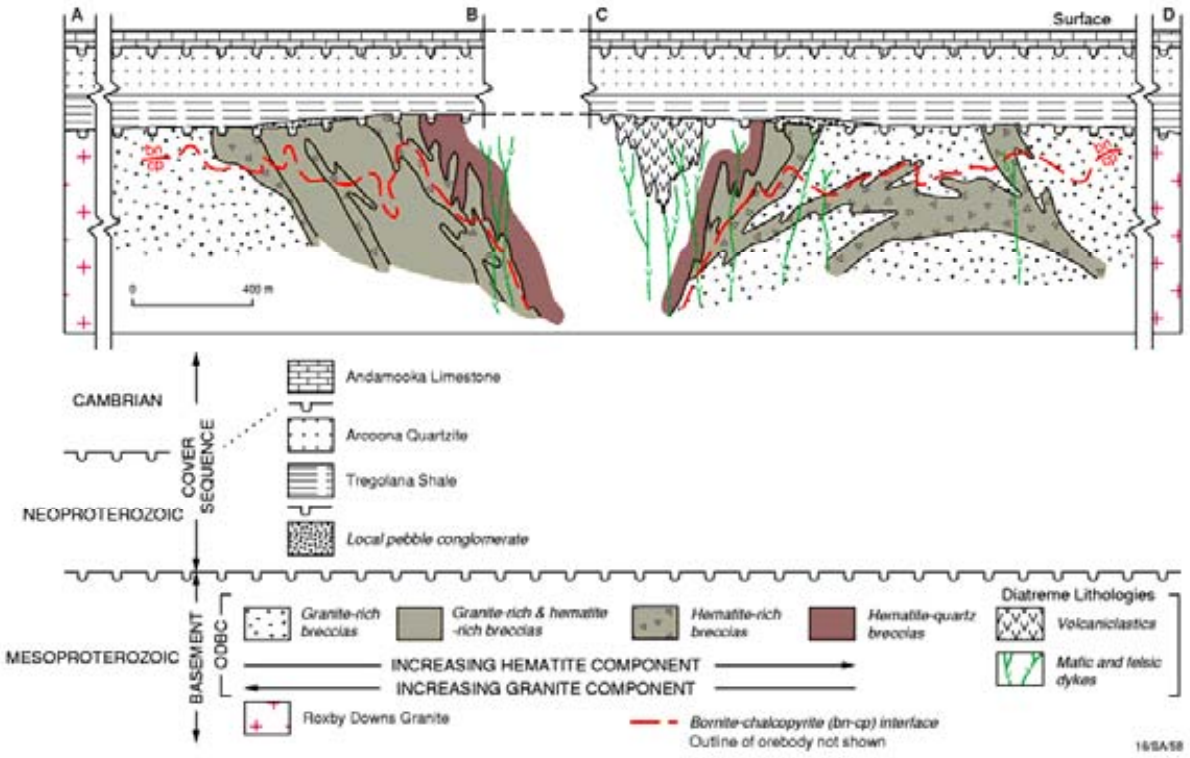

Fig. 9. Simplified geological cross-section of the Olympic Dam Breccia Complex [63]. Refer to Fig. 6 for location of section A–B.

2.3.4. Uranium resources and production in Olympic Dam deposit

The Olympic Dam copper–uranium–gold deposit has the world's largest known resource of low-cost uranium. Initial resources were more than 1.552 Mt U with average grade 0.34 kg/t U (0.034% U). Exploration drilling has discovered major extensions of the deposit to the south-east, which will increase the size of the resources. As at June 2006, the total resources at Olympic Dam were estimated to be 4430 Mt averaging 1.1% Cu, 0.4 kg/t U_3O_8, 0.5 g/t Au and 2.2 g/t Ag [73] which represents 1.503 Mt contained U. The operation is a major producer of uranium, copper, gold and silver. The deposit has significant amounts of rare earth elements (lanthanum and cerium), and has an iron content of about 26% Fe.

The Olympic Dam mine-mill complex began production in 1988. Cumulative production to December 2006 totalled 34 875 t U. BHP Billiton is the owner of the Olympic Dam operation. All production to date has been by underground mining. Consideration is, however, being given to construction of an open pit mine at Olympic Dam. The Olympic Dam processing plant has an annual capacity of 3 930 t U. Consideration is being given to expanding uranium production capacity to 12 720 t U per annum combined from underground and open cut operations by 2013.

The Michelin prospect in the Labrador Central Mineral Belt in Canada is relatively poor in Cu but contains significant resources of U [74].

2.4. Quartz-pebble conglomerate deposits

2.4.1. Definition

Quartz-pebble conglomerate uranium deposits are restricted to early Proterozoic intracratonic basins (older than 2.3–2.4 Ga) downwarped into Archean basement assemblages that include granites. Host rocks for this deposit type typically consist of trough cross-bedded, oligomictic quartz-pebble conglomerate beds with a pyritic matrix interbedded with quartzite and argillite beds. This suite of lithologies typically occurs as basal units in fluvial to deltaic braided stream systems.

Placer uraninite, the principal primary uranium phase, is locally associated with gold, REE and/or other detrital metallic oxide and sulfide minerals. The variable ore mineral assemblages are a function of different geological source provinces. Fluvial transport and accumulation of uraninite depended on the reducing character of the early, oxygen-poor earth atmosphere prior to oxyatmoversion (gradual increase in oxygen content in the earth's atmosphere). Post-depositional redistribution and mineral crystallization mainly by diagenetic processes led to the formation of modified placers composed of a suite of authigenic ore and associated minerals such as brannerite, rutile, anatase, coffinite, pyrite, and others. Two economic subtypes of quartz-pebble conglomerate uranium deposits have been identified: polymetallic (Au+U, Witwatersrand Basin, South Africa and monometallic (Blind River-Elliot Lake area, Canada).

There are two subtypes: Monometallic (or U-dominant with REE) U Deposits and Polymetallic Au with U Deposits.

Example to Monometallic type is Elliot Lake deposit (Canada) [75][76]. Detrital heavy minerals (dominated by uraninite and REE minerals) and later formed authigenic phases occur as disseminated matrix components in pyritic (5 to 20 wt.%), oligomictic quartz-pebble conglomerate horizons (termed reef), from 0.5 to >3.5 m thick. Quartzite units are interbedded with the conglomerate beds. This suite forms the basal section of a sequence, about 50 m thick, in paleovalleys scoured into Archean basement. Uraninite, uranothorite, uranothorianite, monazite, and xenotime are the prevailing detrital minerals. Authigenic minerals include U-Ti-oxide phases (brannerite), coffinite, thucholite, and locally gummite. (Resources+production: >400 000 t U, 0.05 to 0.12 % U; U was the primary commodity produced with occasional recovery of Th and some REE, particularly Y)

2.4.2. Geologic setting of Witwatersrand district, South Africa

Gold-uranium ore and associated minerals in the Witwatersrand deposits occur as detrital and redistributed matrix components in oligomictic quartz-pebble conglomerate horizons in multi-stratigraphic cycles within six large fluvial-deltaic fans on the north and west sides of the Witwatersrand Basin. The ore-hosting fluvial fans are up to 40 km long, 90 km wide across the distal fan base, and are several thousand metres thick. The source for the detrital uranium minerals is believed to have been Archean granitic basement rocks such as the unusually uranium-rich, hydrothermally altered granites identified in the hinterland of the Witwatersrand Basin.

On a regional scale, uranium mineralized reefs occur in all four stratigraphic systems that fill the Witwatersrand Basin. Large concentrations of uranium are restricted to distinct, narrow zones, however, that occupy only about 2% of the entire Upper Witwatersrand System within a belt trending parallel to the former coastline. The most productive reefs occur in the Bird Reef Stage of the Upper Witwatersrand System, which has yielded ca. 80% of past production.

2.4.3. Ore geometry and metallogenesis of Witwatersrand district, South Africa

Host rocks within the Witwatersrand Basin consist of pyritic, oligomictic quartz-pebble conglomerate beds that are commonly only a few cm to several tens of cm thick, which are interbedded with quartzite, arkose, shale and volcanics. Carbonaceous material occurs in several horizons. Detrital ore minerals include uraninite, uranothorite, native gold, and platinoid species (Os, Ir, Ru, Pt). Post depositional modification of the placers generated several generations of a multitude of authigenic ore and associated minerals including brannerite and thucholite [77][78][79][80][81][82][83][84].

On a local scale, the ore minerals tend to have been preferentially concentrated in conglomerate beds less than 30 cm thick that were deposited: 1) immediately above local intraformational disconformities or unconformities, particularly where conglomerates fill depressions or scours in underlying rocks; 2) near the base of conglomerate beds that overlie distinct, partly carbonaceous argillaceous/shaly units; and 3) in generally parallel ‘pay-streaks’ characterized by densely packed, well-rounded and well-sorted pebbles predominantly of quartz with variable amounts of uranium and other heavy minerals.

Individual deposits are several hundred to several thousands of metres long, several tens to several hundreds of metres wide and 5 to 200 cm thick.

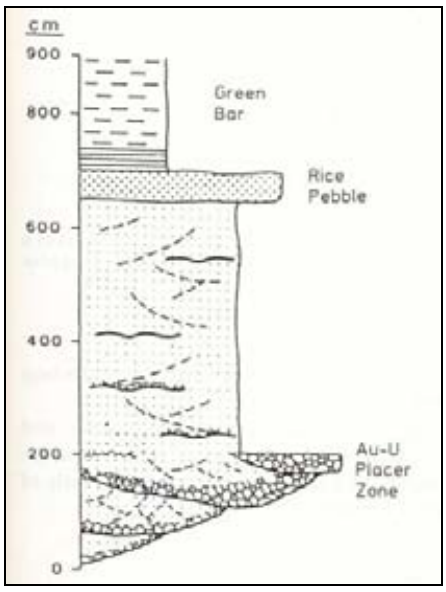

Fig. 10. Witwaterstrand basin, Carletonville Goldfield, lithologic section of the Carbon Leader Formation, Johannesburg Subgroup, showing the position of mineralized comglomerate beds [85].

2.4.4. Uranium resources and production in Witwatersrand basin

Individual deposits in the Witwatersrand Basin contain up to several tens of thousands of t U at average grades ranging from 0.01 to 0.03 % U and locally up to 0.15 % U. Resources including production are >500 000 t U. Uranium production began in the Witwatersrand Basin in 1952; cumulative production through 2004 totaled 154 050 t U. Gold values in the Witwatersrand Basin range from <1 to 25 ppm. Uranium is recovered as a by-product of gold mining operations except in a few now depleted mines, e.g. Africander/Vaal Reefs with 0.12 % U and 1.1 ppm Au.

2.5. Vein type (granite related U deposits)

2.5.1. Definition

The deposit type ‘granite related deposits’, as used in this publication copies ‘vein deposits’, a designation which referred to granite related and undifferentiated deposits. The change in terminology was instituted in an effort to better conform to the practice of relating uranium deposits to specific geologic environments and/or lithologies. Uranium-bearing veins occur in a broad range of lithologies and geologic environments including acidic intrusives (granite, etc.) volcanics, metasediments and sedimentary rocks.

Therefore, the term ‘vein deposits’ is not sufficiently specific to convey a sense of the geology of such deposits. Instead, the term conveys more description of mineral occurrence geometry without providing a geological context.

Two broad subtypes of granite related deposits have been recognized based on their spatial relationship with granitic plutons and surrounding (intruded) host rocks: (1) Endo (or intra-) granitic deposits and related contact-granitic deposits (Limousin-Vendée type); and (2) perigranitic deposits in meta-sediments (monometallic Bohemian and polymetallic Erzgebirge types) and in contact-metamorphic rocks (Iberian type).

Granite related U deposits occur as: (1) true veins and stockworks composed of ore and gangue minerals in granite, contact metamorphic rocks and in adjacent meta-sediments; and (2) disseminated mineralization in episyenite bodies (a dequartzified, micaceous, vuggy alteration product of granite) that are often gradational into veins. In the Hercynian orogenic belt of Europe, these deposits are associated with large batholiths of peraluminous leucogranite modified by late magmatic and/or autometamorphic processes. U mineralization occurs within or in close proximity to a granitic intrusion.

Known granite related U deposits range in age from Proterozoic to Tertiary. Uranium mineralization in granite related deposits generally occurs as pitchblende and/or coffinite, which are commonly accompanied by gangue and alteration minerals. Deposits with simple paragenesis contain pitchblende in association with vary amounts of pyrite/marcasite quartz, hematite, carbonate and minor base metal minerals. Complex deposits contain an important base metal sulfide stage (often with Co-Ni-As stage). In most cases, pitchblende is paragenetically early. The sizes of the vein and stockwork systems that characterize granite related deposits vary widely as to their configuration, size and complexity.

2.5.2. Geologic setting of Margnac, France and Jáchymov, Czech Republic deposits

2.5.2.1. Geologic setting — Endo- (Intra-) granitic deposits [Example Margnac deposit, La Crouzille district, France]

The Margnac deposit is located in the Limousin region, north-western Massif Central (France, N46°00'–E1°19'). It is located within St. Sylvestre leucogranite in the La Crouzille district. Geotectonically favourable leucogranites appear to have been intruded preferentially along narrow, several hundred kilometre-long regional lineaments, which are expressed as elongated gravimetric lows (Peinador Fernandes et al., 1979). Margnac and other vein U deposits in the La Crouzille district occur structurally controlled in a highly differentiated peraluminous leucogranite transected by syn-magmatic mylonite zones and dikes and stocks of variable lithologies. Principal faults within the district trend N-S, NW-SE, NNE-SSW and E-W to ESE-WNW.

The Margnac deposit occurs within coarse- to medium-grained, often porphyritic granite characterized by abundant Al-K phases, mainly Al-rich rock constituants with anomalous concentrations of lithophile elements such as U, Th, Be, Li, F, Sn, and W. Numerous dikes and stocks of peraluminous fine-grained granite with highly variable composition intruded the coarse- to medium-grained facies prior to its final consolidation. A particular group of fine-grained granites were intruded near or into regional syn-magmatic mylonite zones [7].

Pre-ore granite alteration includes albitization, muscovitization, greisenization, dequartzification/episyenitisation, chloritization and argillization. Pre-ore hydrothermal alteration resulted in localized quartz dissolution associated with both destruction of and formation of minerals, a process termed episyenitization by French geoscientists. Two types of episyenite are recognized: early-formed feldspar dominant episyenite (commonly barren of uranium) and later formed mica (muscovite) dominant episyenite (which often — but not necessarily — contain uranium deposits).

2.5.2.2. Geologic setting — perigranitic deposits [Example Jáchymov, Karlovy Vary/Eibenstock Massif, Czech Republic]

Perigranitic U deposits of the Bohemien and Erzgebirge types consist mainly of veins in meta-sediments adjacent to granitic batholiths. Two subtypes of perigranitic deposits have

been recognized: (1) monometallic (essentially pitchblende and gangue minerals) and (2) polymetallic (U, Co, Ni, Bi, Ag or other metals in economic quantities); typical examples are Příbram at the Central Bohemian Pluton and Jáchymov, Karlovy Vary/Eibenstock Pluton, Erzgebirge, respectively. Perigranitic veins can persist to depths of as much as 2 000 m.

Mineralization in the Jáchymov ore field occurs in veins hosted by metasediments intruded by the highly differentiated Karlovy Vary/Eibenstock granite batholith, which includes a younger deuterically altered leucocratic granite facies characterized by high U/Th ratios. This facies underlies and partly surrounds the Jáchymov ore field in a form akin to a half-bowl at a depth of as much as 1 000 m. A contact-metamorphic aureole up to 60 m wide surrounds the granite.

Pre-uranium host rock alteration is reflected by a variety of widespread phenomena that were overprinted by intense silicification. Uranium mineralization related alteration, however, rarely extends more than 10 cm into adjacent wall rocks. Mineralized veins are controlled by several fault systems. The veins preferentially occupy subsidiary faults; they rarely occur in major structures.

2.5.3. Ore geometry and metallogenesis of Margnac, France and Jáchymov, Czech Republic deposits

2.5.3.1. Ore geometry and metallogenesis

Two main ore environments are recognized within the granite that hosts the Margnac deposit: (1) veins cutting the granite which predominantly trend NW-SE (but also E-W in the bottom part of the deposit); and (2) disseminations in mica-episyenite. The mineralogy is very similar in both setting.

Vein-hosted mineralization at Margnac is characterized by a simple mineral association. Pitchblende is the dominant uranium mineral and is mainly accompanied by iron sulphides (pyrite, marcasite) and hematite. Other sulphides of Cu, Pb, Zn, and Mo are scarce. Gangue is present in minor amounts and consists of chalcedony, fluorite, and locally barite and calcite [86][87].

Disseminated mineralization occurs mainly in mica-episyenitic pipes, with lesser amounts occurring in brecciated leucogranite and rarely in feldspar episyenite. Mica-episyenites are commonly only mineralized when intersected by or adjacent to pitchblende veins. Pitchblende and pyrite are the first minerals to form. Pitchblende coats rock faces and penetrates into fractures and/or cleavages.

The primary ore control in the Margnac deposit is structure and secondarily lithology. Mineralized veins (active dilational fractures) commonly trend about NW-SE and to a minor degree E-W, and have steep dip. The veins measure from a few metres to several hundred metres but may extend for up to a kilometre long. Thickness of mineralized veins typically ranges from < 1 to 2 m but can range from a few centimetres up to 15m in highly cataclastic zones. The vertical extent of the vein related ore shoots varies between a few metres and >300 m.

Episyenite-hosted mineralization (vesicular, vuggy mica-episyenite bodies) can range from several tens to several hundreds of square metres in plan view, with vertical extent of between 10 and 300 m. Weathering related processes caused remobilization of original mineralization and re-deposition of uranium as ‘black products’ (neo-pitchblende, para-pitchblende, sooty

pitchblende) below the water table and in the cementation zone, and as multi-coloured hexavalent uranium minerals in the oxidized near surface zone, which commonly extends to a depth of 20 to 30 m and locally to 80m in most of the Hercynian granitic massifs in France.

Formation of granite related uranium deposits in the La Crouzille district began during the final stage of the Hercynian Orogeny, 325 to 300 m.y. ago, which was marked by general uplift associated with intensive magmatic activity in the form of granite, microgranite and lamprophyre dike emplacement. Episyenite formation is estimated at ca. 300 m.y. ago [88].

Isotope age dates of primary pitchblende are ca. 275 to 270 m.y [89]. Several metallogenetic models have been suggested for the formation of Hercynian pitchblende veins in leucogranite. The most favourite model suggests an hypogene convective hydrothermal ore genesis (mixed connate and meteoric waters started circulation in response to tectonic movements and leached uranium for primary pitchblende formation from uraninite of enclosing leucogranites) [86][87][90][91][92].

2.5.3.2. Ore geometry and metallogenesis — perigranitic deposits [Example Jáchymov, Karlovy Vary/Eibenstock Massif, Czech Republic]

The principal uranium minerals in the Jáchymov deposit are pitchblende, coffinite, and alteration products thereof. Associated economic metals include Ag, Co, Ni and Bi (which, along with U, were recovered at various stages of the long history of mining and processing). Sulfides of other metals and hematite also occur. Gangue is abundant and includes carbonates (dominantly dolomite), quartz, albite, adularia, fluorite and barite. Mineral phases occur in several generations; two principal varieties of vein forming mineral assemblages have been identified. Simple veins are composed of pitchblende, carbonate, and gauge with mylonitized rocks, often selvaged by quartz, adularia, albite, and fluorite. These veins occupy structures with lengths ranging from 150 to 400 m and widths from 3 to 25 cm, rarely 50 cm. Complex veins are composed of several generations of pitchblende, carbonate, and younger carbonate-arsenide and quartz-sulfide assemblages, intermixed with breccias and gauge. These veins occupy larger structures, with length of the veins typically exceeding 1 000 m (max. 2 200 m) and widths ranging from 10 to 60 cm.

Mineralization at Jáchymov occurs as erratically distributed ore shoots (a few m^2 to rarely 1 000 m^2 in plan view) separated by barren intervals down to a depth of about 700 m. Ore bearing veins account for less than 10% of the total rock volume. Jáchymov exhibits vertical mineral zonation, which is reflected a by predominance of arsenides and native Ag on the upper levels (down to 400 m), and arsenides and native Bi in the medium to lower levels down to about 700 m below the surface. Most of the uranium mineralization occurs in the lower level. Within and extending from 20 to 120 m away from the contact-metamorphosed zone enveloping the granite, ore structures tend to have reduced uranium mineralization except where wide veins that contain minor amounts of uranium extend down into the granite.

2.5.4. Uranium resources and production in Margnac, France and Jáchymov, Czech Republic deposits

Initial resources at Margnac totalled about 11 000 t U at an average grade of 0.25% U. Within the mineralized veins, the grade is highly variable, ranging between several hundred ppm to as much as several percent U, particularly when veins intersect or follow mafic dikes such as lamprophyres. In the mica-episyenite bodies, the average grade is generally high, exceeding 1% U over limited distances. Where mineralized veins extend into episyenite, the ore grade may range between 1 and 10% U. The Margnac ore has been treated at the Bessines mill.

Approximately 9 050 t U were produced between 1953 and 1995 when the deposit was depleted.

Individual vein systems in the Jáchymov deposit contain from a few tonnes to several hundred t U. Grades range from <0.1 % to several percent U within the same vein system. In addition to uranium, high grades of Ag, Co, and Ni occur in some vein systems. The Jáchymov ore field reportedly yielded almost 10 000 t U at grades from 0.1 to 1 % U.

2.6. Intrusive deposits

2.6.1. Definition

Uranium deposits in intrusive or anatectic rocks consist of disseminated primary, non-refractory uranium minerals dominantly uraninite, uranothorianite and/or uranothorite [93][94]. These deposits are generally low-grade (20–500 ppm), but may contain substantial resources (more than 100 kt U). Five subtypes of intrusive deposits are based on host rock petrology [43][95].

Alaskite type: disseminated uranium occurs in medium- to very coarse-grained alaskite bodies (leucocratic, quartz and alkali feldspar-rich granites) that are discordant to concordant with surrounding folded and highly metamorphosed and migmatized sedimentary rocks [96][97][98][99][100]. The alaskite bodies range in size from small lenses and tabular dikes to large stocks and domes several hundred metres across. No alteration is associated with the uranium mineralization. The main example is Rössing, in Namibia. Other examples include Goanikontes, Ida Dome, Valencia/Trekkopje and SJ Claims (Namibia) and Johan Beetz (Canada). A subtype of the alaskite type deposit, which could also be classified as metasomatic deposits are the ‘Generation four’ type (Upper Proterozoic, 700 to 500 m.y. bp), which is restricted to orogenic belts. This subtype is found in the Damara — Katanga Orogen (part of the Pan-African Orogeny) in Shaba, Democratic Republic of the Congo (Zaire), in Namibia, and in the Brazilian mobile belt (Brazil).

Granite, monzonite type (Bingham Canyon, Utah, USA): very low-grade uranium disseminations occur in highly differentiated granitic to (cupriferous) quartz-monzonitic (copper porphyries) complexes. Because of their very low U content, uranium is recovered only as a by-product of copper heap leaching. Other examples are Twin Buttes (Arizona, USA) and Yerington (Nevada, USA).

Peralkaline syenite type (Kvanefjeld, Greenland): low-grade uranium disseminations occur in peralkaline syenitic domes or stocks. Uranium phases are commonly of a more refractory nature [101][102]. Other examples are Motzfeld (Greenland), Pilanesberg (South Africa), Lolodorf (Cameroon) and Catalao (Brazil).

Carbonatite type (Phalaborwa, South Africa): disseminated uranothorianite occurs in cupriferous carbonatite complexes. Up until 2002, uranium was recovered as a by-product from copper production [103], [104], [105]. Other typical examples are Araxa (Brazil), Sokli (Finland) and Sevathur (India).

Pegmatite type (Bancroft area, Ontario, Canada): uraninite and other uranium-thorium minerals occur in un-zoned granitic and syenitic pegmatitic dykes (siliceous and mafic tendency with aegirine and augite) in sedimentary and igneous rocks, metamorphosed to the amphibolite facies. Deformation and metasomatism commonly follow metamorphism. Hematite is a characteristic alteration product [106]. Pegmatite deposits may average up to

0.08 % U but resources are generally low (a few t U to a few hundred t U). Another example is the Campbell Island Mine (Ontario, Canada).

2.6.2. Geological setting of Rössing deposit, Namibia

The geodynamic settings of intrusive deposits types correspond to syn- to post-orogenic intrusions within intra-cratonic mobile belts. They are commonly in sharp contact with the surrounding rocks and have narrow contact metamorphic aureoles. Uranium-rich alaskite, quartz-monzonite, granite and associated pegmatites are generally considered the product of granitization of uraniferous crustal material (partial melting of sedimentary and volcanic rocks). The Rössing deposit is attributed more to ultrametamorphic-anatectic processes whereas, for granite-monzonite deposit types, magmatic differentiation with uranium retained in late-stage phases is favoured. The content of U, Th, REE, and other metals in the various granitic facies is considered to be a function of their original abundance in the precursor meta-sediments.

A prerequisite for elemental retainment is a dry granitization process in a closed system. These late leucocratic peraluminous Si, Al and alkali-rich facies correspond to highly differentiated granitic complexes. Uranium content is reduced to levels below commercial interest in alaskite bodies when melting is important. Large acid magma volumes such as the typical leucogranites from the French Limousin district are only moderately enriched in uranium (15–30 ppm). Further hydrothermal and structural processes (vesicular episyenite and veins) are necessary in order to create economic ores. Where melting is less intense, however, higher U concentrations are obtained. This condition though necessary, is not sufficient by itself to generate economically attractive disseminated ore bodies in alaskites because of the typically small size of individual alaskite occurrences. Several alaskite occurrences in close proximity are needed to form significant uranium tonnage. For example, large mineralized alaskite bodies in metamorphosed series like those from Mont Laurier or Johan Beetz (Greenville province, Quebec) or those from Charlebois (North Athabasca basin, Canada) have never been mined because they are too disseminated (too high operating costs).

The Rössing deposit is located in the Namib desert, approximately 65 km NE of Swakopmund in western central Namibia. It lies within the 400 to 500 km-wide Upper Proterozoic Damara orogenic belt, which extends from the Atlantic Ocean north-easterly across south-western Africa before submerging beneath the post-Palaeozoic Kalahari Basin. Farther north, it eventually links up with the Lufilian belt of similar age in Zambia-Democratic Republic of the Congo.

Rössing is located on the south-western flank of a regional oval NE-SW trending dome, about 2 km from the contact of a gneissic Proterozoic basement and meta-sediments (schist and graphite- and sulphide-rich marble originated from continental plate-form sediments of the Damara Supergroup deposited between 800 and 1 000 m.y.). There are many alaskitic bodies in the Rössing area. Many others are found in the middle and western parts of the Damara hills which emerged from the northern ‘Congo’ craton merging into the southern ‘Kalahari’ craton, during Pan-African time.

The main constituents of the Rössing host rocks are quartz, microcline, microcline-perthite (sometimes with more than 20% plagioclase), biotite (with local enrichment) and fluorite (as an accessory). Textures are mainly of the pegmatite-type with occurrences of aplite, granite and graphic fabrics. Syntectonic medium-to very coarse-grained alaskites correspond to K-dominant alkali-feldspar granites as defined by [107].

2.6.3. Ore geometry and metallogenesis of Rössing deposit, Namibia

Individual ore shoots in the Rössing area may be several tens of meters to several hundred meters (ca. 700 m) long (trending slightly NE-SW) and several tens to 600 m wide. Mineable ore has been proven to a depth of approximately 300 m (lowest level of the open pit) but drilling has intersected ore grades to a depth of at least 700 m.

The ore minerals at Rössing include primary, variably thoriferous uraninite (few microns to 0.3 mm-sized inclusions in quartz, feldspars and biotite, in intergranular spaces and in veinlets), uranothorianite, uranothorite, betafite, and hexavalent uranium minerals, predominantly yellowish beta-uranophane. Mineralogical distribution of uranium in crude ore is approximately 55% in uraninite, 5% in betafite, and 40% in hexavalent U minerals. Associated minerals include monazite, zircon, apatite, titanite, occasionally pyrite, chalcopyrite, bornite, molybdenite, arsenopyrite, magnetite, hematite, ilmenite, and fluorite. Th/U ratios in the ore are generally below 1 up to 3.

Several metallogenetic models for the origin and evolution of the uraniferous alaskites have been put forward. These models include anatexis of metasediments or partial melting of a uranium-rich source, etc. But because the position, size, and uranium content of the alaskitic intrusions are spatially close to the lower marble band in the Swakop Group, many authors consider that the marble band played a major role as an ore control. The age of both the mineralization and the host alaskite is Cambrian.

2.6.4. Uranium resources and production in Rössing deposit, Namibia

Initial resources at Rössing in the US$ 40/kg U RAR category are estimated at approximately 139 960 t U. Cumulative production since mining began in 1991 has totalled 81 775 t U, all of which has been recovered by open pit mining [6]. The average ore grade at Rössing is 0.03% U, but there are strong grade variations with local grades of up to 1% U. The Rössing mine is the largest uranium open-pit mining operation in the world.

2.7. Caldera related volcanic deposits

2.7.1. Definition

Caldera related volcanic deposits are located within or in close proximity to volcanic calderas that are filled by complex assemblages of mafic to felsic volcanic rocks and intercalated clastic sediments. Mineralization in volcanic deposits is largely structure bound, occurring in intrusive veins or stockworks in volcanic intrusions, diatremes, and flow or bedded pyroclastic units. Smaller ore accumulations occur in strata bound mineralized zones as disseminations and impregnations in permeable and/or reactive flows, flow breccias, tuffs and intercalated pyroclastic and clastic sediments. Uranium mineralization also extends into underlying and adjoining basement rock, where it is concentrated in fractured granite and metamorphic rocks. The main uranium minerals, pitchblende and coffinite, are commonly associated with molybdenum-sulfides and pyrite. Other metallic minerals/elements include minor traces of As, Bi, Hg, Li, Pb, Sb, Sn and W. Associated gangue minerals include fluorite, quartz, carbonates, barite and jarosite.

The uranium deposits of the Streltsovsk district, Russian Federation and the Dornot complex, Mongolia are the most important examples of caldera related volcanic deposits. Other examples include the Gan-Hang volcanic belt, China, Michelin deposit, Labrador, Canada, Nopal/Peña Blanca, Mexico and McDermitt, USA.

2.7.2. Geologic setting of Streltsovskoe deposit, Russian Federation

The Streltsovskoe deposit, the largest deposit in the Streltsovsk district, Russian Federation, lies within a 4 km long × 2.5 km wide structural zone in the eastern part of Streltsovsk caldera, an Upper Jurassic-Lower Cretaceous volcanic-sedimentary complex within the Mongolian-Argunian intracontinental volcanic belt, which developed during Mesozoic tectonic-magmatic activation. Basement rocks in the Streltsovsk district consist of Proterozoic metamorphics (gneiss, schist and dolomitic marble) intruded by Paleozoic leucogranite.

The volcano-sedimentary section in the Streltsovsk district consists of a 1 000 m thick complex comprised of the Upper Jurassic Priargun suite and the Lower Cretaceous Turgin suite, both of which dip to the south-west at 5 to 10. The Priargun suite consists of (from bottom to top): 1) coarse grained basal conglomerate (50 m thick) affected by paleo-weathering, with gravel, sandstone and siltstone seams and lenses; 2) lower basal sheet containing lava horizons and conglomerate lenses, the thickness of which is determined by basement relief but reaching 400 m in thickness; 3) lower trachydacite sheet (from 60 to 350 m) consisting of trachydacite massive and fluidal(?) varieties, tuff, lava and ignimbrite horizons; 4) middle basalt horizon (10 to 240 m thick) consisting of massive basaltic lava, lava-breccia, and conglomerate, which occurs only in the southern part of deposit; 5) upper trachydacite sheet (to 75 m thick); and 6) upper basalt sheet (up to 180 m thick) composed of lava and lava breccia varieties. The Turgin suite consists of: 1) 40 to 90 m thick red conglomerate horizons; 2) 30 to 140 m thick plagioclase trachybasalt horizon; 3) felsite sheet (up to 260 m thick) consisting of individual quartz porphyry units (up to 10 m thick); 4) and fluidal felsite (1 to 15 m thick).

The Streltsovskoe deposit is located at the intersection of the regional, north-west trending Argun fault zone with the north-south trending Central fault zone. Intensive tectonic activity created structural blocks within the caldera. Amplitudes of vertical displacement reach tens of meters.

2.7.3. Ore geometry and metallogenesis of Streltsovskoe deposit, Russian Federation

Uranium mineralization in the Streltsovskoe deposit occurs in five isolated zones (Central, Western, Eastern, Glubinny, Golub), the locations of which are determined by intersecting tectonic zones.

Uranium mineralization within the Streltsovskoe deposit extends over a vertical interval of 480m. About 80% of the deposit's resources occur between 300 and 550 m below the surface. The vertical range of mineralization within individual ore bodies varies from 30 to 90 m and is determined by thickness of individual horizons transsected by fault zones. The shapes of individual ore bodies vary and include veins, stockworks and flat and tabular bodies. Only one steeply dipping vein-hosted ore body within the Streltsovsk fault zone crops out at the surface.

A significant percentage of Streltsovskoe deposit reserves are contained in numerous vein and stockwork ore bodies that lie within the 750 m long × 6 m thick N1 fault zone of the Central sector. Ore grades within this zone average 0.33% U. While all rocks cut by the fault host mineralization, 77% of resources occur in stockwork ore bodies in trachydacite and 16% in basalt. The remaining reserves occur in quartz porphyry and conglomerate. High-grade ore occurs mainly in basalts and associated with large faults complicated by 'feather' jointing.

The principal uranium mineral throughout the Streltsovsk district is pitchblende. Coffinite is of minor importance as are uranium titanites. The main molybdenum mineral is jordisite, which is altered to ilseminite in oxidized zones. Host rock alteration is manifested by hydromicazation, albitization, carbonatization, silicification and pyritization. Isotope dating of pitchblende yields a formation age of 130 m.y.

Felsic volcanics (particularly rhyolitic glassy phases) within Streltsovsk caldera are considered the most favourable source rocks for of the uranium ore. Volcanics are also thought to be the source of the molybdenum. Metal mobilization and transport are attributed to hydrothermal solutions. The first hydrothermal processes are assumed to have been contemporaneous with the final volcanic activity in the caldera. Multiple telescoping attests to repeated remobilization processes. Pathways for solutions and spaces for ore accumulation were provided by permeable faults and pyroclastic and clastic sediments.

Reducing conditions required for reduction and concentration of uranium may have existed at sites where the host volcanics contained abundant sulfides and/or plant remains in intercalated sediments. An additional reductant may have been ferric iron in mafic minerals found in mafic and intermediate volcanics. Physico-chemical conditions, such as effervescence with fractionation of fluid components may have likewise contributed to uranium precipitation.

2.7.4. Uranium resources and production in Streltsovskoe deposit, Russian Federation

Original resources within the Streltsovsk district totaled approximately 240 000 t U. The more than 60 000 t U of which were contained in the Streltsovskoe deposit. Since the discovery of the district in 1963, nine deposits have been brought into production: seven by underground mines and two by open pits. Open pit mining was conducted at Tulukuyevskoye (>35 000 t U) and at Krasny Kamen (<5 000 t U). Both deposits are depleted. Underground mining has taken place at Streltsovskoye (>60 000 t U), Antei (>30 000 t U) and Oktyabrskoe(>15 000 t U), and at the Luchistoye Martovskoye, Vesennee, Yubileinoye and Novogodneye deposits, all of which had original resources ranging between 5 000 and 15 000 t U. In situ ore grades of these deposits commonly range from 0.1 to 0.3 % U, with ore grades in separate ore bodies as high as 1% U.

Processing of the ore is carried out in the hydrometallurgical plant has a nominal capacity of about 3 500 t U/year.

2.8. Metasomatic deposits

2.8.1. Definition

Uranium deposits of this type are related to alkaline metasomatites of sodium or potassium series. The metasomatites are developed in ancient shields and median masses, where they form stockworks controlled by long-lived ancient faults. Sodium metasomatites are predominantly albite in composition, usually with minor carbonate and alkaline amphiboles and pyroxenes — albitites and eisites. Potassium metasomatites are essentially potassium feldspar rocks with minor carbonate (elkonites). Some geologists consider them as gumbeites, which is incorrect, because quartz is unstable in the rearmost zone of these metasomatites.

The largest uranium deposits in sodium metasomatites occur in the Kirovograd Ore District, Ukraine. Other regions with similar deposits are Beaverlodge (Canada), Itatiaia (Brazil), Jaduguda (India), and Kokchetav Massif (Kazakhstan). Uranium deposits in potassium metasomatites are known in the Elkon Horst, the southern Yakutia (Russian Federation).

2.8.2. Uranium deposits in albitites

2.8.2.1. Geologic setting of Kirovograd uranium district, Ukraine

The area is underlain by ancient granitized Archean and Paleoproterozoic crystalline rocks of amphibolite facies. As a result of the intense early Proterozoic granitization, the gneisses alternate with migmatites and granites.

The uranium deposits occur in the central part of a submeridional mobile zone that is located between a granite dome to the east and to the west. The mobile zone was formed in early Proterozoic and repeatedly reactivated over a long time. Migmatites and blastomylonites were formed first and later overprinted by mylonitic and cataclasitic sutures tens of meters in thickness.

Albitites are widespread in the tectonic zones and along feather faults. They form bodies tens to hundreds of meters in lateral and vertical extension within structural zones that can be traced for tens of kilometers on the surface and to depths of 2.5–3 km. Uranium mineralization is controlled by these albitites.

There are also iron-uranium deposits in the eastern part of the area. These ore deposits are genetically related to carbonate-alkaline metasomatism of ferruginous quartzites. The deposits are confined to deep faults which terminates forementioned mobile zone to the east. Characteristics of these uranium ores are their development after magnetite ores and sub-concordance of their bodies with host rocks strongly altered by alkaline and carbonate metasomatism.

The albitites are dated at 1.8–1.9 Ga; the uranium ores, at 1.6–1.7 Ga.

2.8.2.2. Ore geometry and metallogenesis of Kirovograd uranium district, Ukraine

The uranium ore deposits are related to albite-aegirine-riebeckite and albite-chlorite-epidote metasomatites. The former represent altered cataclasites with impregnated uraninite, malacon, apatite, and sphene. The latter are less spread. They contain chlorite, epidote, and calcite instead of amphibole and aegirine, and their ore minerals are pitchblende, uranium-containing leucoxene, coffinite, and a colloform-metacolloidal uranium-titanium silicate. The uranium minerals are located in zones of post-albitization cataclasis, in inner parts of the metasomatic aureole.

The albitite bodies have a zoned structure. This zoning is found as sequential replacement of plagioclase, quartz, and biotite (metamorphic minerals) by albite. Riebeckite, aegirine, chlorite, and epidote were formed in intermediate zones. The albitization is better developed in granites than in gneisses and crystalline schists, which is explained by a higher permeability of the former.

The sodium metasomatites also show a vertical zoning. Albite-aegirine-riebeckite metasomatites are updip substituted by albite-chlorite-epidote metasomatites, and silica is redeposited as veinlets and silicification zones in the upper part of metasomatic columns.

Although all uranium deposits of this area are confined to albitite zones, not all albitites are uranium-bearing. Hence, presence of these metasomatites is not the only prerequisite for uranium ore deposition. Other important ore controlling factors are large permeable

cataclasitic zones, favorable combinations of folds and faults (flexures and junctions), and their mechanical heterogeneity (their difference in the permeability).

The ore bodies have a complicated shape and can be outlined only by sampling. Flattened lenses and column-like stockworks are predominant among them. These bodies form echelon-like series within mineralized albitites. The downdip size of separate bodies is 2–3 times more than their strike length. Their thickness varies from few to 50 m and usually is 10–15 m. Uranium content varies from 0.07 to 0.2 %, with the average of about 0.1 %. The ore mineralization is of the veinlet-disseminated type.

The ores have a rather rich mineral composition including almost all uranium minerals. Predominant among them are davidite, nenadkevite, pitchblende, and coffinite. These are found as fine impregnation (hundredths mm) in assemblage with chlorite, carbonate, and hematite. In addition, uraninite and pitchblende form veinlets with carbonate and hematite.

Sodium metasomatites at iron-uranium deposits are developed after quartz-biotite, amphibole-quartz, and ferruginous hornfelses. They consist of albite, riebeckite, rhodusite, and carbonate, proportion of which depends on the composition of replaced rock. For example, aegirine is more abundant than albite in ferruginous hornfelses and schists, cummingtonite schists are replaced by Mg-Fe carbonates, and quartz interbeds in iron ores are substituted by dolomite. In its turn, the mineralogical composition of uranium ores is a function of the metasomatite composition. Albitites are impregnated with uranium-containing apatite, malacon, and nenadkevite, whereas uraninite is predominant in essentially carbonate metasomatites.

The described uranium deposits were probably formed by deeply generated fluids having caused the Proterozoic tectonic-magmatic rejuvenation. This is confirmed by similar ages of the uranium-bearing albitites, cataclasites, and mylonites (in fault zones), which are also similar to ages of flat tectonic depressions, filled with lower Proterozoic volcanic-sedimentary deposits, and to ages of hypabyssal rapakivi, picritic dykes, and gabbro-diabases. All these magmatic and tectonic products are related to the Proterozoic tectonic-magmatic rejuvenation.

2.8.2.3. Uranium resources and production in Kirovograd uranium district, Ukraine

At present time, Ukrainian uranium resources and reserves are confident data. According to the Red Book 2003, uranium reserves RAR&EAR-I of metasomatic (albitite) deposits are 13 250 t, with mining cost of <US$ 40/kg U, and 42 500 t, with mining cost of <US$ 80/kg U. Uranium resources EARII&SP of the metasomatic deposits are estimated at 133 500 t.

2.8.3. Uranium deposits in potassium metasomatites (elkonites)

2.8.3.1. Geologic setting of Elkon Horst, Russian Federation

The core of the Aldan Shield consists of an Archean-Lower Proterozoic crystalline basement which is exposed in several uplifts including the Au and U bearing Elkon horst. As much as 700 m thick, subhorizontally bedded Vendian-Lower Cambrian limestone and dolomite cover the basement to the north while Lower Jurassic coal bearing continental deposits and pyroclastics fill grabens.

The Elkon horst is a NW-SE elongated, 60 km long and up to 40 km wide uplift in the southern part of the Aldan Shield. Principal lithologies are Archean granulite, amphibolite, gneiss, schist, quartzite and marble. Intense Late Archean-Early Proterozoic granitization

generated leucocratic biotite-microcline granite and migmatite. Only remnants of gneiss and schist are found in the granitized rocks.

Small laccolithlike bodies, stocks, sills and dikes of alkaline and calc-alkaline rocks of the Aldan volcano-plutonic complex were intruded into the aforementioned units particularly within the western part of the Elkon horst during three periods in the Jurassic and Cretaceous.

Faulting affected repeatedly the region, particularly during the Early Proterozoic and Mesozoic and resulted in three prominent fault sets: *ancient*, NW-SE and NW-SE trending faults formed during the Early Proterozoic, ancient faults *reactivated* during the Mesozoic, and *neotectonic* NW-SE and submeridional oriented faults of Mesozoic age. The latter caused block movements and resulted in horst and graben structures.

Several kinds of alteration include from oldest to youngest:

- Post-granitization *potassium-siliceous* metasomatism developed in zonal distribution in the Early Proterozoic granitoids. These metasomatites often contain locally concentrations of disseminated uraninite, cleveite, bröggerite, orthite, thorite, malacon and sphene.

- Multistage Mesozoic, pre-uranium alteration processes generated various mineral assemblages which were superimposed on each other in ore bearing zones. All of them were controlled by Mesozoic neotectonic and reactivated ancient fault zones.

- Oldest is an *albite-sericite-chlorite* facies that zonally overprinted former rock constituents and formed micro-veinlets for up to a few tens of meters from faults.

- A younger and the most prominent pre-uranium alteration assemblage consists of *pyrite-carbonate-potassium feldspar* with dispersed gold, is of tan, greenish-brown or dark grey color and surrounds all ore-bearing structures. This facies overprinted particularly the albite-sericite-chlorite aureoles, and formed micro-veinlets for several hundreds of meters along and downdip of reactivated ancient faults and commonly persists for 6 to 10 m and locally up to 20 m into the wall rocks.

- In the *outer zone*, mafic minerals are completely substituted by dolomite, ankerite, pyrite and marcasite while plagioclase is replaced by sericite and carbonate, magnetite by pyrite, and quartz by calcite. Proportions of carbonate and pyrite are highly variable. Carbonate can amount to 50% as found in the Yuzhnaya zone. Pyrite contains dispersed gold with values of up to 4.5 g/t Au in pyrite concentrate.

- The *inner halo* is characterized besides the above mentioned replacements by a markedly increased K-feldspar content. In result, a dense, dark grey, fine-grained alteration facies evolved composed of 40–75% K-feldspar, 35–50% carbonate, 5–15% pyrite and minor sericite, sphene and apatite. Pyrite concentrates carry as much as 80 g/t of gold.

- Late and post-ore alteration includes carbonatization, silicification, fluoritization, sulfidization, and oxidation. The post-ore emplacement of Mesozoic alkaline intrusions caused fenitization of earlier facies.

- U/Pb isotope dating yield an age of 135 to 130 m.y. for primary brannerite which correlates with the emplacement of the Early Cretaceous intrusions.

2.8.3.2. Ore geometry and metallogenesis of Elkon Horst deposits, Russian Federation

The only primary uranium mineral is a medium to low temperature U-Ti-phase defined as *brannerite*. It commonly occurs in massive, colloform aggregates that encloses small fragments of host rocks, and more rarely as up to 0.08 mm high prismatic crystals. Associated minerals are pyrite and marcasite. They largely predate brannerite. Only a small fraction of them is contemporaneous with brannerite.

Alteration products of brannerite include secondary brannerite, more or less uraniferous TiO_2-phases, U-oxides and, in oxidized intervals, hexavalent U minerals which formed after renewed cataclastic interludes.

Gold is a common constituent of most of the ores but it tends to be not syngenetically related to U. Au mineralization predates and postdates the brannerite formation.

Aggregates of subhedral to rounded uraninite and Ti-oxide phases with or without brannerite occur in the vicinity of Mesozoic magmatic intrusions in the NW segment of the Elkon district. Their generation is attributed to the destruction of brannerite by thermal metamorphism.

A final generation of endogenic mineralization consists of veinlets of dark quartz, dolomite, calcite, fluorite, pyrite, marcasite, and minor baryte, chalcopyrite, sphalerite and galena.

Oxidation of primary ore persists to a depth of some tens of meters below the current surface in most deposits of the Elkon district but may extend to 600 m deep in some ore bearing structures. Characteristic minerals include Fe- and Mn-hydroxides, carbonates, clay minerals, opal, chrysocolla, malachite, azurite, jarosite, various products of decomposed brannerite, uranyl-phosphates, and U adsorbed by Fe-hydroxides and other minerals.

Texture of uraniferous mineralization is dominated by fine- to microclastic breccia and veinlet-breccia. Veinlet and dissemination textures are less frequent.

Coffinite typically occurs in disseminated U mineralization as replacement of pyritized mafic minerals and coatings of Fe-sulfides contained in fissures and voids.

Three uranium ore varieties are distinguish: gold-brannerite, gold-uraninite and brannerite-silver-gold mineralization, and, additionally, three gold ore types which may or may not contain minor uranium. Principal ore zones and deposits of these types are and described further below.

Gold-brannerite mineralization is typical for deposits along the Yuzhnaya, Severnoye, Sokhsolookhsk, Pologaya, Vesennyaya and Agdinsk zones. Ore control is by reactivated ancient and neotectonic NW-SE oriented and steeply SW dipping faults of Mesozoic age and by pyrite-carbonate-potassium feldspar altered rocks. Mineralized zones are traced by blastomylonites imposed on Early Proterozoic metadiorite dikes. Country rocks are Archean-Early Proterozoic ultrametamorphic lithologies.

Gold-brannerite mineralization is of veinlet-disseminated-type and commonly located within gold bearing pyrite-carbonate-potassium feldspar altered zones. Brannerite is the only primary U mineral. Appreciable amounts of gold and silver are bound in pyrite of two, pre-brannerite generations of the pyrite-carbonate-potassium feldspar alteration.

Gold-uraninite mineralization is known from the Nadezhda and Interesnaya zones in the northwestern sector of the Elkon district where Mesozoic stocks and dikes are abundant. Ore control and geological setting are similar to those of the gold-brannerite deposits except that the uraninite is restricted to zones of thermal metamorphism. In contrast to gold-brannerite assemblage, the gold-uraninite mineralization has higher uranium grades. Early pyrite tends to be the essential host of native gold. Concentrates of the early pyrite have gold contents from 9.1 to 24.5 ppm.

Brannerite-silver-gold mineralization is reported from the Fedorov, Marsovaya, Mramornaya and Zvezdnaya zones in the southwestern Elkon district. Ore control and geological setting are similar to those of the gold-brannerite deposits. Ore lodes consist of gold-bearing metasomatic rocks intersected by thin brannerite stringers and a younger generation of small quartz and carbonate veinlets with pyrite, native gold, native silver, and acanthite.

General Shape and Dimensions of Elkon Horst Deposits, Russian Federation

Location, shape, dimensions and internal structure of uranium-gold and uranium-gold-silver deposits are primarily controlled by NW-SE oriented and steeply SW dipping faults.

Deposits consist of intermittently distributed ore bodies which are separated by barren or erratically mineralized ground composed of variably mineralized fractures, joints and disseminations, the distribution, intensity and dimensions of which are a function of the brecciation degree of the host rock.

Ore lodes have a veinlike or columnar configuration and are usually 0.2 to 5 m wide in neotectonic Mesozoic faults but achieve a width of up to 10 m in rejuvenated Proterozoic faults. Lodes have an internal stockwork structure composed of closely spaced brannerite stringers and impregnations that group to en echelon arranged, linear, 500 to 700 m long and 0.5 to more than 10 m wide ore bodies. Some ore zones encompass several of such ore bodies. Ore shoots within these ore bodies carry also gold and locally molybdenum.

Ore bodies are rarely exposed on surface. Upper limit of most ore bodies is at a depth below 200 m. Ore was drill intercepted to a depth of 2 000 m but there is no depth related change in ore mineralogy over the whole vertical interval suggesting that mineralization probably continues into greater depth.

Brannerite-gold ore has uranium contents ranging from 0.02% to 0.2% U and more, and average about 0.1–0.15% U. Gold tenors average 1 to 2 g/t, silver 8 to 15 g/t. Molybdenum grades vary between 0.01 and 0.1 %. *Uraninite-gold ore* averages 0.5 to 1 g/t Au, 10–20 g/t Ag and has U contents exceeding that of the brannerite-gold ore. *Brannerite-gold-silver ore* has average tenors of 3 to 10 g/t Au and 15 to 200 g/t Ag but locally the Au and Ag grades can be substantially higher. U grades are between 0.02 and 0.2% but can exceed 0.5% U. The carbonate content of ore varies between 1.5% CO_2 in silicified ore and 10% CO_2 in other ore types, and the sulfidic sulfur content between 1 and 4% but can be up to 20% S and more.

The ore forming process started with the gold-bearing pyrite-carbonate-orthoclase alteration event with most of the gold contained in pyrite. Subsequently uranium was introduced into the previously altered rocks by hydrothermal fluids. Both processes occurred during the Mesozoic tectono-magmatic activation of the Aldan Shield. Uranium was deposited as brannerite under medium to low temperature conditions at medium to shallow depth and formed structurally controlled deposits in rejuvenated ancient and neotectonic Mesozoic fault

zones. Due to the association of deposits and intrusions in space and time, the author suggests that the hydrothermal process was initiated by the Mesozoic magmatic activity. Uranium probably derived from the Archean granitized rocks which have an elevated uranium content. Uranium dissolution resulted from the interaction of ascending medium temperature, sulfide-carbonate bearing solutions with granitized rocks. Posterior, the Au-Ag mineralization with native gold and silver minerals developed in some of the formerly generated U-Au zones in areas with Mesozoic intrusions as exemplified by the Fedorov zone.

It is noteworthy that there is no vertical zoning in the uranium-bearing zones of the Elkon district except for extensive quartz accumulation in the upper parts of the deposits. Mineralogical and chemical composition of ores are rather uniform over the drill intercepted interval, in the Yuzhnaya zone down to about 2 000 m, which indicates relative stable conditions of ore deposition presumably due to an homogenous environment.

Thermobarometric studies indicate pronounced variations of temperatures during the entire metallogenetic evolution of the Elkon ores and its individual stages. Successive mineral stages started constantly with higher temperatures than those at the end of the previous stage suggesting a multiphase influx of ore-forming fluids.

All post-brannerite processes only altered the original brannerite and redistributed uranium to form coffinite but they did not furnish new uranium.

2.8.3.3. Uranium resources and production

Total resources of the Elkon district are estimated in excess of 200 000 mt U attributed generally to the US$ 80–130/kg U category. Ore grades average 0.1–0.15% U while gold values range from less than 1 ppm to several ppm.

Although the presently known quality of the Elkon deposits combined with the remote location and required deep mining prohibits an economic exploitation of uranium at this stage, the Elkon district is considered a favorable target for additional exploration. This assessment is based on the possibility that further exploration may prove high U grade ore bodies containing sufficiently high tenors of gold to produce it as a by- or co-product.

2.9. Surficial deposits

2.9.1. Definition

Surficial uranium deposits are broadly defined as young (Tertiary to Recent) near-surface uranium concentrations in sediments or soils. These deposits usually have secondary cementing minerals including calcite, gypsum, dolomite, ferric oxide and halite. Uranium deposits in calcrete (calcium and magnesium carbonates) are the largest of the surficial deposits. The calcrete bodies are interbedded with Tertiary sand and clay, which are usually cemented by calcium and magnesium carbonates. Calcrete deposits form in regions where uranium-rich granites were deeply weathered in a semi-arid to arid climate [108]. Surficial uranium deposits also occur in peat bogs and karst caverns.

In Western Australia, surficial calcrete related uranium deposits occur in valley-fill sediments along Tertiary drainage channels (e.g. Yeelirrie) and in playa lake sediments (e.g. Lake Maitland). These deposits overlie Archaean granite and greenstone basement of the northern

portion of the Yilgarn Craton. The main uranium mineral is carnotite (hydrated potassium uranium vanadium oxide).

Calcrete uranium deposits also occur in the Central Namib Desert of Namibia, the largest being the Langer Heinrich deposit. Other small deposits are Trekkopje, Tubas and Aussinanis.

2.9.2. Geologic setting of Yeelirrie deposit, Australia

The Yeelirrie deposit in Western Australia occurs within valley calcretes lying along the drainage channel of a broad flat valley located in the northern part of the Yilgarn Craton. The Yeelirrie catchment area is developed almost entirely on highly weathered granitic rocks. Along the extreme western margins the drainage has encroached onto mafic volcanics and intrusives of the Montague Range greenstone belt [109].

The present day ephemeral drainage is generally regarded as the remains of an extensive Early Cretaceous river system that drained the Yilgarn Craton. Rejuvenation in Tertiary time etched this mature pattern into a lateritised peneplain [110]. Calcrete is developed at the top of the alluvial sediments filling the palaeochannel, and represents a late-stage modification of the alluvial valley-fill sediments. As yet, the precise age of the calcrete is unresolved, but it is probable that calcrete formation extended over a considerable period in recent geological time, even to the present when some varieties are still being formed [110].

2.9.3. Ore geometry and metallogenesis of Yeelirrie deposit, Australia

In the general area of uranium mineralisation at Yeelirrie, the valley-fill sediments comprise three main lithological units [111]: overburden, calcrete and a clay–quartz unit (combined thickness about 30 m). The overburden (1–2 m thick) of sandy, friable grey–brown soil is locally indurated by silica and passes down into carbonate-rich loam.

Two types of calcrete are present within the calcrete layer — one is a pale brown, friable, ‘earthy’ type and the other is a white, hard, nodular, ‘porcellanous’ type, which is commonly riddled with voids. The earthy calcrete forms a fairly continuous layer that grades upwards into the overlying soils. The porcellanous calcrete forms discrete, bulbous masses that commonly truncate the horizontal layering in the earthy calcrete, and appear to be growth mounds. The carbonate content in the porcellanous variety is commonly 70%, whereas the earthy variety has much lower carbonate content.

The calcrete is underlain by a clay–quartz unit (alluvium), which extends down to decomposed basement. The boundary between the calcrete and the alluvium is transitional. The alluvium consists of red clay with disseminated detrital quartz grains and quartz-rich bands, thin seams of celestite, or thin arkose layers overlying the basement.

The Yeelirrie deposit is a horizontal sheet approximately 9 km long and up to 1.5 km wide. The bulk of the mineralisation is confined to the interval between 4 m and 8 m below the surface, with approximately 90% of the mineralization occurring below the water table. The average thickness of mineralised material assaying 0.10% U_3O_8 or greater is 3 m [112]. Approximately 90% of the mineralisation is in a zone 4 m thick at the transition between the calcrete and the clay–quartz.

Carnotite is the only important uranium mineral at Yeelirrie, occurring as a thin film coating cavities and fractures, or disseminated through the earthy calcrete. The northern Yilgarn catchment areas of which Yeelirrie is a part contain extensive areas of Archean greenstones and granites. The granitic rocks which contain between 2 and 25 ppm U were the soruces of U and K. Vandaium was most probably sourced from the greenstones. These same terrains may also have been sources for V and K. Oxidizing waters draining these granitic terrains mobilized uranium as uranyl complexes, which were transported in laterally circulating, slightly oxidizing groundwater [113]. The weakly oxidizing conditions acted as a geochemical barrier in which dissolved V^{4+} was oxidized to V^{5+}, thereby establishing the conditions required for carnotite precipitation — reaction of V^{5+} with $(UO_2)^{2+}$ and K^+ already in solution [114]. Evaporative concentration of ionic species may have contributed to increasing ore concentrations.

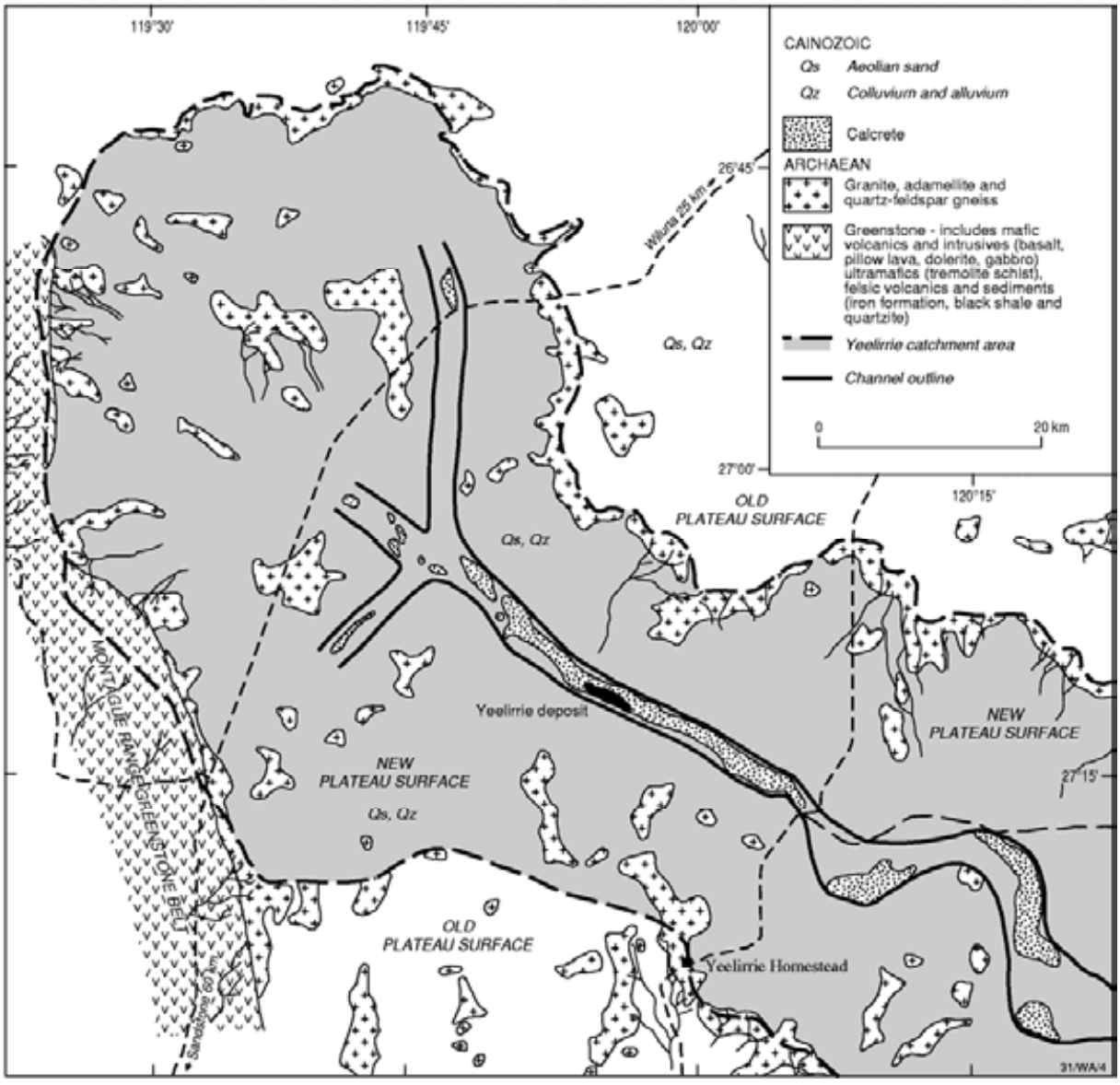

Fig. 11. Regional geological setting of the Yeelirrie deposit [109].

2.9.4. Uranium resources and production in Yeelirrie deposit, Australia

The Yeelirrie deposit is by far the world's largest surficial deposit, with resources totaling 44 430 t U at an average grade of 0.13% U.Other significant deposits in Western Australia include Lake Way, Centipede, Thatcher Soak and Lake Maitland.

Yeelirrie resource totals are as follows:

Prime ore	27 080 t U	Ave. grade 0.2% U
Intermediate ore	17 350 t U	Ave. grade 0.08% U
Total resources	44 430 t U	Ave. grade 0.13% U

2.10. Collapse breccia pipe deposits

2.10.1. Definition

Collapse breccia pipe deposits occur as vertical chimney-like structures that are filled with down-dropped fragments. Uranium mineralization, which was introduced into the pipes by ascending groundwater and was deposited in response to changes in temperature and/or pressure or to changes in chemical environment, occurs in the interstices between breccia fragments and in fractures in the annular ring that separates the breccia-filled column from the surrounding wall rock. Examples include the Hack Canyon deposit complex and the Orphan deposit, northwestern Arizona, USA.

2.10.2. Geologic setting of Arizona strip

Uraniferous collapse breccia pipe deposits have been identified in northwestern Arizona, USA, in the 10 000 km^2 Arizona Strip uranium district. The pipes have their origins in cave systems formed during development of karst topography in the Mississippian Redwall Limestone. The karst Redwall surface was covered by up to 800 m of shallow marine to continental sediments ranging in age from Pennsylvanian to Triassic. The pipes were formed by progressive upward stoping caused by groundwater ascending along near-vertical zones of weakness (faults, joints and fractures). The stoping process, which involved both chemical disaggregation and mechanical failure of roof and wall rock, was dependent on continual creation of space within the pipe structure. Syndepositional thickening of sedimentary units of varying ages indicates that pipe formation began as early as early Pennsylvanian time and continued intermittently through Triassic time.

Breccia pipes on the Arizona Strip extend up to 630 m vertically and cross a wide range of lithological units. The stoping process formed a breccia-filled column of down-dropped, lithologically variable breccia clasts ranging in size from individual sand grains to blocks several metres in diameter. Breccia fragments have been identified that have been displaced up to 350 m below their units of origin.

2.10.3. Ore geometry and metallogenesis of Arizona strip

The breccia pipes of the Arizona Strip are comprised of three interrelated parts — the cone of collapse, the throat of the pipe and the halo of alteration. The cone of collapse, which overlies the breccia filled throat of the pipe, is defined by beds that are infolded into the pipe structure, but are not necessarily brecciated. Concentric bands of inward dipping beds typically define the outer edge of the collapse cone at the surface. Recognition of the collapse cone from aerial photography is usually the first step in breccia pipe exploration.

The breccia column within the throat of the pipe is complex and variable both in composition and lateral and vertical distribution. The breccia-filled throat of the pipe is separated from the

surrounding country rock by the annular fracture system or annular ring. The country rock is typically slightly infolded into the annular ring. The transition from breccia column to country rock is generally abrupt. Breccia pipes vary in diameter with depth, depending on the permeability of the surrounding country rocks and their chemical susceptibility to stoping fluids. Pipes typically average about 30 m in diameter in impermeable units such as the Hermit Shale and up to 60 m in more permeable stratigraphic intervals.

The halo of alteration is represented by undisturbed country rock that has been chemically altered, typically by changing ferric iron to ferrous iron. The width of the halo of alteration depends on the permeability of the surrounding country rock, but it typically extends only a few tens of metres beyond the annular fracture system.

Metallogenesis of the breccia pipes began with Late Triassic emergence of highlands to the south of the Arizona Strip accompanied by arc volcanism [115]. North-flowing groundwater dispersal patterns flushed long stagnant brines that contained dissolved base metals and petroleum fluids northward. The breccia filled pipes served as vertical permeability pathways for ascending fluids during the mineralizing periods. Base metals were precipitated from these brines, which ranged in temperature between 80 ^{o}Cand 170^{o} C [116]. Petroleum residues (pyrobitumen) were also deposited in some pipes from the same circulating brines that transported the base metals. As uplift continued, oxidizing waters in the recharge area leached uranium from eroding volcanic and crystalline terrains. The dissolved uranium was transported by north-flowing groundwater systems and was precipitated by reducing environments within the pipes. The age of the uranium mineralization on the Arizona Strip is estimated to be between 260 and 200 million years before present [115]. Younger age dates have been measured in some of the deposits, which are likely the result of remobilization and re-precipitation of the uranium.

Uranium mineralization in the Arizona Strip breccia pipes has been documented to extend over a vertical range of nearly 400 m. Ore grade mineralization occurs in the breccia filled throat, associated with the annular fracture system and in minor amounts outside of the pipe in the alteration halo. The relative importance of each of these ore environments varies from pipe to pipe. A majority of the ore produced at the Orphan mine came from the annular ring, while resources in other pipes are largely associated with the breccia column itself.

2.10.4. Uranium resources and production

Uranium was recovered from Arizona Strip mines intermittently between 1956 and 1990, with cumulative production having totaled 8 960 t U at an average grade of 0.5% U. Production stopped in 1990 because of low uranium prices. Though uranium is the primary commercial product associated with the collapse breccia pipes, copper and silver have been recovered in commercial quantities; small amounts of gold and vanadium have also been recovered. For example, between 1956 and 1969, the Orphan Mine produced 1 600 t U, 3 030 tonnes of copper, 107 000 oz. of silver and 1.5 tonnes of vanadium [117]. Mineralized zones within the breccia pipes frequently contain sub-economic concentrations of other base and precious metals.

Total uranium resources plus past production associated with confirmed ore bearing collapse breccia pipes in the Arizona Strip uranium district with sufficient drilling to calculate resources are estimated at about 18 160 t U. There are, however, a large number of breccia pipes that have confirmed ore grade mineralization but with insufficient drilling on which to base resource calculations. Individual deposits range between 380 and 2300 t U with average grades of between 0.4 and 0.8% U.

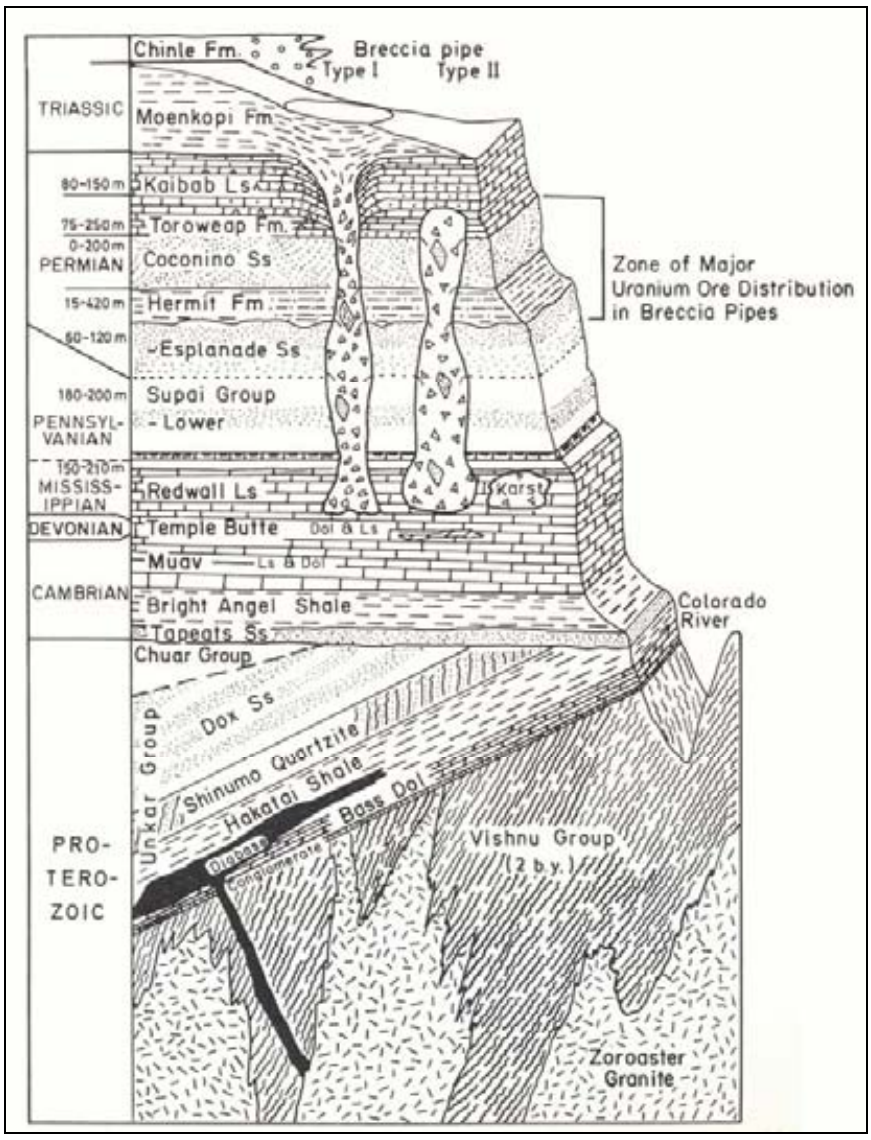

Fig. 12. Arizona Strip area, diagrammatic stratigraphic section and position of collapse breccia pipes [114].

2.11. Phosphorite deposits

2.11.1. Definition

Uraniferous phosphorite deposits consist of syn-sedimentary, stratiform, disseminated uranium in marine phosphate-rich rocks or phosphorite deposits that formed in continental shelf environments (Modified after Dahlkamp [114]). The uranium mineralization is substituted for Ca in cryptocrystalline fluor-carbonate apatite grains. Phosphorite deposits constitute large uranium resources, but are very low grade (25–150 ppm). Phosphate rock is a key raw material for the world's chemical fertilizer industry. Therefore, uranium can only be recovered as a by-product of phosphoric acid production. Examples of phosphorite deposits include New Wales Florida (land pebble phosphate) (USA), Gantour (Morocco) and Al-Abiad (Jordan). Other types of phosphorite deposits include: 1) Organic phosphate such as the argillaceous marine sediments enriched in phosphatized fish bones with U-REE-Re-Sc mineralization in the Melovoe deposit, Kazakhstan; 2) Continental phosphorite deposits such as the Bakouma deposit in Central African Republic (considered by some to be a 'paleo karst'

deposit); and 3) Igneous phosphates including the Itataia deposit in Brazil and deposits on the Kola Pennisula, Russian Federation.

2.11.2. Geologic setting

Phosphorite deposits were deposited on continental shelves in shallow marine environments. The depositional process involves mixing of upwelling of deep, cold seawater and warm ocean currents or warm shallow shelf waters [118]. Cold water can dissolve more CO_2 and apatite [$Ca_5(PO_4)_3F$] than can warm water. Therefore, PO_4 averages 0.3 ppm in cold water but only 0.003 to 0.01 ppm in warm shallow water. As deep, apatite-saturated water is warmed CO_2 is degassed and pH rises. Apatite is less soluble in alkaline water, so calcium phosphate precipitates from the supersaturated waters. If upwelling is sustained the deposits may become very thick. Phosphorite deposits range from Precambrian to recent in age. They appear to have formed at various times and places within 40^o of latitude north or south of the paleoequator [118].

There are two main subtypes of phosphorite deposits: bedded deposits and nodular deposits.

2.11.2.1. Subtype 1: Bedded phosphorite deposits

Bedded phosphorite deposits were deposited in distal continental shelf environments where upwelling P-enriched seawater provided a renewable source of P and where upwelling U-enriched water flooded the phosphorite accumulations. These environments were characterized by very slow rates of deposition. Phosphate deposits hosted in the Phosphoria Formation, Idaho, USA are representative examples of the bedded phosphorite subtype.

Bedded phosphorite deposits are composed of bedded fluor-carbonate apatite, which occurs as oolites, pisolites, pellets and laminae and as phosphatic fossil fragments mixed with clay-rich and carbonaceous fine-grained detritus [114]. They typically grade into black shales in a basinward direction and into chert beds in a landward direction and are over and underlain by pyritic chert, mudstone and black shale. Average grades in bedded Phosphorite deposits range between 50 and 300 ppm, with layers locally enriched to 600 ppm.

2.11.2.2. Subtype 2: Nodular phosphorite deposits

Nodular phosphorite deposits were deposited nearer shore in shallower water than their bedded counterparts. They are represented by reworked phosphatic pebbly sandstones with nodules and sand sized fluor-carbonate apatite mixed with clay minerals and marine sands. The nodular phosphorite deposits are interbedded with marine sands and shallow water carbonates and evaporites. The Land Pebble district, Florida, USA is a representative of the nodular Phosphorite deposit subtype.

Reworking and re-exposure of the apatite particles to uranium bearing seawater during marine transgressions leads to a variation of nodular phosphorite deposits termed land pebble phosphorite. Nodular phosphorite deposits typically average 10 to 20% P_2O_5 and 20 to 80 ppm U. Land pebble phosphorites in the Pliocene Bone Valley Formation in Florida contain fluor-carbonate apatite nodules and grains that are enriched up to 30% P_2O_5 and 500 ppm U. Weathering has produced a unit in the Bone Valley Formation in which the apatite is further enriched locally to several thousand ppm U [114].

2.11.2.3. Subtype 3: Continental phosphorite deposits

The only known continental phosphorite deposit is Bakouma (Central African Republic) with resources of 17 000 t U at an average grade of 0.24%. Mineralization at Bakouma occurs in 10 lenses of various sizes (500 to 6400 t) and grades (0.18 to 0.32%). Uranium occurs within fluorapatites in the basal formations and is concentrated in secondary minerals (autunite, torbernite) in the surficial formations.

2.11.3. Ore geometry and metallogenesis

Marine phosphorite deposits are characterized by their broad regional extent. The bedded phosphorite deposits of the Phosphoria Formation extend over an area of several thousand km^2. The Mead Peak Phosphatic Shale Member, the main phosphate member of the Phosphoria Formation, varies in thickness from 60 to 150m and averages 11 to 12% P_2O_5 [114]. The upper and lower 1 to 3m of the Mead Peak Member, however, average 25 to 35% P; uranium content is also higher in the upper and lower units of the Mead Peak Member.

The lower Bone Valley Formation in Florida, in which the land pebble phosphorite deposits occur, covers an area of about 2 500 km^2. Mineralized beds in the Bone Valley district average between 5 and 7 metres. Total resources of this district are estimated at 420 000 t U. The average grade of the land pebble mineralization is 150 ppm U.

Uranium enrichment in marine phosphorite deposits is thought to have been the result of extraction of U from seawater and syngenetic incorporation into cryptocrystalline fluor-carbonate apatite. The slow rate of deposition that characterizes bedded phosphates permitted longer exposure of apatite grains, which in turn allowed U from seawater to replace Ca in the apatite. Bedded phosphorite deposits are characterized by the noticeable absence of carbonate beds. The low concentration of CO_2^{+2} ions that must have characterized the marine waters in phosphorite depositional environments allowed U to remain in solution and to interact with the apatite.

The phosphorite deposits in Morocco range from Upper Cretaceous to Eocene in age. The Eocene age Khouribga deposit is 5 m thick and contains up to 36% P_2O_5 with uranium values of around 150 ppm U and local enrichment in some layers to 500–600 ppm. The phosphate consists of 0.1 to 0.2 mm diameter grains of F-collophanite enclosed in a clayey and calcareous matrix that is locally impregnated with opal. The phosphate grains often have quartz or zircon grains at their centres, which served as the nucleus of phosphate precipitation.

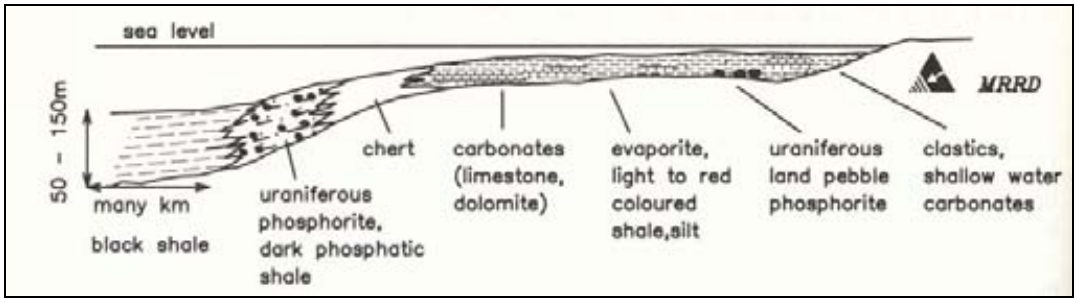

Fig. 13. Phosphorite uranium deposit type [114].

2.11.4. Uranium resources and production in phosphorite deposits

The 2003 Red Book states that resources contained in worldwide phosphate deposits potentially total 22 million t U, but does not list any corroboration of this total. Barthel [119] lists phosphate resources as totalling between 7 million and 7.2 million t U. Phosphate related resources in Morocco reportedly total 6.53 million t U or approximately 93% of the worldwide total. Other countries with significant phosphate related resources include Brazil, Egypt, Jordon, Mexico, Syria and the USA.

Worldwide production totals for uranium recovery from phosphate deposits are not available. However, it is known that about 690 t U were recovered from processing Moroccan phosphate rock in Belgium; at least 18 200 t U were recovered in the USA (in 1980 there were eight plants recovering uranium from phosphoric acid manufacturing in the USA alone) and 6 000 t U were recovered from processing marine organic deposits (fish bones) in Kazakhstan. A small amount of uranium was also recovered in Canada from processing US phosphate rock. Recovery of uranium from marine phosphorite deposits uses well established technology, which has been used in Belgium and the USA as recently as 1998 and 1999, respectively. The uranium produced as a by-product of phosphoric acid production in Belgium, which processed phosphate rock imported from Morocco, was controlled by Prayon-Rupel Technologies, S.A. The Uncle Sam uranium production facility, the last operating plant in the USA, which had a production capacity of about 300 t U per year, is owned by IMC-Agrico Company.

2.12. Black shale deposits

2.12.1. Definition

Stratiform black shale hosted uranium mineralization consists of syngenetic, uniformly disseminated uranium adsorbed onto organic and/or clay particles in organic-rich, pyritic marine shale with thin coalified, phosphatic and/or silty intercalations. The organic matter is of a sapropelic-bituminous or humic, coaly nature derived from planktonic marine algae and land plant debris (e.g. wood spores). Limestone, sand/siltstone, and shale strata complete the stratigraphic sequence. Discrete primary uranium minerals are absent. Other metals (Cu, Cr, Mo, Mn, REE, V and P) occur in small quantities.

2.12.2. Geologic setting of Ranstad deposits, Sweden

The black shale formations that host uraniferous black shale deposits were deposited in shallow, partially closed epicontinental basins within tectonically stable terrane [114]. Low rates of deposition, brackish to normal marine salinities and anaerobic, strongly reducing conditions characterized the environments in which the black shales were deposited.

2.12.3. Ore geometry and metallogenesis of Ranstad deposits, Sweden

Mineralized black shale beds are of fairly uniform thickness (few metres to tens of metres), geographically extensive (several hundred to 10 000 km^2), and host enormous quantities of uranium but at very low concentrations. Higher concentrations are confined to beds (cm to m thick) that are rich in organics, particularly humic-coaly material. If phosphate nodules are present, they normally contain more uranium than the surrounding shale.

Based on the organic substances with which the uranium is associated two subtypes of black shales are distinguished: uranium associated (1) with humic/kolm in alum shale (Ranstad

type); and (2) with bituminous/sapropelic black shale (Chattanooga type). The Ranstad deposits in Sweden have been selected as the type example for uraniferous black shale deposits. The principal uranium host rock is the kolm horizon, which is characterized by nodular or concretionary bodies of coal within black bituminous alum shales of Cambrian age. The flat-lying black shale unit rests on Cambrian sandstone and is covered by Ordovician Limestone. The kolm-bearing alum shale covers an area of about 500 km^2. Thickness of the alum shale is 15 m; the kolm horizon varies in thickness from 2.5 to 4 m.

Uranium mineralization in the Ranstad black shale deposits is stratiform and is adsorbed on organic matter and, in particular, on kolm nodules. The kolm contains about 30 % ash. Nodules may contain up to 80% organics and up to 0.4% U. Average values for the kolm horizon are: 300 to 380 ppm U (alum shale ca. 200 ppm U), 22% organic material, 13 % pyrite, 6.5% S, 0.065% V, 0.03% Mo, 0.02% Ni, 0.4% Mg, 0.7% P, and high Al and K contents.

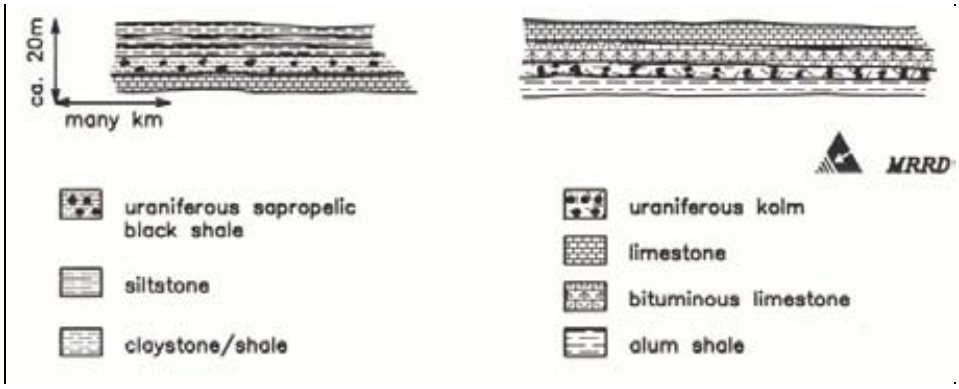

Fig. 14. Black shale uranium type [120].

2.12.4. Uranium resources and production from Ranstad deposits, Sweden

The Ranstad occurrence is estimated to contain 250 000 t U at 200–300 ppm U, including 65 000 t U averaging about 300 ppm U. Approximately 200 t U were produced from the Ranstad alum shale in the 1960s. Global uranium resources associated with black shale deposits are estimated to total approximately 4.4 million t U [121].

2.13. Metamorphic deposits [Example: Mary Kathleen deposit, Queensland, Australia]

2.13.1. Definition

Metamorphic uranium deposits result from regional metamorphism of uraniferous sediments or volcanics. Accordingly, they occur in metasediments and/or metavolcanics in which the uranium mineralization resulted directly from metamorphic processes. Examples include the Mary Kathleen deposit, Australia and the Forstau deposit, Austria [65].

2.13.2. Geologic setting of Mary Kathleen deposit, Queensland, Australia

The Mount Isa Inlier in western Queensland, Australia is subdivided by major north-striking faults into three broad tectonic belts — Western Succession, Kalkadoon–Leichhardt Belt and Eastern Succession — which comprise Palaeoproterozoic metasediments, volcanics and intrusive rocks. The easternmost of these tectonic belts, the Eastern Succession, is subdivided

from west to east into the Mary Kathleen, Quamby–Malbon and Cloncurry–Selwyn zones [122][123]. The Mary Kathleen zone, which hosts a number of uranium deposits, is 10–20km wide and more than 200 km long. It is comprised of a sequence of Palaeoproterozoic shallow-water shelf sediments that have undergone complex folding, regional metamorphism, and granitic intrusion and metasomatism.

Uranium mineralisation in the Mary Kathleen zone is hosted by skarns within metamorphosed calcareous rocks of the Corella Formation, a sequence of contact and regionally metamorphosed evaporitic calc-silicate rocks with marble, metapelites, metasammites and minor metavolcanics, which has been dated at 1 780–1 760 Ma.

Four phases of deformation related hydrothermal activity are recognised in the Palaeoproterozoic metasediments of the Mary Kathleen zone that occurred from at least 1 750 Ma to 1 100 Ma. Intense metasomatism occurred during all four phases, caused by reactions with highly saline fluids derived in part from the evaporitic Corella Formation sediments.

2.13.3. Ore geometry and metallogenesis of Mary Kathleen deposit, Queensland, Australia

The Mary Kathleen deposit is considered to be a skarn-hosted metamorphic–hydrothermal deposit. Uranium–rare earth mineralisation is hosted by a skarn that formed during a period of regional metamorphism and deformation. U mineralisation and the host skarn body are closely associated with a major shear zone that was active during deformation and regional metamorphism. Several other small uranium prospects also occur in metasediments and skarns of the Palaeoproterozoic Corella Formation in the Mary Kathleen zone [124].

The Mary Kathleen deposit occurs along the axial trace of a tight syncline (the Mary Kathleen Syncline), which formed during the second phase of deformation. The main rock types in the syncline are hornfelsed calc-silicate rocks, skarn, cobble conglomerate, ‘igneous textured granofels’, diorite, calc-silicate granofels, quartzite, amphibolite and impure marble [125]. The western limb of this syncline is cut by the Mary Kathleen shear zone, and the eastern limb by the Burstall Granite. Slightly younger rhyolite dikes west of the granite have similar compositions and an identical radiometric age. The Burstall Granite and the rhyolite dikes have elevated uranium and thorium contents.

The Mary Kathleen shear zone has a north–south regional trend and is approximately parallel to the axial trace of the Mary Kathleen Syncline, except in the vicinity of the ore body. Here the shear zone wraps around the skarn to form a bulge, in a departure from its regional trend. Exposures in the Mary Kathleen open pit show that the shear zone truncates the host skarn and skarns are absent to the west of the shear zone. However, the shear does not truncate ore zones [126]. Most of the vertical movement along the shear zone occurred late in the second phase of regional metamorphism.

The skarns and metamorphosed carbonates along the eastern limb of the Mary Kathleen Syncline were formed during emplacement of the Burstall Granite. The age of these phase 1 skarns is 1766 ± 80 Ma, which overlaps that of the granite [127][128]. At the Mary Kathleen deposit and the nearby Elaine prospect, metamorphosed carbonates typically contain calcite, mostly andradite garnet, clinopyroxene, wollastonite, K-feldspar and minor scapolite with uranium and REE. Maas and others [128]concluded that uranium and REE enrichment also occurred at this time (1 766 ± 80 Ma) in the skarn at or near the present ore body.

Approximately 200–250 Ma later, metasomatism associated with phase 2 deformation and intrusion produced a second generation of skarns containing andradite garnet, K-feldspar, albite, epidote, scapolite and ferrohastingsite together with uranium and REE mineralisation [129]. There was widespread garnet veining and replacement of previous skarn mineral assemblages.

Age dating of uraninite has yielded 1 550 ± 15 Ma [130], which is approximately the same age as the second phase of deformation. Field relationships indicate that ore formation occurred after the folding but was synchronous with or predated shearing along the Mary Kathleen shear under amphibolite facies metamorphism [131]. Brecciation and reworking of earlier skarns took place during phase 2 skarn formation. During this phase, the previously existing uranium–REE mineralisation may have been reworked and possibly upgraded.

Uranium–REE mineralisation occurs within the skarn and is surrounded by an extensive irregular alteration zone consisting mainly of garnet (andradite–grossularite) with lesser amounts of diopside, scapolite and feldspar. Where alteration is incomplete, garnet and diopside form veins and lit-par-lit injections. In the centre of the ore body, alteration is virtually complete and only small remnants of altered diorite and cobble conglomerate remain [132].

The Mary Kathleen mineralisation changes gradually with depth. Down to about 100 m the ore body consists of several large irregular lenses of high-grade ore dipping at 30–50°W and extending over a zone up to 100m wide. With increasing depth, the lenses become a series of narrow, irregular, steep zones that are sub parallel to the Mary Kathleen Shear.

Large irregular zones of allanite (a complex rare-earth silicate) occur in a honeycomb pattern throughout the alteration zone. Uraninite is disseminated throughout the allanite zones as ovoid grains 0.01–0.1 mm across; most of them are surrounded by a thin shell of silica, pyrite, or radiogenic galena [132]. Other gangue minerals include hornblende, prehnite and calcite. Sulphides occur as irregular pods of massive sulphide and as disseminations. The cores of the massive sulphide pods contain up to 95% pyrrhotite, with minor chalcopyrite, diopside, allanite and garnet. The pods are rimmed by narrow zones of disseminated pyrrhotite and chalcopyrite. Minor amounts of pyrite, marcasite, galena, sphalerite, molybdenite, pentlandite, bornite and linnaeite are also present. Although sulphides are locally abundant, the average sulphide content of the ore body is only about 2%. The main REE are lanthanum and cerium, which comprise about 85% of the rare-earth content [133].

Maas and others [128] proposed that the ore body formed during phase 2 skarn development and that the higher grade U-REE ore formed by enrichment of earlier-formed low-grade mineralisation. The earlier mineralisation formed during the development of phase 1 skarns, which were produced by high temperature metamorphism and metasomatism of the Corella Formation during intrusion of the Burstall Granite. The granite is fractionated, oxidised and uranium-rich with an average content of 7–10 ppm U. The reworking of the skarns during phase 2 deformation was associated with shearing and was also associated with oxidising fluids with high salt content derived from evaporitic minerals in the Corella Formation.

Oliver and others [126][131] have proposed an alternative origin for the deposit, whereby reworking of the skarn occurred during phase 2 deformation, with large-scale fluid circulation introducing uranium and rare-earth mineralisation from an external source via the Mary Kathleen shear.

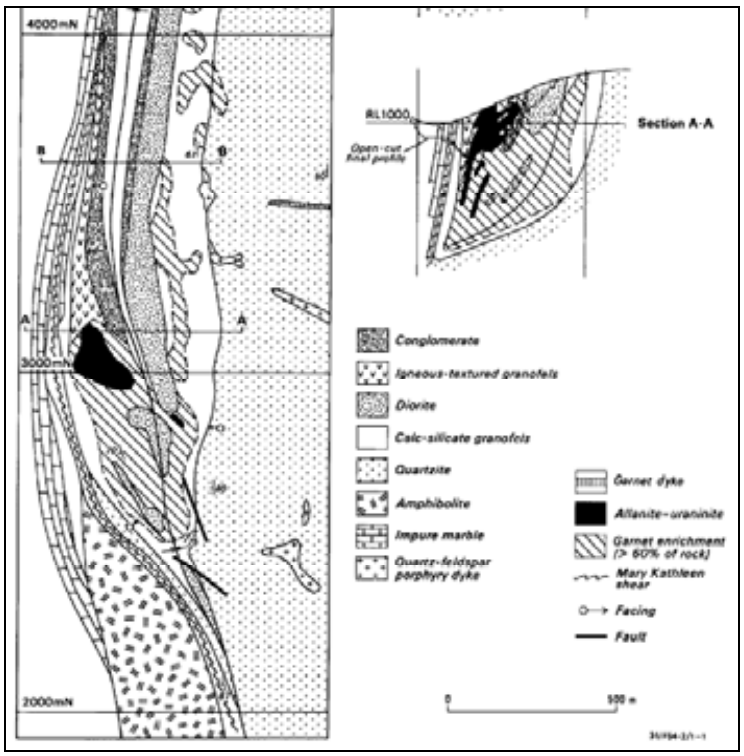

Fig. 15. Geology of the Mary Kathleen deposit [125].

2.13.4. Uranium resources and production

Initial resources for the Mary Kathleen deposit were estimated to have totalled 10 150 t U at an average grade of 0.11% U [133]. Mining of the Mary Kathleen ore body took place during two periods: 1958 to 1963, and 1976 to 1982. Total production during these periods was 7532 t U. After mining ended, the resources below the open cut were estimated to be 1018 t U [132]. The company reported that these reserves could not be extracted at a profit because of high mining costs and the low prices for spot-market sales at that time.

2.14. Other deposit types

The preceding list includes all deposit types that are known to host uranium deposits of significant commercial interest. There are, however, other deposit types that host uranium, which either because of their low ore-grades or small size, are of limited commercial interest. For completeness, however, summary definitions for these deposits follow.

2.14.1. Uraniferous coal and lignite deposits

Elevated uranium content occurs in lignite/coal, and in clay and sandstone immediately adjacent to lignite. Examples of uranium occurrences in coal/lignite include deposits in the Serres Basin (Greece), in North and South Dakota (USA), Koldjat and Nizhne Iliyskoe deposits (Kazakhstan), Melovoe (Russian Federation) and Freital (Germany). Uranium grades are typically very low (20–60 ppm), but some layers are enriched in uranium with values above 0.1%U. For example, in Harding County, South Dakota, USA, grades of 0.1% up to several percent have been recorded in Paleocene lignite layers. The Hilltop mine produced 232 t U at an average grade of 0.28%.

2.14.2. Limestone and paleokarst deposits

The most important examples of uranium occurrences hosted in limestones are the deposits in the Todilto Limestone in the Grants district (New Mexico, USA), where uraninite was precipitated in the presence of organic matter in intra-formational folds and associated fractures in the limestones. From 1950 through 1981, mines in the Grants district yielded 2 566 t U from the Todilto Limestone, amounting to slightly more than 2% of the total uranium produced from the Grants district [134][135]. More than 100 uranium mines and occurrences are found in the Todilto Limestone in New Mexico; 42 mines have documented uranium production [136]. The Todilto uranium deposits are 150–155 Ma, based on U-Pb isotopic dating and are older than the 130 Ma Morrison sandstone uranium deposits [137].

Paleokarst-hosted uranium deposits in organic matter in clay-rich Devonian-Carboniferous carbonates are an economically important new type of uranium deposit in South China. The deposits, represented by Sanqilinyi, Sanbaqi and Saqisan, are characterized by their occurrence in collapse breccias and by their mineral association of uraninite, coffinite, carbonates and Fe, Cu, Pb, Zn, Ni sulfides. The breccias occurred mainly along fault zones and unconformities between different strata which permitted access to groundwater, leading to karst formation and eventually to the formation of solution-collapse breccia. Small quantities of uranium have also been mined from limestone collapse breccias that cover the floors of karst caverns in the Mississippian Madison Limestone in the Pryor Mountains, Wyoming, USA. The Pryor Mountain deposits are small, usually only a few tens of t U; ore grades range between 0.4 to 0.7% U and 0.1 to 1% V_2O_5 [114].

Limestone hosted uranium mineralization has also been mined from the Mailu-Suu and Shakoptar deposits in Kyrgyzstan.

2.14.3. By-product–copper processing

Uranium mineralization occurs in low concentrations (50–200 ppm) in many metalliferous deposits. In the past, uranium has been recovered as a by-product from concentrates derived from processing of copper ores at Palabora (South Africa), Bingham Canyon (USA) and the Singbhum district (India).

3. WORLD DISTRIBUTION OF URANIUM DEPOSITS

3.1. UDEPO CD-ROM

A CD-ROM has been prepared to help readers of this IAEA-TECDOC to provide detailed information on the worldwide uranium deposits as a supplementary tool. The CD-ROM has been formulated so that any internet browser is capable of showing the content of the CD-ROM. However, the CD-ROM has been fully tested on MS Internet Explorer Version 6 and 7. Other browser might show some differences in the operation of the CD-ROM.

In addition to the information provided in UDEPO CD-ROM, more details, summary tables with the recent updates can be found at the UDEPO internet site at http://www-nfcis.iaea.org.

3.1.1. Deposit list

The home page to the UDEPO CD-ROM is UDEPOMain.html. The home page will be opened automatically by the system if Autorun feature of CD-ROM device is enabled in the computer. Otherwise the users can open the UDEPOMain.html page easily by double clicking on the name of the file in Windows Explorer.

The home page of the UDEPO CD-ROM will show the list of uranium deposits which UDEPO database stores (Fig. 16). The complete list includes 874 deposits. The list can be filtered by using the filters in the upper part of the table. The list can also be sorted by any of the fields by clicking the column headings of the table. By default the paging is enabled and set to 20 deposits per page. However, paging can be disabled by pressing 'Show All Rows' button in the top of the table. The footer part of the table shows the total number of deposits and the number of deposits which match the selected filters (the number is displayed in red color). The footer also hosts the paging information and links to go to the next or previous page.

3.1.2. Deposit details

Clicking on the name of the deposit or DepositID in the deposit list opens the deposit report page which is giving more details about the selected uranium deposit (Fig. 17). Geological or technical details about the selected uranium deposit are given in this page.

3.1.3. Country maps

Country maps are provided in UDEPO CD-ROM showing the locations, types and sizes of the deposits in the selected country (Fig. 18). The country can be selected from the combobox which is located in the over of the map. There are two map images in the page. Left and big image shows the details of the selected area from the right and small image. The detailed map can be scrolled using the red box in the small map. The user can also open the high resolution image by clicking on the big map any time.

Fig. 16. Home page of the UDEPO CD-ROM (deposit list).

Fig. 17. Deposit details page from UDEPO CD-ROM.

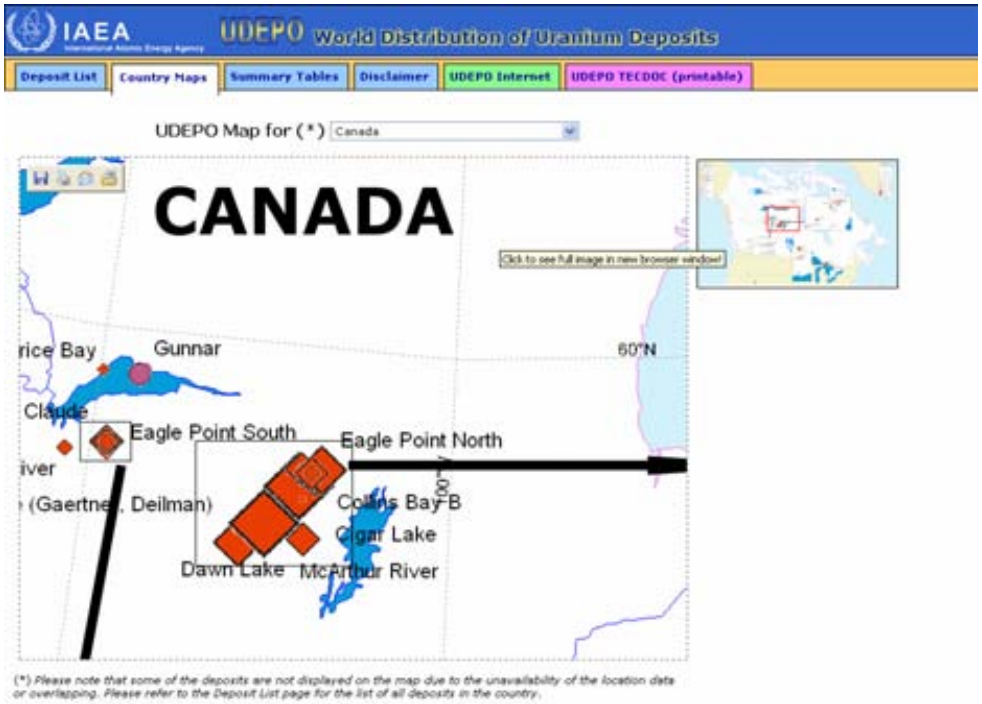

Fig. 18. Country maps page from UDEPO CD-ROM.

3.1.4. Worldwide summary tables

The third page in the UDEPO CD-ROM is the Summary Tables page which hosts a number of statistical or summary tables to illustrate the worldwide overview of the uranium deposits (Fig. 19). There are a number of different tables and they can be selected by clicking on the radio button which resides on the left part of the table caption.

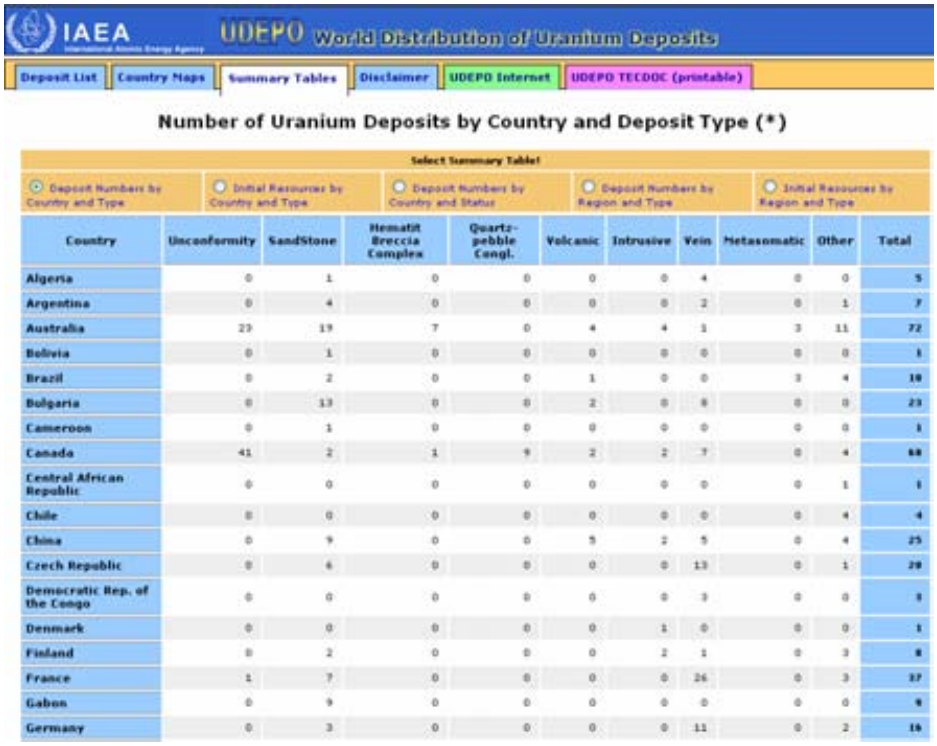

Fig. 19. Summary Tables page from UDEPO CD-ROM.

3.2. Directory of uranium deposits

This section includes a number of tables generated using the data from the database.

3.2.1. The list of uranium deposits: Sorted by country and name (as of March 2009).

Country	DepID	Deposit Name	Deposit Type	Status	Resource Range
Algeria	1	Abankor	Vein	Dormant	5,000–10,000
Algeria	2	Daira	Vein	Dormant	UNKNOWN
Algeria	3	Tahaggart	Surficial	Dormant	1,000–2,500
Algeria	4	Timgaouine	Vein	Dormant	10,000–25,000
Algeria	5	Tinef	Vein	Dormant	UNKNOWN
Argentina	6	Cerro Solo	Sandstone–Tabular	Dormant	2,500–5,000
Argentina	7	Don Otto	Sandstone–Tabular	Depleted	500–1,000
Argentina	8	Dr. Baulles	Sandstone–Tabular	Dormant	10,000–25,000
Argentina	9	Huemul	Sandstone–Tabular	Dormant	< 500
Argentina	10	La Estela	Vein	Depleted	< 500
Argentina	11	Rodolfo	Surficial	Dormant	1,000–2,500
Argentina	12	Schlagintweit	Vein	Dormant	1,000–2,500
Australia	13	Anderson's Lode	Metasomatite	Exploration	2,500–5,000
Australia	14	Angela	Sandstone–Roll Front	Dormant	5,000–10,000
Australia	15	Angelo River A	Unconformity-Proterozoic Fracture bound	Dormant	500–1,000

Country	DepID	Deposit Name	Deposit Type	Status	Resource Range
Australia	16	Armchair Streitberg	Hematite Breccia Complex	Exploration	1,000–2,500
Australia	17	Ben Lomond	Volcanic	Dormant	5,000–10,000
Australia	18	Bennetts Well	Sandstone–Roll Front	Dormant	1,000–2,500
Australia	19	Beverley	Sandstone–Basal Channel	Operating	10,000–25,000
Australia	20	Bigrlyi	Sandstone–Roll Front	Dormant	5,000–10,000
Australia	21	Caramal	Unconformity-Proterozoic Fracture bound	Exploration	500–1,000
Australia	22	Centipede	Surficial	Dormant	2,500–5,000
Australia	1296	Central 50	Volcanic	Exploration	500–1,000
Australia	23	Coronation Hill	Unconformity-Proterozoic Fracture bound	Dormant	1,000–2,500
Australia	24	Crocker Well	Intrusive	Exploration	2,500–5,000
Australia	25	Dam	Unconformity-Proterozoic Fracture bound	Dormant	500–1,000
Australia	26	Dyson's	Unconformity-Proterozoic Fracture bound	Depleted	< 500
Australia	27	East Kalkaroo	Sandstone–Roll Front	Exploration	500–1,000
Australia	29	Goulds Dam–Billeroo	Sandstone–Roll Front	Exploration	5,000–10,000
Australia	30	Hades Flat	Unconformity-Proterozoic Fracture bound	Dormant	500–1,000
Australia	31	Hodgkinson	Hematite Breccia Complex	Dormant	< 500
Australia	32	Honeymoon	Sandstone–Roll Front	Development	1,000–2,500
Australia	33	Huarabagoo	Vein	Dormant	2,500–5,000
Australia	34	Jabiluka 1 Orebody	Unconformity-Proterozoic Fracture bound	Dormant	2,500–5,000
Australia	951	Jabiluka 2 Orebody	Unconformity-Proterozoic Fracture bound	Dormant	> 100,000
Australia	980	Jailor Bore	Surficial	Exploration	500–1,000
Australia	35	Junnagunna	Sandstone–Tabular	Dormant	2,500–5,000
Australia	36	Kintyre	Unconformity-Proterozoic Fracture bound	Dormant	25,000–50,000
Australia	37	Koongarra 1 Orebody	Unconformity-Proterozoic Fracture bound	Dormant	10,000–25,000
Australia	950	Koongarra 2 Orebody	Unconformity-Proterozoic Fracture bound	Dormant	1,000–2,500
Australia	945	Kylie	Unconformity-Proterozoic Fracture bound	Exploration	UNKNOWN
Australia	38	Lake Maitland	Surficial	Development	5,000–10,000
Australia	39	Lake Mason	Surficial	Dormant	1,000–2,500
Australia	40	Lake Raeside	Surficial	Dormant	1,000–2,500
Australia	41	Lake Way	Surficial	Exploration	2,500–5,000
Australia	42	Malbooma	Sandstone–Tabular	Dormant	2,500–5,000
Australia	43	Manyingee	Sandstone–Roll Front	Dormant	10,000–25,000
Australia	44	Mary Kathleen	Metamorphic	Depleted	10,000–25,000
Australia	45	Maureen	Volcanic	Dormant	1,000–2,500
Australia	46	Mount Fitch	Unconformity-Proterozoic Fracture bound	Dormant	2,500–5,000
Australia	47	Mount Gee	Hematite Breccia Complex	Exploration	10,000–25,000
Australia	48	Mount Painter	Hematite Breccia Complex	Exploration	5,000–10,000
Australia	944	Mount Victoria	Intrusive	Dormant	< 500
Australia	49	Mulga Rock Deposits	Sandstone–Tabular	Dormant	10,000–25,000
Australia	50	Nabarlek	Unconformity-Proterozoic Fracture bound	Exploration	5,000–10,000
Australia	51	Napperby	Surficial	Dormant	500–1,000
Australia	979	Nolans Bore	Intrusive	Exploration	1,000–2,500
Australia	52	Nowthana	Surficial	Dormant	1,000–2,500
Australia	53	Olympic Dam	Hematite Breccia Complex	Operating	> 100,000
Australia	947	Oobagooma	Sandstone–Roll Front	Dormant	5,000–10,000
Australia	54	Outcamp	Sandstone–Tabular	Dormant	500–1,000
Australia	943	Pamela	Sandstone–Roll Front	Dormant	UNKNOWN
Australia	55	Paralana-Pepegoona	Sandstone–Roll Front	Exploration	500–1,000
Australia	977	Prominent Hill	Hematite Breccia Complex	Development	10,000–25,000
Australia	56	Radium Hill	Intrusive	Depleted	500–1,000
Australia	58	Radium Ridge	Hematite Breccia Complex	Dormant	1,000–2,500

Country	DepID	Deposit Name	Deposit Type	Status	Resource Range
Australia	59	Ranger 68	Unconformity-Proterozoic Fracture bound	Dormant	2,500–5,000
Australia	948	Ranger No. 1 Orebody	Unconformity-Proterozoic Fracture bound	Depleted	25,000–50,000
Australia	952	Ranger No. 3 Orebody	Unconformity-Proterozoic Fracture bound	Operating	> 100,000
Australia	60	Redtree	Sandstone–Tabular	Exploration	10,000–25,000
Australia	61	Rum Jungle Creek South	Unconformity-Proterozoic Fracture bound	Depleted	1,000–2,500
Australia	62	Skal	Metasomatite	Exploration	2,500–5,000
Australia	28	South Alligator River District	Unconformity-Proterozoic Fracture bound	Depleted	500–1,000
Australia	63	Sue	Sandstone–Tabular	Dormant	500–1,000
Australia	64	Thatcher Soak	Surficial	Dormant	2,500–5,000
Australia	65	Trident	Volcanic	Dormant	< 500
Australia	66	Turee Creek	Unconformity-Proterozoic Fracture bound	Dormant	UNKNOWN
Australia	67	Two-Gee	Volcanic	Dormant	500–1,000
Australia	68	Valhalla	Metasomatite	Exploration	10,000–25,000
Australia	69	Walbiri	Sandstone–Tabular	Dormant	500–1,000
Australia	70	Warrior	Sandstone–Tabular	Exploration	2,500–5,000
Australia	72	White's	Unconformity-Proterozoic Fracture bound	Depleted	500–1,000
Australia	73	Yeelirrie	Surficial	Dormant	25,000–50,000
Bolivia	74	Cotaje	Sandstone–Tabular	Dormant	500–1,000
Botswana	1124	Mokobaesi	Surficial	Exploration	5,000–10,000
Botswana	1258	Serule	Sandstone–Basal Channel	Exploration	25,000–50,000
Brazil	75	Amorinopolis	Sandstone–Tabular	Dormant	2,500–5,000
Brazil	76	Campos Belos	Vein	Closed	< 500
Brazil	77	Espinharas	Metasomatite	Dormant	5,000–10,000
Brazil	78	Figueira	Sandstone–Tabular	Dormant	5,000–10,000
Brazil	79	Gandarela	Unknown	Dormant	1,000–2,500
Brazil	80	Itataia	Metasomatite	Development	> 100,000
Brazil	81	Lagoa Real	Metasomatite	Operating	50,000–100,000
Brazil	82	Pocos De Caldas	Volcanic	Reclamation	10,000–25,000
Brazil	83	Serra Des Gaivotas	Quartz-pebble Conglomerate	Feasibility study	UNKNOWN
Brazil	84	Serrotes Baixos	Unknown	Unknown	UNKNOWN
Bulgaria	85	Beslet	Vein	Depleted	500–1,000
Bulgaria	86	Biala Voda	Vein	Closed	1,000–2,500
Bulgaria	87	Bukhovo District	Vein	Depleted	5,000–10,000
Bulgaria	88	Dospat	Sandstone–Tectonic/Lithologic	Depleted	500–1,000
Bulgaria	89	Eleshnitsa District	Sandstone–Tabular	Closed	5,000–10,000
Bulgaria	90	Gabra	Sandstone–Tabular	Closed	< 500
Bulgaria	91	Gradevo	Sandstone–Tabular	Fully explored	500–1,000
Bulgaria	92	Igralishte	Surficial	Depleted	500–1,000
Bulgaria	1127	Isgrew	Sandstone–Roll Front	Depleted	500–1,000
Bulgaria	1128	Kostenetz	Vein	Depleted	< 500
Bulgaria	93	Kurrilo	Sandstone–Tectonic/Lithologic	Depleted	500–1,000
Bulgaria	1130	Marritza District	Sandstone–Roll Front	Dormant	2,500–5,000
Bulgaria	94	Melnik	Sandstone–Tabular	Depleted	500–1,000
Bulgaria	95	Momino District	Sandstone–Roll Front	Closed	2,500–5,000
Bulgaria	1244	Narretshen	Vein	Depleted	500–1,000
Bulgaria	1133	Okop-Tenevo	Sandstone–Tabular	Depleted	1,000–2,500
Bulgaria	96	Partisanska Polana	Vein	Depleted	< 500
Bulgaria	97	Pravoslaven, Haskovo	Sandstone–Roll Front	Closed	10,000–25,000
Bulgaria	98	Pripetchen-Deltshevo	Sandstone–Tabular	Dormant	500–1,000
Bulgaria	99	Proboinitsa	Vein	Closed	500–1,000
Bulgaria	100	Rosen	Vein	Depleted	500–1,000
Bulgaria	101	Sarnitsa and Planinetz	Volcanic	Depleted	1,000–2,500
Bulgaria	102	Saslyka Paleochannel	Sandstone–Roll Front	Closed	1,000–2,500
Bulgaria	103	Sborishte	Vein	Closed	500–1,000

Country	DepID	Deposit Name	Deposit Type	Status	Resource Range
Bulgaria	104	Simitli	Sandstone–Tabular	Closed	2,500–5,000
Bulgaria	105	Sliven	Vein	Depleted	500–1,000
Bulgaria	106	Smolian	Volcanic	Closed	2,500–5,000
Bulgaria	107	Smolianovtzi	Sandstone–Tabular	Depleted	1,000–2,500
Bulgaria	1245	Zdravetz	Vein	Dormant	1,000–2,500
Cameroon	155	Kitongo	Metasomatite	Exploration	10,000–25,000
Canada	1247	Abeta	Quartz-pebble Conglomerate	Dormant	2,500–5,000
Canada	981	Ace-Fay-Verna	Vein	Depleted	10,000–25,000
Canada	109	Agnew Lake	Quartz-pebble Conglomerate	Depleted	2,500–5,000
Canada	1138	Allied Zones	Intrusive	Dormant	2,500–5,000
Canada	982	Andrew Lake	Unconformity-Proterozoic Fracture bound	Feasibility study	10,000–25,000
Canada	1139	Apple	Quartz-pebble Conglomerate	Dormant	2,500–5,000
Canada	1038	Axe Lake	Intrusive	Unknown	500–1,000
Canada	1039	Baie Johan Beetz	Intrusive	Unknown	10,000–25,000
Canada	1248	Banana Lake	Quartz-pebble Conglomerate	Unknown	25,000–50,000
Canada	111	Bancroft	Intrusive	Dormant	2,500–5,000
Canada	1041	Bicroft	Intrusive	Depleted	1,000–2,500
Canada	1042	BJ	Unconformity-Proterozoic Fracture bound	Dormant	UNKNOWN
Canada	112	Blizzard	Sandstone–Basal Channel	Dormant	2,500–5,000
Canada	1043	Blue Rock	Intrusive	Unknown	UNKNOWN
Canada	983	Bong Grid	Unconformity-Proterozoic Fracture bound	Exploration	1,000–2,500
Canada	1141	Buckels	Quartz-pebble Conglomerate	Closed	500–1,000
Canada	1142	Calumet-Contact	Metasomatite	Unknown	500–1,000
Canada	1048	Canadian Dyno	Intrusive	Closed	1,000–2,500
Canada	1143	Can-Met	Quartz-pebble Conglomerate	Closed	5,000–10,000
Canada	1249	Capri 2	Intrusive	Unknown	< 500
Canada	984	Caribou	Unconformity-Proterozoic Clay bound	Dormant	1,000–2,500
Canada	993	Cayzor	Vein	Depleted	500–1,000
Canada	1051	Centennial	Unconformity-Proterozoic Fracture bound	Exploration	UNKNOWN
Canada	113	Cigar Lake	Unconformity-Proterozoic Fracture bound	Development	> 100,000
Canada	114	Cluff Lake: Claude	Unconformity-Proterozoic Fracture bound	Depleted	10,000–25,000
Canada	117	Cluff Lake: D	Unconformity-Proterozoic Fracture bound	Depleted	2,500–5,000
Canada	999	Cluff Lake: Dominique-Jeanine	Unconformity-Proterozoic Fracture bound	Depleted	1,000–2,500
Canada	998	Cluff Lake: Dominique-Peter	Unconformity-Proterozoic Fracture bound	Depleted	10,000–25,000
Canada	115	Cluff Lake: N	Unconformity-Proterozoic Fracture bound	Depleted	1,000–2,500
Canada	1250	Cluff Lake: OP	Unconformity-Proterozoic Fracture bound	Depleted	1,000–2,500
Canada	116	Collins Bay A	Unconformity-Proterozoic Clay bound	Closed	5,000–10,000
Canada	1000	Collins Bay B	Unconformity-Proterozoic Clay bound	Depleted	10,000–25,000
Canada	1001	Collins Bay D	Unconformity-Proterozoic Fracture bound	Depleted	10,000–25,000
Canada	1251	Conecho	Quartz-pebble Conglomerate	Dormant	1,000–2500
Canada	1058	Cup Lake	Sandstone–Basal Channel	Dormant	< 500
Canada	118	Dawn Lake	Unconformity-Proterozoic Fracture bound	Dormant	2,500–5,000

Country	DepID	Deposit Name	Deposit Type	Status	Resource Range
Canada	126	Deilmann	Unconformity-Proterozoic Fracture bound	Depleted	25,000–50,000
Canada	119	Denison	Quartz-pebble Conglomerate	Closed	> 100,000
Canada	1252	Double S	Intrusive	Exploration	5,000–10,000
Canada	122	Eagle Point	Unconformity-Proterozoic Fracture bound	Operating	25,000–50,000
Canada	1145	Eco Ridge Mine (Elliot Lake)	Quartz-pebble Conglomerate	Exploration	10,000–25,000
Canada	1010	Eldorado (Port Radium)	Vein	Depleted	2,500–5,000
Canada	123	Eldorado-Hab	Vein	Depleted	500–1,000
Canada	1064	Empire B Zone	Intrusive	Unknown	500–1,000
Canada	985	End Grid	Unconformity-Proterozoic Fracture bound	Feasibility study	10,000–25,000
Canada	1065	Fish Hook Bay Mine	Vein	Depleted	< 500
Canada	986	Fond du Lac	Unconformity-Proterozoic Fracture bound	Dormant	< 500
Canada	1253	Gaertner	Unconformity-Proterozoic Fracture bound	Depleted	25,000–50,000
Canada	1067	Gear	Volcanic	Dormant	< 500
Canada	120	Greyhawk	Intrusive	Closed	500–1,000
Canada	124	Gunnar	Vein	Depleted	10,000–25,000
Canada	1069	Hab	Vein	Depleted	500–1,000
Canada	1147	Haynes	Sandstone–Basal Channel	Dormant	500–1,000
Canada	988	Horseshoe	Unconformity-Proterozoic Fracture bound	Exploration	5,000–10,000
Canada	121	Houseshol	Unknown	Unknown	5,000–10,000
Canada	1148	Hydraulic Lake	Sandstone–Basal Channel	Dormant	1,000–2,500
Canada	1073	Inda	Volcanic	Dormant	500–1,000
Canada	1075	Jacques Lake	Volcanic	Exploration	5,000–10,000
Canada	125	Jeb	Unconformity-Proterozoic Clay bound	Depleted	1,000–2,500
Canada	1003	Kiggavik Centre	Unconformity-Proterozoic Fracture bound	Feasibility study	2,500–5,000
Canada	1004	Kiggavik East	Unconformity-Proterozoic Fracture bound	Feasibility study	500–1,000
Canada	127	Kiggavik Main	Unconformity-Proterozoic Fracture bound	Feasibility study	10,000–25,000
Canada	128	Kitts	Volcanic	Dormant	1,000–2,500
Canada	1150	L	Unconformity-Proterozoic Fracture bound	Dormant	1,000–2,500
Canada	1078	Lac Cinquante	Vein	Exploration	2,500–5,000
Canada	1152	Lac Gayot	Other	Exploration	25,000–50,000
Canada	137	Lacnor	Quartz-pebble Conglomerate	Depleted	5,000–10,000
Canada	1079	Lake Cinch Mine	Vein	Dormant	< 500
Canada	1080	LaRocque Lake	Unconformity-Proterozoic Clay bound	Dormant	1,000–2,500
Canada	129	Lorado	Vein	Dormant	500–1,000
Canada	130	Madawaska	Intrusive	Closed	2,500–5,000
Canada	1083	Matoush	Other	Development	5,000–10,000
Canada	131	Maurice Bay	Unconformity-Proterozoic Fracture bound	Dormant	500–1,000
Canada	991	Maverick Zone	Unconformity-Proterozoic Fracture bound	Exploration	UNKNOWN
Canada	989	Maybelle River	Unconformity-Proterozoic Fracture bound	Exploration	UNKNOWN
Canada	132	McArthur River	Unconformity-Proterozoic Fracture bound	Operating	> 100,000
Canada	133	McClean Lake (N, SE, SW, S)	Unconformity-Proterozoic Clay bound	Dormant	10,000–25,000
Canada	134	Michelin	Volcanic	Exploration	25,000–50,000
Canada	135	Midwest	Unconformity-Proterozoic Fracture bound	Dormant	10,000–25,000
Canada	1082	Midwest A	Unconformity-Proterozoic Fracture bound	Exploration	2,500–5,000

Country	DepID	Deposit Name	Deposit Type	Status	Resource Range
Canada	1254	Millaqua	Quartz-pebble Conglomerate	Dormant	2,500–5,000
Canada	990	Millennium	Unconformity-Proterozoic Fracture bound	Exploration	10,000–25,000
Canada	142	Milliken	Quartz-pebble Conglomerate	Dormant	5,000–10,000
Canada	1088	Mont Laurier	Intrusive	Exploration	< 500
Canada	1090	Moran C	Vein	Exploration	2,500–5,000
Canada	1091	Mountain Lake	Sandstone–Tabular	Dormant	2,500–5,000
Canada	1093	Nash	Volcanic	Exploration	500–1,000
Canada	136	Nordic	Quartz-pebble Conglomerate	Dormant	10,000–25,000
Canada	1298	North Shore Double S Zone	Intrusive	Exploration	5,000–10,000
Canada	1299	North Shore Middle Zone	Intrusive	Exploration	5,000–10,000
Canada	1300	North Shore TJ Zone	Intrusive	Exploration	2,500–5,000
Canada	992	P Patch	Unconformity-Proterozoic Fracture bound	Exploration	5,000–10,000
Canada	138	Panel	Quartz-pebble Conglomerate	Unknown	10,000–25,000
Canada	1100	Paul Bay	Unconformity-Proterozoic Fracture bound	Dormant	5,000–10,000
Canada	140	Pronto	Quartz-pebble Conglomerate	Depleted	1,000–2,500
Canada	141	Quirke	Quartz-pebble Conglomerate	Closed	25,000–50,000
Canada	143	Rabbit Lake	Unconformity-Proterozoic Fracture bound	Depleted	10,000–25,000
Canada	1102	Rainbow	Volcanic	Exploration	1,000–2,500
Canada	144	Raven	Unconformity-Proterozoic Fracture bound	Exploration	2,500–5,000
Canada	1155	Rayrock	Vein	Depleted	< 500
Canada	145	Rexspar	Volcanic	Dormant	500–1,000
Canada	994	Shea Creek Anne	Unconformity-Proterozoic Fracture bound	Exploration	UNKNOWN
Canada	995	Shea Creek Colette	Unconformity-Proterozoic Fracture bound	Exploration	UNKNOWN
Canada	996	Shea Creek Kianna	Unconformity-Proterozoic Fracture bound	Exploration	UNKNOWN
Canada	1255	Silvermaque	Quartz-pebble Conglomerate	Unknown	2,500–5,000
Canada	139	Spanish American	Quartz-pebble Conglomerate	Closed	2,500–5,000
Canada	147	Stanleigh	Quartz-pebble Conglomerate	Closed	25,000–50,000
Canada	1156	Stanrock	Quartz-pebble Conglomerate	Unknown	5,000–10,000
Canada	148	Sue A	Unconformity-Proterozoic Clay bound	Dormant	500–1,000
Canada	1005	Sue B	Unconformity-Proterozoic Clay bound	Dormant	500–1,000
Canada	1006	Sue C	Unconformity-Proterozoic Fracture bound	Depleted	10,000–25,000
Canada	1256	Sue CQ	Unconformity-Proterozoic Clay bound	Unknown	UNKNOWN
Canada	1007	Sue D	Unconformity-Proterozoic Fracture bound	Dormant	1,000–2,500
Canada	1008	Sue E	Unconformity-Proterozoic Fracture bound	Dormant	2,500–5,000
Canada	1110	Tamarack	Unconformity-Proterozoic Clay bound	Dormant	5,000–10,000
Canada	1111	Thorburn Lake	Unconformity-Proterozoic Clay bound	Dormant	500–1,000
Canada	1114	Tyee	Sandstone–Basal Channel	Dormant	500–1,000
Canada	149	West Bear	Unconformity-Proterozoic Clay bound	Dormant	500–1,000

Country	DepID	Deposit Name	Deposit Type	Status	Resource Range
Canada	1117	Wolf Lake	Unconformity-Proterozoic Fracture bound	Dormant	1,000–2,500
Central African Republic	108	Bakouma	Phosphorite	Development	10,000–25,000
Chile	150	Bahia Inglesia	Phosphorite	Unknown	UNKNOWN
Chile	152	Estacion Romero	Metasomatite	Unknown	500–1,000
Chile	153	Mejillones	Phosphorite	Unknown	UNKNOWN
Chile	154	Prospecto Cerro Carmen	Metasomatite	Unknown	2,500–5,000
China	158	Baiyanghe, Junggar-Tien Shan U province	Volcanic	Depleted	500–1,000
China	156	Bashibulak, Junggar-Tien Shan U province	Sandstone–Tabular	Exploration	2,500–5,000
China	157	Beimianshi, South China U province	Sandstone–Basal Channel	Dormant	2,500–5,000
China	159	Bentou, South China U province	Other	Exploration	500–1,000
China	160	Chanziping, South China U province+B22	Other	Exploration	2,500–5,000
China	162	Chengzishan, (Tengchong mine) West Yunna	Sandstone–Basal Channel	Dormant	5,000–10,000
China	161	Chenjiazhung (Danfeng), Qilian-Quiling U	Intrusive	Exploration	500–1,000
China	163	Daladi, Junggar-Tien Shan U province	Lignite	Depleted	500–1,000
China	164	Guixi, South China U province	Volcanic	Depleted	500–1,000
China	165	Guyuan, Yinshan-Liahoe U province	Volcanic	Exploration	2,500–5,000
China	166	Hongshiquan, Qilian-Quiling U province	Intrusive	Exploration	500–1,000
China	167	Jiling, Qilian-Quiling U province	Vein	Exploration	500–1,000
China	168	Jinyinzhai	Vein	Depleted	5,000–10,000
China	169	Kujie'ertai, Junggar-Tien Shan U provinc	Sandstone–Roll Front	Operating	10,000–25,000
China	170	Lianshanguan, Yinshan-Liahoe U province	Vein	Operating	2,500–5,000
China	171	Mengqiuguer, Junggar-Tien Shan U provinc	Lignite	Depleted	500–1,000
China	172	Nuheting, Yinshan-Liahoe U province	Sandstone–Tabular	Exploration	10,000–25,000
China	173	Puquitang	Sandstone–Tabular	Depleted	500–1,000
China	174	Quinglong, Yinshan-Liahoe U province	Sandstone–Basal Channel	Dormant	5,000–10,000
China	1120	Shihongtan, Junggar-Tien Shan U Province	Sandstone–Roll Front	Operating	2,500–5,000
China	175	Tengchong, West Yunnan U province	Sandstone–Roll Front	Operating	2,500–5,000
China	176	Xiangcao	Sandstone–Roll Front	Exploration	1,000–2,500
China	180	Xiangshan (Zoujiashan), South China U province	Volcanic	Operating	10,000–25,000
China	179	Xiazhuang (Xiwang), South China U Province	Vein	Depleted	5,000–10,000
China	1121	Zaohuohao,Yinshan-Liahoe U province	Sandstone–Roll Front	Exploration	5,000–10,000
Colombia	1305	Berlin	Black Shales	Exploration	2,500–5,000
Czech Republic	181	Brevniste	Sandstone–Tabular	Depleted	10,000–25,000
Czech Republic	183	Dylen	Vein	Depleted	2,500–5,000
Czech Republic	184	Hamr	Sandstone–Tabular	Dormant	25,000–50,000
Czech Republic	185	Horni Slavkov	Vein	Depleted	2,500–5,000
Czech Republic	186	Hvezdov	Sandstone–Tabular	Dormant	10,000–25,000
Czech Republic	187	Jachymov	Vein	Depleted	10,000–25,000
Czech Republic	188	Jasenice	Vein	Depleted	2,500–5,000

Country	DepID	Deposit Name	Deposit Type	Status	Resource Range
Czech Republic	189	Javornik-Zalesi	Vein	Depleted	2,500–5,000
Czech Republic	190	Licomerice-Brezinka	Vein	Depleted	2,500–5,000
Czech Republic	191	Mimon	Sandstone–Tabular	Depleted	10,000–25,000
Czech Republic	192	Okrouhla Radoun	Vein	Depleted	2,500–5,000
Czech Republic	193	Olsi	Vein	Depleted	2,500–5,000
Czech Republic	194	Osecna-Kotel	Sandstone–Tabular	Dormant	25,000–50,000
Czech Republic	182	Polna	Vein	Dormant	1,000–2,500
Czech Republic	1160	Predborice	Vein	Depleted	< 500
Czech Republic	195	Pribram	Vein	Depleted	25,000–50,000
Czech Republic	196	Rozna	Vein	Operating	10,000–25,000
Czech Republic	1161	Slavkovice-Petrovice	Vein	Depleted	< 500
Czech Republic	1158	Sokolov Tertiary Basin	Lignite	Dormant	1,000–2,500
Czech Republic	197	Straz	Sandstone–Tabular	Operating	25,000–50,000
Czech Republic	198	Vitkov II	Vein	Depleted	10,000–25,000
Czech Republic	199	Vnitrosudetska Panev	Other	Depleted	2,500–5,000
Czech Republic	200	Zadni Chodov	Vein	Depleted	10,000–25,000
Democratic Rep. of the Congo	1163	Kalongwe	Vein	Dormant	< 500
Democratic Rep. of the Congo	1164	Kambove West	Vein	Depleted	1,000–2,500
Democratic Rep. of the Congo	433	Kamoto Principal	Vein	Dormant	1,000–2,500
Democratic Rep. of the Congo	434	Kasompi East	Vein	Dormant	500–1,000
Democratic Rep. of the Congo	1165	Luena Basin	Lignite	Dormant	5,000–10,000
Democratic Rep. of the Congo	1166	Musonoi Extension	Vein	Depleted	2,500–5,000
Democratic Rep. of the Congo	435	Shinkolobwe-Kasolo	Vein	Depleted	25,000–50,000
Democratic Rep. of the Congo	1167	Swambo	Vein	Dormant	500–1,000
Denmark	201	Kvanefjeld	Intrusive	Exploration	25,000–50,000
Finland	202	Kesankitunturi	Sandstone–Tabular	Dormant	500–1,000
Finland	203	Nuottijarvi	Phosphorite	Dormant	1,000–2,500
Finland	204	Pahtavuoma-U	Vein	Dormant	500–1,000
Finland	205	Palmottu	Intrusive	Exploration	1,000–2,500
Finland	206	Paukkajanvaara	Sandstone–Tabular	Reclaimed	< 500
Finland	207	Sokli	Intrusive	Dormant	2,500–5,000
Finland	208	Talvivaara	Black Shales	Development	2,500–5,000
Finland	209	Vihanti-U	Phosphorite	Reclamation	500–1,000
France	1266	Vendée District	Vein	Depleted	1,000–2,500
France	956	Ambert (District)	Vein	Depleted	< 500
France	1261	Augères	Vein	Depleted	500–1,000
France	210	Bellezane	Vein	Depleted	2,500–5,000
France	221	Bernardan (Le)	Vein	Depleted	5,000–10,000
France	211	Bertholene	Unconformity-Proterozoic Fracture bound	Depleted	500–1,000
France	218	Besse (La) District	Vein	Depleted	1,000–2,500
France	225	Bois Noirs (Les)	Vein	Depleted	5,000–10,000
France	969	Bondons (Les)	Vein	Depleted	< 500
France	967	Bretagne (District)	Vein	Depleted	1,000–2,500
France	226	Brugeaud (Le)	Vein	Depleted	1,000–2,500
France	222	Cellier (Le)–Villeret (Le)	Vein	Depleted	1,000–2,500
France	212	Cerilly (District)	Sandstone–Tabular	Depleted	1,000–2,500
France	219	Chapelle-Largeau (La)-Bel Air	Vein	Depleted	500–1,000
France	223	Chardon (Le)	Vein	Depleted	2,500–5,000
France	958	Château-Chinon (District)	Vein	Depleted	< 500
France	220	Commanderie (La)	Vein	Depleted	2,500–5,000
France	971	Corrèze (District)	Vein	Depleted	< 500
France	213	Coutras	Sandstone–Tabular	Dormant	10,000–25,000
France	972	Creuse (District)	Vein	Depleted	500–1,000

Country	DepID	Deposit Name	Deposit Type	Status	Resource Range
France	939	Ecarpiere (L')	Vein	Depleted	2,500–5,000
France	963	Failles Sud et Centrales	Sandstone–Tectonic/Lithologic	Depleted	500–1,000
France	215	Fanay–Les Sagnes	Vein	Depleted	2,500–5,000
France	224	Fraisse (Le)-Les Gorces	Vein	Depleted	1,000–2,500
France	216	Grury-Luzy district	Vein	Depleted	500–1,000
France	217	Hyverneresse	Vein	Depleted	500–1,000
France	230	Lodève District	Sandstone–Tectonic/Lithologic	Depleted	500–1,000
France	227	Loges (Les)	Vein	Depleted	500–1,000
France	1262	Marche District	Vein	Depleted	500–1,000
France	961	Mares (Les)	Sandstone–Tectonic/Lithologic	Depleted	500–1,000
France	232	Margnac-Peny	Vein	Depleted	5,000–10,000
France	1263	Mas d'Alary	Vein	Depleted	1,000–2,500
France	231	Mas Lavayre	Sandstone–Tectonic/Lithologic	Depleted	10,000–25,000
France	233	Montulat	Vein	Dormant	1,000–2,500
France	234	Pen Ar Ran	Vein	Depleted	500–1,000
France	235	Piegut- La Cote Moreau	Vein	Depleted	< 500
France	228	Pierres-Plantées (Les)	Vein	Depleted	1,000–2,500
France	237	Saint Hippolyte	Black Shales	Dormant	1,000–2,500
France	236	Saint.Pierre Du Cantal	Sandstone–Basal Channel	Depleted	1,000–2,500
France	1264	Schaenzel	Black Shales	Dormant	500–1,000
France	974	Siège MCO	Vein	Depleted	1,000–2,500
France	1265	Teufelsloch-Warik	Black Shales	Dormant	1,000–2,500
France	965	Vénachat	Vein	Depleted	500–1,000
Gabon	242	Mounana	Sandstone–Tectonic/Lithologic	Depleted	5,000–10,000
Gabon	239	Bangombé	Sandstone–Tectonic/Lithologic	Dormant	< 500
Gabon	240	Boyindzi	Sandstone–Tectonic/Lithologic	Depleted	1,000–2,500
Gabon	241	Mikouloungou	Sandstone–Tectonic/Lithologic	Depleted	1,000–2,500
Gabon	243	Okélobondo Nord	Sandstone–Tectonic/Lithologic	Depleted	1,000–2,500
Gabon	900	Okélobondo Satellite Nord	Sandstone–Tabular	Depleted	< 500
Gabon	899	Okélobondo Satellite Sud	Sandstone–Tabular	Depleted	< 500
Gabon	898	Okélobondo Sud	Sandstone–Tectonic/Lithologic	Depleted	1,000–2,500
Gabon	244	Oklo	Sandstone–Tectonic/Lithologic	Depleted	10,000–25,000
Germany	245	Annaberg	Vein	Depleted	500–1,000
Germany	246	Antonsthal (Weisser Hirsch)	Vein	Depleted	500–1,000
Germany	247	Culmitzsch	Sandstone–Tabular	Depleted	10,000–25,000
Germany	248	Freital-Gittersee	Lignite	Closed	2,500–5,000
Germany	249	Grossschloppen	Vein	Dormant	1,000–2,500
Germany	250	Johanngeorgenstadt	Vein	Depleted	5,000–10,000
Germany	251	Koenigstein	Sandstone–Tabular	Depleted	10,000–25,000
Germany	252	Menzenschwand	Vein	Dormant	2,500–5,000
Germany	253	Muellenbach	Sandstone–Tabular	Dormant	2,500–5,000
Germany	255	Niederschlema-Alberoda	Vein	Depleted	> 100,000
Germany	953	Oberschlema	Vein	Unknown	5,000–10,000
Germany	254	Ronneburg Ore Field	Black Shales	Closed	> 100,000
Germany	256	Schneckenstein	Vein	Depleted	500–1,000
Germany	257	Tellerhauser	Vein	Closed	1,000–2,500
Germany	258	Waeldel & Hoehensteinweg/Poppenreuth	Vein	Dormant	1,000–2,500
Germany	259	Zobes	Vein	Depleted	5,000–10,000

Country	DepID	Deposit Name	Deposit Type	Status	Resource Range
Guinea	1267	Firawa	Vein	Exploration	UNKNOWN
Guyana	1306	Aricheng	Vein	Exploration	2,500–5,000
Hungary	260	Mecsek	Sandstone–Tabular	Closed	25,000–50,000
India	261	Bhatin	Vein	Operating	1,000–2,500
India	262	Domiasat	Sandstone–Tabular	Fully explored	5,000–10,000
India	263	Jaduguda	Vein	Operating	5,000–10,000
India	264	Koppunuru	Unconformity-Proterozoic Fracture bound	Exploration	500–1,000
India	265	Lambapur	Unconformity-Proterozoic Fracture bound	Fully explored	1,000–2,500
India	266	Narwapahar	Vein	Operating	10,000–25,000
India	273	Peddagattu	Unconformity-Proterozoic Fracture bound	Exploration	5,000–10,000
India	268	Rohil	Metasomatite	Exploration	2,500–5,000
India	269	Tummalapalle–Rachakuntapalle	Other	Operating	10,000–25,000
India	270	Turamdih	Vein	Operating	2,500–5,000
India	272	Wahkyn	Sandstone–Tabular	Exploration	2,500–5,000
Indonesia	954	Lemajung	Vein	Dormant	500–1,000
Indonesia	274	Remaja-Hitam	Vein	Dormant	1,000–2,500
Indonesia	267	Rirang	Vein	Dormant	< 500
Iran, Islamic Republic of	275	Saghand	Metasomatite	Development	1,000–2,500
Italy	276	Novazza	Volcanic	Dormant	1,000–2,500
Italy	955	Valvedello	Volcanic	Dormant	2,500–5,000
Japan	281	Ningyo-Toge Ore Field	Sandstone–Roll Front	Dormant	1,000–2,500
Japan	282	Tono Ore Field	Sandstone–Roll Front	Dormant	5,000–10,000
Jordan	277	Al-Abiad	Phosphorite	Dormant	UNKNOWN
Jordan	278	Al-Hassa	Phosphorite	Dormant	UNKNOWN
Jordan	279	Eshidia	Phosphorite	Dormant	UNKNOWN
Jordan	280	Ruseita	Phosphorite	Dormant	UNKNOWN
Jordan	1168	Siwaqa	Phosphorite	Dormant	25,000–50,000
Kazakhstan	283	Agashskoe	Vein	Dormant	5,000–10,000
Kazakhstan	1169	Akdala	Unknown	Unknown	10,000–25,000
Kazakhstan	285	Assarchik	Sandstone–Roll Front	Dormant	10,000–25,000
Kazakhstan	286	Balkashinskoye	Vein	Dormant	2,500–5,000
Kazakhstan	288	Bezymyannoye	Volcanic	Dormant	500–1,000
Kazakhstan	289	Botaburum	Vein	Depleted	5,000–10,000
Kazakhstan	290	Budennovskoye	Sandstone–Roll Front	Standby	25,000–50,000
Kazakhstan	291	Burlukskoye	Vein	Dormant	2,500–5,000
Kazakhstan	292	Chaglinskoye	Vein	Dormant	10,000–25,000
Kazakhstan	293	Chayan	Sandstone–Roll Front	Dormant	500–1,000
Kazakhstan	294	Daba	Volcanic	Dormant	5,000–10,000
Kazakhstan	295	Dergachevskoye	Vein	Depleted	500–1,000
Kazakhstan	297	Djusandalynskoye	Vein	Partially explored	5,000–10,000
Kazakhstan	298	Dzhidely	Volcanic	Depleted	2,500–5,000
Kazakhstan	299	Fevralskoe	Vein	Dormant	2,500–5,000
Kazakhstan	300	Glubinnoe	Vein	Dormant	5,000–10,000
Kazakhstan	301	Grachevskoye	Vein	Depleted	10,000–25,000
Kazakhstan	302	Granitnoye	Surficial	Dormant	500–1,000
Kazakhstan	303	Inkai	Sandstone–Roll Front	Development	50,000–100,000
Kazakhstan	304	Irkol	Sandstone–Roll Front	Dormant	25,000–50,000
Kazakhstan	305	Ishimskoye	Vein	Depleted	5,000–10,000
Kazakhstan	306	Kamyshevoe	Vein	Dormant	10,000–25,000
Kazakhstan	307	Kanzhugan	Sandstone–Roll Front	Operating	50,000–100,000
Kazakhstan	308	Karakoyn	Sandstone–Roll Front	Dormant	UNKNOWN
Kazakhstan	309	Karamurun North	Sandstone–Roll Front	Operating	25,000–50,000
Kazakhstan	310	Karamurun South	Sandstone–Roll Front	Operating	25,000–50,000
Kazakhstan	311	Karyntarynskoye	Phosphorite	Dormant	UNKNOWN
Kazakhstan	313	Kharasan	Sandstone–Roll Front	Development	50,000–100,000
Kazakhstan	314	Koksorskoe	Vein	Dormant	500–1,000
Kazakhstan	315	Koldzhat	Lignite	Dormant	25,000–50,000
Kazakhstan	316	Kopalysai	Sandstone–Roll Front	Dormant	1,000–2,500

Country	DepID	Deposit Name	Deposit Type	Status	Resource Range
Kazakhstan	317	Kostobe	Volcanic	Depleted	500–1,000
Kazakhstan	320	Kurdai	Vein	Depleted	1,000–2,500
Kazakhstan	322	Kyzylkol	Vein	Depleted	500–1,000
Kazakhstan	321	Kyzylsai	Vein	Depleted	2,500–5,000
Kazakhstan	323	Kyzyltu	Sandstone–Roll Front	Dormant	10,000–25,000
Kazakhstan	325	Lunnoye	Sandstone–Roll Front	Dormant	500–1,000
Kazakhstan	326	Manybai	Vein	Depleted	10,000–25,000
Kazakhstan	327	Melovoye	Phosphorite	Depleted	25,000–50,000
Kazakhstan	328	Moynkum	Sandstone–Roll Front	Operating	50,000–100,000
Kazakhstan	329	Mynkuduk	Sandstone–Roll Front	Operating	> 100,000
Kazakhstan	330	Nizhneylyiskoye	Lignite	Dormant	25,000–50,000
Kazakhstan	332	Panfilovskoye	Vein	Dormant	1,000–2,500
Kazakhstan	333	Semizbai	Sandstone–Basal Channel	Dormant	10,000–25,000
Kazakhstan	334	Shatskoe	Vein	Dormant	500–1,000
Kazakhstan	335	Shokpak	Vein	Dormant	2,500–5,000
Kazakhstan	336	Sholak-Espe	Sandstone–Roll Front	Dormant	5,000–10,000
Kazakhstan	337	Shorly	Volcanic	Dormant	1,000–2,500
Kazakhstan	338	Slavyanskoye	Vein	Dormant	5,000–10,000
Kazakhstan	1170	South Inkai	Sandstone–Roll Front	Operating	10,000–25,000
Kazakhstan	339	Suluchekinskoye	Sandstone–Roll Front	Dormant	25,000–50,000
Kazakhstan	341	Talas	Sandstone–Basal Channel	Dormant	500–1,000
Kazakhstan	342	Tasmurunskoye	Phosphorite	Dormant	2,500–5,000
Kazakhstan	343	Tastykolskoye	Vein	Depleted	1,000–2,500
Kazakhstan	344	Taybagarskoye	Phosphorite	Dormant	5,000–10,000
Kazakhstan	345	Tomakskoye	Phosphorite	Dormant	5,000–10,000
Kazakhstan	942	Tortkuduk	Sandstone–Roll Front	Development	25,000–50,000
Kazakhstan	346	Ulken-Akzhal	Volcanic	Dormant	1,000–2,500
Kazakhstan	347	Uvanas	Sandstone–Roll Front	Operating	10,000–25,000
Kazakhstan	348	Victorovskoe	Vein	Dormant	2,500–5,000
Kazakhstan	349	Vostok	Vein	Operating	10,000–25,000
Kazakhstan	350	Yuzhno-Manybayskoe	Vein	Dormant	500–1,000
Kazakhstan	353	Zaozernoye	Vein	Dormant	10,000–25,000
Kazakhstan	352	Zarechnoye	Sandstone–Roll Front	Development	10,000–25,000
Kazakhstan	354	Zhalpak	Sandstone–Roll Front	Dormant	10,000–25,000
Kazakhstan	355	Zhautkan	Sandstone–Roll Front	Dormant	2,500–5,000
Kazakhstan	356	Zvyozdnoe	Vein	Development	5,000–10,000
Korea, Republic of	436	Ogcheon Deposits	Black Shales	Dormant	10,000–25,000
Kyrgyzstan	1171	Aramsu	Unknown	Exploration	UNKNOWN
Kyrgyzstan	357	Mailisai	Vein	Depleted	500–1,000
Kyrgyzstan	358	Mailisu	Vein	Depleted	1,000–2,500
Kyrgyzstan	359	Shakaptar	Vein	Depleted	500–1,000
Kyrgyzstan	1174	Sogul	Black Shales	Exploration	UNKNOWN
Kyrgyzstan	1175	Sumsar	Unknown	Exploration	UNKNOWN
Kyrgyzstan	360	Turakovak	Lignite	Depleted	2,500–5,000
Madagascar	361	Antsirabe	Sandstone–Tabular	Dormant	< 500
Madagascar	362	Folakara	Sandstone–Roll Front	Dormant	5,000–10,000
Madagascar	363	Tranomaro	Intrusive	Exploration	1,000–2,500
Malawi	1268	Kanyika	Intrusive	Exploration	2,500–5,000
Malawi	372	Kayelekera	Sandstone–Tabular	Development	5,000–10,000
Mali	1176	Falea	Sandstone–Roll Front	Exploration	2,500–5,000
Mauritania	1177	Bir En Nar	Vein	Exploration	UNKNOWN
Mexico	364	Coneto	Volcanic	Dormant	500–1,000
Mexico	365	El Chapote-Diana	Sandstone–Roll Front	Dormant	1,000–2,500
Mexico	369	El Nopal	Volcanic	Dormant	1,000–2,500
Mexico	366	La Coma	Sandstone–Roll Front	Dormant	500–1,000
Mexico	367	La Sierrita	Sandstone–Roll Front	Dormant	2,500–5,000
Mexico	368	Los Amoles	Volcanic	Dormant	1,000–2,500
Mexico	370	Santa Catarina Tayata	Volcanic	Dormant	< 500
Mexico	371	Santo Domingo	Phosphorite	Dormant	50,000–100,000
Mongolia	373	Dornod (District)	Volcanic	Dormant	25,000–50,000
Mongolia	374	Gurvanbulak	Volcanic	Dormant	10,000–25,000
Mongolia	1178	Khairkhan	Sandstone–Tabular	Exploration	2,500–5,000
Mongolia	375	Kharat	Sandstone–Tabular	Dormant	10,000–25,000

Country	DepID	Deposit Name	Deposit Type	Status	Resource Range
Mongolia	376	Mardaingol	Volcanic	Dormant	1,000–2,500
Mongolia	377	Nars	Sandstone–Tabular	Dormant	2,500–5,000
Mongolia	378	Nemer	Volcanic	Dormant	2,500–5,000
Mongolia	1179	Ulaan Nuur	Sandstone–Tabular	Exploration	5,000–10,000
Morocco	379	Gantour, Ganntour	Phosphorite	Dormant	25,000–50,000
Morocco	380	Khouribga (Uran)	Phosphorite	Dormant	25,000–50,000
Morocco	381	Meskala (Uran)	Phosphorite	Dormant	25,000–50,000
Morocco	382	Oued Eddahab (Uran)	Phosphorite	Dormant	25,000–50,000
Namibia	383	Auris	Intrusive	Dormant	500–1,000
Namibia	1180	Aussinanis	Surficial	Exploration	2,500–5,000
Namibia	384	Engo Valley	Sandstone–Basal Channel	Exploration	1,000–2500
Namibia	1269	Garnet Valley	Intrusive	Exploration	10,000–25,000
Namibia	385	Goanikontes	Intrusive	Dormant	5,000–10,000
Namibia	1181	Goanikontes Anomaly A	Intrusive	Exploration	25,000–50,000
Namibia	386	Hakskeen	Surficial	Dormant	500–1,000
Namibia	1182	Ida Central	Intrusive	Exploration	1,000–2,500
Namibia	1183	Klein Spitzkoppe	Unknown	Unknown	1,000–2,500
Namibia	387	Klein Trekkopje	Surficial	Development	25,000–50,000
Namibia	388	Langer Heinrich	Surficial	Operating	25,000–50,000
Namibia	1184	Marenica	Surficial	Exploration	5,000–10,000
Namibia	389	Mile 72	Surficial	Dormant	< 500
Namibia	1270	Namib Park	Surficial	Exploration	2,500–5,000
Namibia	1271	New Camp	Intrusive	Exploration	1,000–2,500
Namibia	1272	Oryx	Surficial	Exploration	2,500–5,000
Namibia	1273	Oryx extension	Surficial	Exploration	500–1,000
Namibia	1307	Oshively	Intrusive	Exploration	2,500–5,000
Namibia	390	Roessing	Intrusive	Operating	> 100,000
Namibia	1274	Rossing South	Intrusive	Exploration	25,000–50,000
Namibia	1185	Trekkopje	Surficial	Development	2,500–5,000
Namibia	1186	Tubas	Surficial	Exploration	10,000–25,000
Namibia	391	Tumas	Surficial	Exploration	2,500–5,000
Namibia	392	Valencia	Intrusive	Exploration	10,000–25,000
Niger	404	Abakorum	Sandstone–Tabular	Dormant	10,000–25,000
Niger	396	Akola	Sandstone–Tabular	Operating	25,000–50,000
Niger	397	Akouta Nord	Sandstone–Tabular	Operating	25,000–50,000
Niger	398	Akouta Sud	Sandstone–Tabular	Dormant	10,000–25,000
Niger	1187	Arcadie	Sandstone–Tabular	Dormant	5,000–10,000
Niger	1188	Argus	Sandstone–Tabular	Dormant	1,000–2,500
Niger	399	Ariege	Sandstone–Tabular	Operating	10,000–25,000
Niger	401	Arlette	Sandstone–Tabular	Depleted	10,000–25,000
Niger	403	Artois	Sandstone–Tabular	Development	10,000–25,000
Niger	1189	Azelik	Sandstone–Tabular	Exploration	10,000–25,000
Niger	897	Ebala	Sandstone–Tabular	Exploration	25,000–50,000
Niger	394	Ebba Nord	Sandstone–Tabular	Development	10,000–25,000
Niger	395	Ebba Sud	Sandstone–Tabular	Development	5,000–10,000
Niger	405	Imouraren	Sandstone–Roll Front	Development	> 100,000
Niger	1275	In Gall	Sandstone–Tabular	Exploration	1,000–2,500
Niger	1190	Madaouela	Sandstone–Tabular	Exploration	5,000–10,000
Niger	895	Marianne	Sandstone–Roll Front	Exploration	2,500–5,000
Niger	896	Marthe	Sandstone–Roll Front	Exploration	UNKNOWN
Niger	894	Maryline	Sandstone–Roll Front	Exploration	2,500–5,000
Niger	1191	Nord Somair	Sandstone–Tabular	Dormant	10,000–25,000
Niger	890	Tabelle	Sandstone–Tabular	Development	2,500–5,000
Niger	892	Takriza	Sandstone–Tabular	Depleted	5,000–10,000
Niger	893	Tamgak	Sandstone–Tabular	Exploration	25,000–50,000
Niger	407	Tamou	Sandstone–Tabular	Operating	10,000–25,000
Niger	1192	Taossa	Sandstone–Tabular	Dormant	2,500–5,000
Niger	408	Taza Nord	Sandstone–Tabular	Depleted	2,500–5,000
Niger	891	Taza Sud	Sandstone–Tabular	Depleted	5,000–10,000
Niger	1193	Teguidda	Sandstone–Tabular	Dormant	10,000–25,000
Pakistan	409	Baghal Chur	Sandstone–Roll Front	Depleted	< 500
Pakistan	410	Qabul Khel	Sandstone–Tabular	Development	500–1,000
Paraguay	1195	Yuti	Volcanic	Exploration	2,500–5,000

Country	DepID	Deposit Name	Deposit Type	Status	Resource Range
Peru	411	Colquijirca	Other	Dormant	500–1,000
Peru	1196	Corachapi	Volcanic	Exploration	2,500–5,000
Peru	412	Macusani District	Volcanic	Exploration	2,500–5,000
Peru	413	Turmalina	Collapse Breccia Pipe	Dormant	500–1,000
Peru	414	Vilacabamba	Vein	Dormant	500–1,000
Poland	415	Gzmiaca	Sandstone–Tabular	Dormant	1,000–2,500
Poland	416	Kowary	Vein	Dormant	500–1,000
Poland	417	Krynica Morska	Sandstone–Tabular	Dormant	2,500–5,000
Poland	418	Okrzeszyn	Other	Dormant	1,000–2,500
Poland	419	Radoniow	Vein	Dormant	500–1,000
Poland	420	Rajsk	Black Shales	Dormant	5,000–10,000
Poland	421	Wambierzyce	Black Shales	Dormant	1,000–2,500
Portugal	422	Bica	Vein	Depleted	UNKNOWN
Portugal	423	Castelejo	Vein	Depleted	UNKNOWN
Portugal	424	Chavelhos	Vein	Dormant	UNKNOWN
Portugal	425	Cunha Baixa	Vein	Depleted	UNKNOWN
Portugal	426	Freixiosa	Vein	Dormant	UNKNOWN
Portugal	427	Mestras	Vein	Dormant	UNKNOWN
Portugal	428	Nisa	Vein	Dormant	2,500–5,000
Portugal	429	Pedreiros	Vein	Depleted	UNKNOWN
Portugal	430	Pinhal Do Souto	Vein	Dormant	UNKNOWN
Portugal	431	Quinta Do Bispo	Vein	Depleted	UNKNOWN
Portugal	432	Urgeirica	Vein	Depleted	1,000–2,500
Romania	437	Arieseni	Vein	Closed	500–1,000
Romania	438	Avram Iancu	Vein	Closed	500–1,000
Romania	439	Baita Bihor	Sandstone–Tabular	Closed	10,000–25,000
Romania	440	Bicazu Ardelean	Vein	Dormant	500–1,000
Romania	441	Botusana	Vein	Closed	1,000–2,500
Romania	442	Budurease	Sandstone–Tabular	Fully explored	500–1,000
Romania	443	Ciudanovita	Sandstone–Tabular	Depleted	500–1,000
Romania	444	Conop	Vein	Dormant	500–1,000
Romania	445	Crucea	Vein	Operating	2,500–5,000
Romania	446	Dobrei North	Sandstone–Tabular	Closed	500–1,000
Romania	447	Dobrei South	Sandstone–Tabular	Operating	1,000–2,500
Romania	448	Hojda Magura	Vein	Dormant	500–1,000
Romania	450	Ilisova	Volcanic	Dormant	500–1,000
Romania	451	Milova	Vein	Dormant	500–1,000
Romania	452	Natra	Sandstone–Tabular	Depleted	500–1,000
Romania	453	Paiuseni	Vein	Dormant	500–1,000
Romania	454	Rachitele	Sandstone–Tabular	Dormant	500–1,000
Romania	455	Ranusa	Sandstone–Tabular	Dormant	1,000–2,500
Romania	456	Tulghes	Vein	Operating	5,000–10,000
Russian Federation	457	Agdinskoye	Metasomatite	Dormant	1,000–2,500
Russian Federation	460	Antei	Vein	Operating	25,000–50,000
Russian Federation	461	Argunskoye	Vein	Development	25,000–50,000
Russian Federation	463	Badyelskoye	Lignite	Dormant	5,000–10,000
Russian Federation	1197	Barun-Ulacha	Volcanic	Dormant	1,000–2,500
Russian Federation	466	Belskoje	Lignite	Dormant	5,000–10,000
Russian Federation	468	Beryozovoye	Vein	Development	2,500–5,000
Russian Federation	469	Beshtau	Vein	Depleted	500–1,000
Russian Federation	472	Briketno-Zheltuhinskoye	Lignite	Dormant	5,000–10,000
Russian Federation	474	Buyanovskoye	Sandstone–Roll Front	Dormant	5,000–10,000
Russian Federation	475	Bykogorskoye	Vein	Depleted	1,000–2,500
Russian Federation	477	Bytuguchag	Vein	Depleted	2,500–5,000
Russian Federation	478	Chaika	Volcanic	Dormant	2,500–5,000
Russian Federation	479	Chaplinskoye	Volcanic	Dormant	2,500–5,000
Russian Federation	481	Cherepanovskoye	Surficial	Dormant	2,500–5,000
Russian Federation	482	Crystalnoye	Vein	Dormant	2,500–5,000
Russian Federation	485	Dalmatovskoye	Sandstone–Basal Channel	Operating	10,000–25,000
Russian Federation	483	Dalneye	Volcanic	Dormant	2,500–5,000
Russian Federation	484	Dobrovolnoye	Sandstone–Basal Channel	Dormant	5,000–10,000
Russian Federation	486	Druzhnoye	Metasomatite	Development	50,000–100,000
Russian Federation	487	Dybryn	Sandstone–Basal Channel	Development	2,500–5,000

Country	DepID	Deposit Name	Deposit Type	Status	Resource Range
Russian Federation	488	Dzhigda	Unknown	Exploration	2,500–5,000
Russian Federation	492	Gornoye	Vein	Development	5,000–10,000
Russian Federation	493	Imskoye	Sandstone–Roll Front	Fully explored	10,000–25,000
Russian Federation	494	Interesnoye	Metasomatite	Development	2,500–5,000
Russian Federation	495	Istochnoe	Sandstone–Basal Channel	Exploration	1,000–2,500
Russian Federation	497	Karhu	Unconformity-Proterozoic Fracture bound	Exploration	10,000–25,000
Russian Federation	500	Kedrovoye	Sandstone–Roll Front	Dormant	2,500–5,000
Russian Federation	503	Khiagdinskoye	Sandstone–Basal Channel	Development	10,000–25,000
Russian Federation	504	Khokhlovskoye	Sandstone–Basal Channel	Exploration	10,000–25,000
Russian Federation	505	Kolichikan	Sandstone–Basal Channel	Development	2,500–5,000
Russian Federation	507	Koretkondinskoe	Sandstone–Basal Channel	Exploration	2,500–5,000
Russian Federation	508	Kosmozero	Metasomatite	Exploration	2,500–5,000
Russian Federation	509	Krasnyi Kamen	Vein	Depleted	500–1,000
Russian Federation	512	Labyshkoye	Vein	Dormant	1,000–2,500
Russian Federation	513	Lastochka	Volcanic	Dormant	2,500–5,000
Russian Federation	515	Luchistoye	Volcanic	Operating	10,000–25,000
Russian Federation	516	Malinovskoye	Sandstone–Basal Channel	Exploration	10,000–25,000
Russian Federation	517	Malo-Tulukuevskoye	Volcanic	Development	10,000–25,000
Russian Federation	518	Martovskoye	Volcanic	Operating	2,500–5,000
Russian Federation	520	Meridionalnoye	Vein	Dormant	2,500–5,000
Russian Federation	521	Molodezhnoye	Vein	Dormant	2,500–5,000
Russian Federation	522	Namaru	Sandstone–Basal Channel	Exploration	2,500–5,000
Russian Federation	524	Novogodneye	Vein	Operating	2,500–5,000
Russian Federation	526	Oktyabrskoye	Volcanic	Operating	10,000–25,000
Russian Federation	527	Olovskoye	Volcanic	Development	10,000–25,000
Russian Federation	528	Osenneye	Vein	Dormant	2,500–5,000
Russian Federation	530	Prigorodnoye	Sandstone–Roll Front	Dormant	2,500–5,000
Russian Federation	531	Primorskoye	Sandstone–Roll Front	Dormant	5,000–10,000
Russian Federation	533	Pyatilentneye	Vein	Dormant	2,500–5,000
Russian Federation	534	Radionovskoye	Surficial	Dormant	2,500–5,000
Russian Federation	537	Repyovskoye	Lignite	Dormant	2,500–5,000
Russian Federation	538	Rjabinovoye	Volcanic	Dormant	2,500–5,000
Russian Federation	539	Sanarskoye	Surficial	Depleted	2,500–5,000
Russian Federation	1238	Severnoe	Metasomatite	Development	50,000–100,000
Russian Federation	544	Shirondukuevskoye	Volcanic	Dormant	5,000–10,000
Russian Federation	549	Solonechnoye	Volcanic	Dormant	1,000–2,500
Russian Federation	550	Srednaya Padma	Metasomatite	Dormant	2,500–5,000
Russian Federation	551	Stepnovskoye	Phosphorite	Dormant	10,000–25,000
Russian Federation	553	Stepnoye	Sandstone–Tabular	Dormant	10,000–25,000
Russian Federation	555	Streltsovskoye	Volcanic	Operating	50,000–100,000
Russian Federation	559	Tetrakhskoye	Sandstone–Basal Channel	Exploration	5,000–10,000
Russian Federation	562	Tsarevskoye	Metasomatite	Dormant	2,500–5,000
Russian Federation	563	Tsentralnoye	Lignite	Dormant	2,500–5,000
Russian Federation	564	Tulukuevskoye	Vein	Depleted	25,000–50,000
Russian Federation	565	Urulynguevskoye	Vein	Dormant	2,500–5,000
Russian Federation	566	Ust-Uyukskoye	Sandstone–Tabular	Dormant	10,000–25,000
Russian Federation	567	Verkhnaya Padma	Metasomatite	Partially explored	500–1,000
Russian Federation	568	Vershinnoye	Sandstone–Basal Channel	Exploration	5,000–10,000
Russian Federation	571	Vesenneye-Padma	Metasomatite	Dormant	500–1,000
Russian Federation	569	Vesenneye-Streltsovsk	Volcanic	Dormant	500–1,000
Russian Federation	572	Vinogradovskoye	Surficial	Exploration	2,500–5,000
Russian Federation	573	Vitlausskoye	Surficial	Dormant	2,500–5,000
Russian Federation	576	Yubileinoye	Volcanic	Operating	5,000–10,000
Russian Federation	578	Yugo-Zapadonoye	Vein	Dormant	2,500–5,000
Russian Federation	489	Yuzhnoe (Elkon; Kurung; Elkonskoe Plato; Druzhnoye, Neprohodimoe)	Metasomatite	Development	> 100,000
Russian Federation	580	Zheglovskoe	Sandstone–Basal Channel	Exploration	10,000–25,000
Russian Federation	581	Zherlovoye	Vein	Operating	2,500–5,000
Russian Federation	583	Zjulzinskoye	Sandstone–Roll Front	Exploration	2,500–5,000
Russian Federation	584	Zmeika	Vein	Depleted	2,500–5,000

Country	DepID	Deposit Name	Deposit Type	Status	Resource Range
Saudi Arabia	1200	Ghurayyah	Intrusive	Exploration	25,000–50,000
Senegal	1201	Saraya	Vein	Exploration	1,000–2,500
Serbia	852	Cigankulja	Vein	Unknown	500–1,000
Serbia	853	Dojkinci	Sandstone–Tabular	Unknown	1,000–2,500
Serbia	854	Mezdreja	Vein	Unknown	500–1,000
Serbia	855	Paun Stena	Vein	Unknown	500–1,000
Serbia	856	Ribarice	Sandstone–Tabular	Unknown	500–1,000
Serbia	857	Srednje Brdo	Sandstone–Tabular	Unknown	500–1,000
Serbia	858	Srneci Do	Vein	Unknown	1,000–2,500
Slovakia	1203	Kuriskova	Volcanic	Exploration	10,000–25,000
Slovakia	1204	Novoveska Huta	Volcanic	Exploration	5,000–10,000
Slovenia	605	Krivorvsk	Unknown	Unknown	UNKNOWN
Slovenia	606	Zirovski Vrh	Sandstone–Roll Front	Dormant	5,000–10,000
Somalia	603	Alio Ghelle	Metasomatite	Dormant	5,000–10,000
Somalia	604	Dusa Mareb	Surficial	Dormant	5,000–10,000
Somalia	1276	Mudug Province	Surficial	Dormant	2,500–5,000
South Africa	1208	Beaufort West	Sandstone–Tabular	Unknown	10,000–25,000
South Africa	1277	Beisa	Quartz-pebble Conglomerate	Unknown	UNKNOWN
South Africa	585	Blyvooruitzicht	Quartz-pebble Conglomerate	Development	UNKNOWN
South Africa	586	Buffelsfontein	Quartz-pebble Conglomerate	Development	5,000–10,000
South Africa	587	Chemwes-Stilfontein	Quartz-pebble Conglomerate	Dormant	UNKNOWN
South Africa	1279	Cooke Section (Randfontein mine)	Quartz-pebble Conglomerate	Unknown	50,000–100,000
South Africa	1209	Denny Dalton	Quartz-pebble Conglomerate	Unknown	5,000–10,000
South Africa	588	Driefontein Mine	Quartz-pebble Conglomerate	Dormant	UNKNOWN
South Africa	1280	East Rand (tailing project)	Quartz-pebble Conglomerate	Dormant	5,000–10,000
South Africa	596	Ezulwini	Quartz-pebble Conglomerate	Development	50,000–100,000
South Africa	589	Free State Geduld Mine	Quartz-pebble Conglomerate	Dormant	5,000–10,000
South Africa	590	Harmony	Quartz-pebble Conglomerate	Dormant	UNKNOWN
South Africa	591	Hartebeestfontein	Quartz-pebble Conglomerate	Operating	5,000–10,000
South Africa	1281	Henkries	Quartz-pebble Conglomerate	Dormant	1,000–2,500
South Africa	1282	Klerksdorp	Quartz-pebble Conglomerate	Unknown	UNKNOWN
South Africa	592	Loraine	Quartz-pebble Conglomerate	Dormant	UNKNOWN
South Africa	1207	Mudug Province	Unknown	Unknown	2,500–5,000
South Africa	1283	Old Randfontein Section	Quartz-pebble Conglomerate	Dormant	50,000–100,000
South Africa	593	Phalabora	Intrusive	Closed	2,500–5,000
South Africa	594	President Brand Mine	Quartz-pebble Conglomerate	Operating	2,500–5,000
South Africa	595	President Steyn	Quartz-pebble Conglomerate	Operating	5,000–10,000
South Africa	1212	Rietkuil Dominion	Quartz-pebble Conglomerate	Exploration	25,000–50,000
South Africa	1213	Ryst Kuil	Sandstone–Basal Channel	Exploration	10,000–25,000
South Africa	597	St.Helena (Beisa Section)	Quartz-pebble Conglomerate	Dormant	10,000–25,000
South Africa	598	Vaal Reefs Mines	Quartz-pebble Conglomerate	Operating	50,000–100,000
South Africa	1286	Vaal River area	Quartz-pebble Conglomerate	Operating	50,000–100,000
South Africa	600	Western Area Mine	Quartz-pebble Conglomerate	Closed	UNKNOWN

Country	DepID	Deposit Name	Deposit Type	Status	Resource Range
South Africa	601	Western Deep Levels Mine	Quartz-pebble Conglomerate	Dormant	10,000–25,000
South Africa	602	Western Holdings	Quartz-pebble Conglomerate	Unknown	UNKNOWN
South Africa	599	Western Rand Goldfields Mines (Uranium Section)	Quartz-pebble Conglomerate	Development	UNKNOWN
Spain	607	Acehuche Ceclavin	Unknown	Unknown	UNKNOWN
Spain	608	Alameda	Unknown	Unknown	UNKNOWN
Spain	609	Andujar	Vein	Dormant	UNKNOWN
Spain	610	Cabeza de Araya	Unknown	Unknown	UNKNOWN
Spain	1308	El Olivar	Vein	Exploration	500–1,000
Spain	612	El Pedregal	Vein	Dormant	1,000–2,500
Spain	613	Ezperanza	Unknown	Unknown	UNKNOWN
Spain	1215	Gambuta	Vein	Exploration	2,500–5,000
Spain	614	Intermedia	Vein	Dormant	UNKNOWN
Spain	615	Mazarete	Sandstone–Tabular	Dormant	2,500–5,000
Spain	616	Mina Fe	Vein	Depleted	5,000–10,000
Spain	617	Navalmoral	Unknown	Unknown	UNKNOWN
Spain	618	Retortillo	Vein	Exploration	2,500–5,000
Spain	1309	Santidad	Vein	Exploration	1,000–2,500
Spain	619	Villavieja	Unknown	Unknown	UNKNOWN
Spain	611	Zarcina	Vein	Dormant	500–1,000
Spain	1310	Zona 7	Vein	Exploration	< 500
Sweden	620	Arvidsjaur	Metasomatite	Dormant	UNKNOWN
Sweden	1217	Bjorkramyran	Vein	Dormant	1,000–2,500
Sweden	1218	Duobblon	Volcanic	Dormant	2,500–5,000
Sweden	1219	Klappibacken	Vein	Exploration	1,000–2,500
Sweden	1220	Kvarnan	Metamorphic	Dormant	1,000–2,500
Sweden	1221	Lilljuthatten	Vein	Dormant	1,000–2,500
Sweden	1311	MMS Vicken	Black Shales	Exploration	2,500–5,000
Sweden	621	Pleutajokk	Metasomatite	Dormant	2,500–5,000
Sweden	622	Ranstad	Black Shales	Dormant	50,000–100,000
Sweden	1223	Sagtjarn	Intrusive	Dormant	< 500
Sweden	1225	Tasjo	Phosphorite	Dormant	25,000–50,000
Tajikistan	623	Adrasman	Vein	Depleted	500–1,000
Tajikistan	624	Taboshary	Vein	Depleted	1,000–2,500
Turkey	628	Demirtepe	Vein	Dormant	1,000–2,500
Turkey	629	Fakili	Unknown	Dormant	< 500
Turkey	630	Kucukcavdar	Unknown	Dormant	< 500
Turkey	631	Manisa-Koprubasi	Sandstone–Basal Channel	Dormant	2,500–5,000
Turkey	632	Yozgat-Sorgun	Sandstone–Basal Channel	Dormant	2,500–5,000
Turkmenistan	625	Bailik	Black Shales	Dormant	5,000–10,000
Turkmenistan	626	Sernoye	Vein	Depleted	5,000–10,000
Ukraine	633	Adamovskoye	Other	Dormant	1,000–2,500
Ukraine	634	Berekskoye	Other	Dormant	500–1,000
Ukraine	635	Bratskoye	Other	Depleted	1,000–2,500
Ukraine	636	Chervonoyarskoye	Other	Dormant	500–1,000
Ukraine	637	Devladovskoye	Sandstone–Basal Channel	Depleted	1,000–2,500
Ukraine	1227	Ingulskii	Metasomatite	Operating	25,000–50,000
Ukraine	638	Kalinovskoje	Intrusive	Dormant	5,000–10,000
Ukraine	639	Krasnooskol'Skoye	Other	Dormant	500–1,000
Ukraine	640	Lozovatskoye	Intrusive	Dormant	1,000–2,500
Ukraine	641	Markovskoye	Other	Dormant	1,000–2,500
Ukraine	642	Michurinskoje	Metasomatite	Operating	10,000–25,000
Ukraine	643	Nickolaevskoye	Sandstone–Basal Channel	Dormant	1,000–2,500
Ukraine	644	Nickolo-Kozelskoye	Quartz-pebble Conglomerate	Dormant	1,000–2,500
Ukraine	645	Novogoor'Evskoye	Other	Dormant	1,000–2,500
Ukraine	646	Pervomayskoye	Vein	Depleted	10,000–25,000
Ukraine	647	Sadovoye	Other	Dormant	500–1,000
Ukraine	648	Saphonovskoye	Sandstone–Basal Channel	Dormant	2,500–5,000
Ukraine	649	Severinskoye	Metasomatite	Dormant	25,000–50,000

Country	DepID	Deposit Name	Deposit Type	Status	Resource Range
Ukraine	650	Surskoye	Other	Dormant	1,000–2,500
Ukraine	651	Vatutinskoye	Metasomatite	Operating	25,000–50,000
Ukraine	652	Yuzhnoye	Intrusive	Dormant	5,000–10,000
Ukraine	653	Zheltorechenskoye	Vein	Depleted	10,000–25,000
United Republic of Tanzania	1290	Nyota	Surficial	Exploration	10,000–25,000
United Republic of Tanzania	1288	Henri	Sandstone–Roll Front	Exploration	UNKNOWN
United Republic of Tanzania	1289	Manyoni C1	Surficial	Exploration	5,000–10,000
USA	654	Abbe	Sandstone–Tabular	Depleted	< 500
USA	655	Alta Mesa	Sandstone–Roll Front	Operating	2,500–5,000
USA	656	Alta Verde	Sandstone–Roll Front	Dormant	2,500–5,000
USA	924	Alzada	Sandstone–Roll Front	Dormant	1,000–2,500
USA	657	Ambrosia Lake (Dysart)	Sandstone–Tabular	Closed	50,000–100,000
USA	658	Anderson	Volcanic	Dormant	10,000–25,000
USA	659	Arizona 1	Collapse Breccia Pipe	Dormant	1,000–2,500
USA	660	Bear Creek	Sandstone–Roll Front	Depleted	2,500–5,000
USA	661	Benevides	Sandstone–Roll Front	Depleted	1,000–2,500
USA	662	Bernabe-Montano	Sandstone–Tabular	Dormant	5,000–10,000
USA	663	Big Buck / Velvet	Sandstone–Tabular	Dormant	2,500–5,000
USA	916	Big Eagle	Sandstone–Tabular	Closed	UNKNOWN
USA	664	Big Eagle Phase 2 / Green Mountain	Sandstone–Tabular	Dormant	10,000–25,000
USA	665	Big Gypsum Creek-Hamm Canyon	Sandstone–Tabular	Dormant	500–1,000
USA	666	Big Red	Sandstone–Roll Front	Dormant	1,000–2,500
USA	668	Bison Basin	Sandstone–Roll Front	Depleted	1,000–2,500
USA	669	Bokan Mountain	Intrusive	Depleted	500–1,000
USA	670	Borrego Pass	Sandstone–Roll Front	Dormant	5,000–10,000
USA	671	Bruni	Sandstone–Roll Front	Dormant	1,000–2,500
USA	672	Buckhingham	Sandstone–Roll Front	Dormant	500–1,000
USA	673	Bull Canyon	Sandstone–Tabular	Dormant	1,000–2,500
USA	937	Bullfrog	Sandstone–Tabular	Exploration	10,000–25,000
USA	674	Burns Ranch	Sandstone–Roll Front	Depleted	1,000–2,500
USA	675	Butler-Weddington	Sandstone–Roll Front	Depleted	2,500–5,000
USA	676	Calamity-N. Outlaw-Flaptop	Sandstone–Tabular	Dormant	1,000–2,500
USA	927	Canyon	Sandstone–Roll Front	Dormant	1,000–2,500
USA	677	Canyon	Collapse Breccia Pipe	Dormant	1,000–2,500
USA	678	Carpenter Flats	Sandstone–Tabular	Depleted	< 500
USA	679	Cedar Hills	Sandstone–Roll Front	Dormant	1,000–2,500
USA	680	Central Florida	Phosphorite	Closed	> 100,000
USA	681	Chapman	Sandstone–Roll Front	Dormant	500–1,000
USA	682	Charlie	Sandstone–Roll Front	Dormant	1,000–2,500
USA	683	Christensen Ranch	Sandstone–Roll Front	Closed	10,000–25,000
USA	929	Church Rock Section 17	Sandstone–Roll Front	Dormant	2,500–5,000
USA	928	Church Rock Section 8	Sandstone–Roll Front	Dormant	2,500–5,000
USA	684	Churchrock	Sandstone–Tabular	Dormant	50,000–100,000
USA	685	Churchrock NE	Sandstone–Roll Front	Dormant	10,000–25,000
USA	686	Clay West	Sandstone–Roll Front	Depleted	2,500–5,000
USA	687	Cliffside (Section 36)	Sandstone–Tabular	Depleted	25,000–50,000
USA	910	Collins Draw	Sandstone–Roll Front	Unknown	UNKNOWN
USA	688	Copper Mountain	Vein	Dormant	2,500–5,000
USA	689	Crooks Gap	Sandstone–Roll Front	Dormant	10,000–25,000
USA	690	Crow Butte	Sandstone–Roll Front	Operating	10,000–25,000
USA	691	Crownpoint	Sandstone–Tabular	Dormant	25,000–50,000
USA	692	Dalton Pass	Sandstone–Tabular	Dormant	5,000–10,000
USA	693	Day Loma	Sandstone–Roll Front	Depleted	2,500–5,000
USA	917	Desert View / Green Mountain	Sandstone–Tabular	Dormant	UNKNOWN
USA	694	Dewey Burdock	Sandstone–Roll Front	Development	2,500–5,000
USA	695	East Florida District	Phosphorite	Closed	> 100,000
USA	696	East Gas Hills	Sandstone–Roll Front	Depleted	2,500–5,000

Country	DepID	Deposit Name	Deposit Type	Status	Resource Range
USA	922	Edgemont District	Sandstone–Roll Front	Depleted	UNKNOWN
USA	697	EZ-2	Collapse Breccia Pipe	Dormant	500–1,000
USA	698	Faith	Collapse Breccia Pipe	Dormant	500–1,000
USA	699	Fernandez Main Ranch	Sandstone–Roll Front	Dormant	2,500–5,000
USA	1314	FMC Claim	Sandstone–Roll Front	Exploration	1,000–2,500
USA	700	Gas Hills Cameco	Sandstone–Roll Front	Development	5,000–10,000
USA	901	Grace #1	Sandstone–Tabular	Dormant	UNKNOWN
USA	902	Grace #2	Sandstone–Tabular	Dormant	UNKNOWN
USA	702	Grover	Sandstone–Roll Front	Dormant	< 500
USA	935	Gruy Ranch	Sandstone–Roll Front	Exploration	< 500
USA	703	Hack Canyon	Collapse Breccia Pipe	Depleted	2,500–5,000
USA	704	Hanson	Sandstone–Basal Channel	Dormant	10,000–25,000
USA	705	Happy Jack	Sandstone–Tabular	Depleted	1,000–2,500
USA	706	Hauber	Sandstone–Roll Front	Dormant	UNKNOWN
USA	707	Hermit	Collapse Breccia Pipe	Depleted	1,000–2,500
USA	708	Hershey	Sandstone–Tabular	Depleted	500–1,000
USA	709	Hideout	Sandstone–Tabular	Depleted	< 500
USA	710	Highland	Sandstone–Roll Front	Operating	10,000–25,000
USA	903	Hobson	Sandstone–Roll Front	Depleted	1,000–2,500
USA	711	Holiday-El Mesquite	Sandstone–Roll Front	Depleted	2,500–5,000
USA	713	Irigaray	Sandstone–Roll Front	Depleted	2,500–5,000
USA	714	J.J.	Sandstone–Roll Front	Dormant	5,000–10,000
USA	716	Jackpile	Sandstone–Tabular	Depleted	25,000–50,000
USA	701	Jackpot / Green Mountain	Sandstone–Roll Front	Dormant	10,000–25,000
USA	717	John Brown	Sandstone–Tabular	Depleted	2,500–5,000
USA	718	Johnny-M	Sandstone–Tabular	Dormant	5,000–10,000
USA	920	Juniper	Sandstone–Roll Front	Exploration	1,000–2,500
USA	719	Kanab North	Collapse Breccia Pipe	Dormant	1,000–2,500
USA	720	Keota	Sandstone–Roll Front	Dormant	2,500–5,000
USA	721	King Solomon	Sandstone–Tabular	Depleted	1,000–2,500
USA	722	Kingsville Dome	Sandstone–Roll Front	Dormant	2,500–5,000
USA	723	L Bar	Sandstone–Tabular	Depleted	2,500–5,000
USA	724	La Jara Mesa	Sandstone–Roll Front	Dormant	2,500–5,000
USA	725	La Sal Creek	Sandstone–Tabular	Dormant	500–1,000
USA	726	Lamprecht-Felder	Sandstone–Roll Front	Depleted	2,500–5,000
USA	727	Las Palmas	Sandstone–Roll Front	Depleted	1,000–2,500
USA	728	Lee	Sandstone–Tabular	Dormant	2,500–5,000
USA	729	Legin-Charles T-Deremo	Sandstone–Tabular	Closed	2,500–5,000
USA	730	Leuenberger	Sandstone–Roll Front	Dormant	1,000–2,500
USA	731	Long And Horse Mesas	Sandstone–Tabular	Depleted	500–1,000
USA	732	Long Park	Sandstone–Tabular	Dormant	2,500–5,000
USA	733	Los Ochos	Vein	Dormant	500–1,000
USA	734	Lower And Radium Groups	Sandstone–Tabular	Depleted	500–1,000
USA	735	Lucky Mc Mine	Sandstone–Roll Front	Depleted	10,000–25,000
USA	736	Lukachukai Mountains	Sandstone–Tabular	Dormant	1,000–2,500
USA	737	Mancos	Sandstone–Roll Front	Dormant	1,000–2,500
USA	738	Mariano Lake	Sandstone–Tabular	Dormant	10,000–25,000
USA	739	Marquez Canyon	Sandstone–Tabular	Dormant	5,000–10,000
USA	740	Marquez Grant	Sandstone–Tabular	Dormant	1,000–2,500
USA	741	Marysvale	Volcanic	Dormant	500–1,000
USA	742	Mcdermitt	Volcanic	Dormant	5,000–10,000
USA	743	Mi Vida / Lisbon Valley	Sandstone–Tabular	Depleted	10,000–25,000
USA	744	Midnite	Vein	Dormant	2,500–5,000
USA	745	Monogram Mesa	Sandstone–Tabular	Dormant	2,500–5,000
USA	746	Monument No.2	Sandstone–Tabular	Depleted	1,000–2,500
USA	747	Moonlight	Sandstone–Tabular	Depleted	500–1,000
USA	919	Moonshine Springs	Sandstone–Tabular	Dormant	1,000–2,500
USA	748	Moore Ranch	Sandstone–Roll Front	Development	1,000–2,500
USA	749	Mrak	Sandstone–Roll Front	Depleted	500–1,000
USA	750	Mt. Lucas	Sandstone–Roll Front	Depleted	1,000–2,500

Country	DepID	Deposit Name	Deposit Type	Status	Resource Range
USA	751	Mt. Taylor	Sandstone–Tabular	Dormant	25,000–50,000
USA	752	Narrow Canyon	Sandstone–Roll Front	Dormant	2,500–5,000
USA	753	Nell	Sandstone–Roll Front	Dormant	500–1,000
USA	1312	Nichols Ranch	Sandstone–Roll Front	Exploration	500–1,000
USA	755	Nine Mile Lake	Sandstone–Roll Front	Dormant	1,000–2,500
USA	756	North Butte / Brown	Sandstone–Roll Front	Dormant	2,500–5,000
USA	757	North Florida	Phosphorite	Dormant	50,000–100,000
USA	758	Northeast Florida District	Phosphorite	Dormant	> 100,000
USA	931	Northwest Unit	Sandstone–Roll Front	Exploration	1,000–2,500
USA	759	Nose Rock	Sandstone–Tabular	Dormant	10,000–25,000
USA	760	O'Hern	Sandstone–Roll Front	Depleted	< 500
USA	761	Orphan Lode	Collapse Breccia Pipe	Depleted	1,000–2,500
USA	762	Oshoto Deposit	Sandstone–Roll Front	Dormant	1,000–2,500
USA	905	Palangana	Sandstone–Roll Front	Development	1,000–2,500
USA	763	Pandora	Sandstone–Tabular	Operating	500–1,000
USA	764	Panna Maria	Sandstone–Roll Front	Depleted	5,000–10,000
USA	765	Pawnee	Sandstone–Roll Front	Depleted	500–1,000
USA	930	Peach	Sandstone–Roll Front	Development	2,500–5,000
USA	766	Peterson Ranch	Sandstone–Roll Front	Dormant	1,000–2,500
USA	767	Petrotomics / Dave	Sandstone–Roll Front	Dormant	10,000–25,000
USA	768	Piedre Lumbre	Sandstone–Roll Front	Dormant	500–1,000
USA	769	Pigeon	Collapse Breccia Pipe	Depleted	1,000–2,500
USA	770	Pinenut	Collapse Breccia Pipe	Dormant	1,000–2,500
USA	918	Pinetree	Sandstone–Roll Front	Development	1,000–2,500
USA	771	Pitch	Vein	Depleted	500–1,000
USA	772	Poison Canyon	Sandstone–Tabular	Depleted	500–1,000
USA	773	Ramco	Unknown	Unknown	UNKNOWN
USA	774	Red Desert Basin	Unknown	Unknown	UNKNOWN
USA	1313	Reno Creek SouthWest	Sandstone–Roll Front	Exploration	1,000–2,500
USA	775	Reno Creek West	Sandstone–Roll Front	Exploration	2,500–5,000
USA	932	Reynolds Ranch	Sandstone–Roll Front	Development	5,000–10,000
USA	776	Rhode Ranch	Sandstone–Roll Front	Depleted	2,500–5,000
USA	777	Rio Puerco	Sandstone–Tabular	Dormant	1,000–2,500
USA	778	Rob Rollo	Sandstone–Tabular	Depleted	1,000–2,500
USA	779	Roca Honda	Sandstone–Roll Front	Dormant	1,000–2,500
USA	780	Rosita	Sandstone–Roll Front	Depleted	1,000–2,500
USA	781	Ruby	Sandstone–Tabular	Depleted	2,500–5,000
USA	782	Ruby Ranch	Sandstone–Tabular	Dormant	1,000–2,500
USA	783	Ruth	Sandstone–Roll Front	Dormant	500–1,000
USA	784	Sage	Collapse Breccia Pipe	Dormant	1,000–2,500
USA	785	Saint Anthony	Sandstone–Roll Front	Dormant	2,500–5,000
USA	786	San Antonio Valley	Sandstone–Tabular	Dormant	1,000–2,500
USA	787	Sand Creek	Sandstone–Roll Front	Dormant	500–1,000
USA	789	Schwartzwalder	Vein	Depleted	2,500–5,000
USA	790	Section 32	Sandstone–Roll Front	Dormant	1,000–2,500
USA	791	Sharp Canyon	Sandstone–Tabular	Dormant	500–1,000
USA	792	Sherwood Mine	Sandstone–Basal Channel	Depleted	5,000–10,000
USA	793	Shinarump	Sandstone–Tabular	Depleted	500–1,000
USA	933	Shirley Basin Cameco	Sandstone–Roll Front	Exploration	1,000–2,500
USA	794	Shirley Basin Mine	Sandstone–Roll Front	Closed	10,000–25,000
USA	796	Slick Rock	Sandstone–Tabular	Dormant	1,000–2,500
USA	797	Smith Ranch	Sandstone–Roll Front	Operating	5,000–10,000
USA	798	South Florida District	Phosphorite	Dormant	UNKNOWN
USA	799	South Morton Ranch	Sandstone–Roll Front	Dormant	5,000–10,000
USA	800	Sundance	Unknown	Unknown	UNKNOWN
USA	801	Swanson	Metasomatite	Dormant	10,000–25,000
USA	1315	SWD Claims	Sandstone–Roll Front	Exploration	500–1,000
USA	802	Sweetwater Mine	Sandstone–Roll Front	Depleted	5,000–10,000
USA	803	Taylor Ranch	Unknown	Dormant	2,500–5,000
USA	804	Temple Mountain	Sandstone–Tabular	Dormant	500–1,000
USA	805	Tony M. / Shootering Canyon	Sandstone–Tabular	Operating	1,000–2,500

Country	DepID	Deposit Name	Deposit Type	Status	Resource Range
USA	806	Trevino	Sandstone–Roll Front	Depleted	1,000–2,500
USA	936	Uravan District	Sandstone–Tabular	Operating	2,500–5,000
USA	809	Uravan-Atkinson Mesas	Sandstone–Tabular	Dormant	2,500–5,000
USA	810	Vanadium	Sandstone–Tabular	Dormant	5,000–10,000
USA	811	Vanura	Sandstone–Tabular	Depleted	1,000–2,500
USA	921	Vasquez	Sandstone–Roll Front	Unknown	1,000–2,500
USA	934	West Cole	Sandstone–Roll Front	Depleted	< 500
USA	812	West Gas Hills	Sandstone–Roll Front	Depleted	5,000–10,000
USA	813	West Largo	Sandstone–Tabular	Dormant	5,000–10,000
USA	814	Whiskey Peak / Green Mountain	Sandstone–Roll Front	Dormant	5,000–10,000
USA	904	Zamzov	Sandstone–Roll Front	Depleted	UNKNOWN
Uzbekistan	815	Agron	Sandstone–Roll Front	Operating	5,000–10,000
Uzbekistan	816	Aktau	Sandstone–Roll Front	Dormant	5,000–10,000
Uzbekistan	817	Alatanga	Vein	Depleted	2,500–5,000
Uzbekistan	818	Alendy	Sandstone–Roll Front	Operating	10,000–25,000
Uzbekistan	819	Altyntau	Black Shales	Dormant	500–1,000
Uzbekistan	820	Aulbek	Sandstone–Roll Front	Operating	10,000–25,000
Uzbekistan	822	Bakhaly	Sandstone–Roll Front	Dormant	1,000–2,500
Uzbekistan	823	Beshkak	Sandstone–Roll Front	Operating	5,000–10,000
Uzbekistan	824	Bukeenai	Sandstone–Roll Front	Operating	25,000–50,000
Uzbekistan	825	Charkasar	Vein	Depleted	1,000–2,500
Uzbekistan	826	Chauli	Volcanic	Depleted	2,500–5,000
Uzbekistan	827	Djantuar	Black Shales	Dormant	10,000–25,000
Uzbekistan	828	Kanimekh	Sandstone–Roll Front	Operating	10,000–25,000
Uzbekistan	829	Kattasai	Vein	Depleted	1,000–2,500
Uzbekistan	830	Kendyktjube	Sandstone–Roll Front	Operating	10,000–25,000
Uzbekistan	831	Ketmenchi	Sandstone–Roll Front	Operating	10,000–25,000
Uzbekistan	832	Koscheka	Black Shales	Dormant	1,000–2,500
Uzbekistan	833	Lyavlyakan	Sandstone–Roll Front	Operating	5,000–10,000
Uzbekistan	834	Mailikatan	Vein	Depleted	1,000–2,500
Uzbekistan	840	Mayzak	Sandstone–Roll Front	Dormant	2,500–5,000
Uzbekistan	835	Meylysai	Sandstone–Roll Front	Dormant	2,500–5,000
Uzbekistan	836	Nagornoye	Sandstone–Roll Front	Dormant	2,500–5,000
Uzbekistan	837	Rudnoye	Black Shales	Dormant	2,500–5,000
Uzbekistan	838	Sabyrsay	Sandstone–Roll Front	Operating	10,000–25,000
Uzbekistan	839	Severny Kanimekh	Sandstone–Roll Front	Operating	10,000–25,000
Uzbekistan	841	Shark	Sandstone–Roll Front	Operating	1,000–2,500
Uzbekistan	842	Sugraly	Sandstone–Roll Front	Operating	25,000–50,000
Uzbekistan	843	Terekuduk	Sandstone–Roll Front	Dormant	500–1,000
Uzbekistan	844	Tokhumbet	Sandstone–Roll Front	Dormant	2,500–5,000
Uzbekistan	845	Tutly	Sandstone–Roll Front	Operating	2,500–5,000
Uzbekistan	846	Uchkuduk	Sandstone–Roll Front	Operating	25,000–50,000
Uzbekistan	847	Ulus	Unknown	Unknown	500–1,000
Uzbekistan	848	Varadzhan	Sandstone–Roll Front	Dormant	500–1,000
Uzbekistan	849	Yuzhny Bukinai	Sandstone–Roll Front	Operating	10,000–25,000
Vietnam	850	An Diem	Sandstone–Tabular	Exploration	5,000–10,000
Vietnam	851	Khe Hoa-Khe Cao	Sandstone–Tabular	Exploration	5,000–10,000
Zambia	1230	Bungua	Unknown	Exploration	UNKNOWN
Zambia	1231	Dibwe	Sandstone–Tabular	Exploration	2,500–5,000
Zambia	1232	Gwabe	Sandstone–Tabular	Exploration	500–1,000
Zambia	1234	Lumwana	Unknown	Feasibility study	5,000–10,000
Zambia	1235	Mutanga	Unknown	Exploration	2,500–5,000
Zambia	1237	Njame	Sandstone–Tabular	Exploration	2,500–5,000
Zimbabwe	859	Kanyemba	Sandstone–Tabular	Dormant	1,000–2,500
Zimbabwe	1291	Kawanga	Vein	Dormant	2,500–5,000

3.2.2. Initial resources by country and deposit type

TABLE 11. INITIAL RESOURCES BY COUNTRY AND DEPOSIT TYPE

Dep. Type / Country	Unconformity	Sandstone	Hematite Breccia Comp.	Quartz-Pebble	Volcanic	Intrusive	Vein	Metasomatite	Other	Total
Algeria	0	0	0	0	0	0	19,400	0	1,500	**20,900**
Argentina	0	17,520	0	0	0	0	1,720	0	1,285	**20,525**
Australia	429,713	92,389	1,939,970	0	9,814	9,747	2,679	29,934	79,484	**2,593,730**
Bolivia	0	500	0	0	0	0	0	0	0	**500**
Botswana	0	36,575	0	0	0	0	0	0	7,731	**44,306**
Brazil	0	11,240	0	0	22,700	0	424	285,505	0	**319,869**
Bulgaria	0	33,580	0	0	3,600	0	11,380	0	500	**49,060**
Cameroon	0	0	0	0	0	0	0	11,130	0	**11,130**
Canada	635,922	9,544	0	427,051	43,226	60,522	44,085	680	54,225	**1,275,260**
Central African Republic	0	0	0	0	0	0	0	0	16,700	**16,700**
Chile	0	0	0	0	0	0	0	2,900	0	**2,900**
China	0	47,500	0	0	10,000	0	8,000	0	2,500	**68,000**
Colombia	0	0	0	0	0	0	0	0	4,965	**4,965**
Czech Republic	0	140,000	0	0	0	0	89,925	0	3,500	**233,425**
Democratic Rep. of the Congo	0	0	0	0	0	0	33,490	0	0	**33,490**
Denmark	0	0	0	0	0	27,000	0	0	0	**27,000**
Finland	0	950	0	0	0	3,500	500	0	4,710	**9,660**
France	744	36,767	0	0	0	0	69,368	0	3,963	**110,842**
Gabon	0	153,898	0	0	0	0	0	0	0	**153,898**
Germany	0	39,920	0	0	0	0	127,165	0	167,440	**334,525**
Guinea	0	0	0	0	0	0	0	0	0	**0**
Guyana	0	0	0	0	0	0	2,735	0	0	**2,735**
Hungary	0	32,800	0	0	0	0	0	0	0	**32,800**
India	8,070	13,081	0	0	0	0	25,850	3,500	12,555	**63,056**
Indonesia	0	0	0	0	0	0	1,670	0	0	**1,670**
Iran, Islamic Republic of	0	0	0	0	0	0	0	1,367	0	**1,367**

Dep. Type Country	Unconformity	Sandstone	Hematite Breccia Comp.	Quartz-Pebble	Volcanic	Intrusive	Vein	Metasomatite	Other	Total
Italy	0	0	0	0	4,800	0	0	0	0	**4,800**
Japan	0	7,500	0	0	0	0	0	0	0	**7,500**
Jordan	0	0	0	0	0	0	0	0	29,000	**29,000**
Kazakhstan	0	623,720	0	0	16,600	0	171,175	0	139,500	**950,995**
Korea, Republic of	0	0	0	0	0	0	0	0	14,800	**14,800**
Kyrgyzstan	0	0	0	0	0	0	2,850	0	3,200	**6,050**
Madagascar	0	5,100	0	0	0	0	0	0	0	**5,100**
Malawi	0	8,547	0	0	0	3,290	0	0	0	**11,837**
Mali	0	4,240	0	0	0	0	0	0	0	**4,240**
Mauritania	0	0	0	0	0	0	0	0	0	**0**
Mexico	0	6,145	0	0	4,485	0	0	0	51,000	**61,630**
Mongolia	0	26,177	0	0	50,389	0	0	0	0	**76,566**
Morocco	0	0	0	0	0	0	0	0	132,000	**132,000**
Namibia	0	1,638	0	0	0	278,240	0	0	126,010	**405,888**
Niger	0	456,887	0	0	0	0	0	0	0	**456,887**
Pakistan	0	100	0	0	0	0	0	0	0	**100**
Paraguay	0	0	0	0	2,700	0	0	0	0	**2,700**
Peru	0	0	0	0	2,800	0	500	0	1,000	**4,300**
Poland	0	3,600	0	0	0	0	1,000	0	9,124	**13,724**
Portugal	0	0	0	0	0	0	5,360	0	0	**5,360**
Romania	0	24,361	0	0	0	0	12,710	0	0	**37,071**
Russian Federation	0	154,110	0	0	152,865	0	133,405	426,265	41,940	**908,585**
Saudi Arabia	0	0	0	0	0	40,000	0	0	0	**40,000**
Senegal	0	0	0	0	0	0	1,462	0	0	**1,462**
Serbia	0	3,446	0	0	0	0	3,255	0	0	**6,701**
Slovakia	0	0	0	0	19,065	0	0	0	0	**19,065**
Slovenia	0	8,500	0	0	0	0	0	0	0	**8,500**
Somalia	0	0	0	0	0	0	0	5,350	10,600	**15,950**
South Africa	0	47,640	0	388,081	0	4,300	0	0	4,200	**444,221**
Spain	0	4,800	0	0	0	0	21,598	0	0	**26,398**
Sweden	0	0	0	0	4,400	438	4,243	4,000	122,522	**135,603**

Dep. Type Country	Unconformity	Sandstone	Hematite Breccia Comp.	Quartz-Pebble	Volcanic	Intrusive	Vein	Metasomatite	Other	Total
Tajikistan	0	0	0	0	0	0	1,400	0	0	**1,400**
Turkey	0	6,702	0	0	0	0	1,729	0	698	**9,129**
Turkmenistan	0	0	0	0	0	0	7,000	0	5,000	**12,000**
Ukraine	0	6,380	0	2,090	0	14,855	25,400	114,990	11,225	**174,940**
United Republic of Tanzania	0	0	0	0	0	0	0	0	19,650	**19,650**
USA	0	805,213	0	0	31,500	600	14,730	13,000	786,756	**1,651,800**
Uzbekistan	0	253,955	0	0	4,500	0	8,830	0	16,495	**283,780**
Vietnam	0	15,580	0	0	0	0	0	0	0	**15,580**
Zambia	0	7,210	0	0	0	0	0	0	12,772	**19,982**
Zimbabwe	0	2,000	0	0	0	0	3,000	0	0	**5,000**
Total	**1,074,449**	**3,149,815**	**1,939,970**	**817,222**	**383,444**	**442,492**	**858,038**	**898,621**	**1,898,550**	**11,462,607**

3.2.3. Deposit numbers by country and deposit type

TABLE 12. DEPOSIT NUMBERS BY COUNTRY AND DEPOSIT TYPE.

Dep. Type / Country	Unconformity	Sandstone	Hematite Breccia Comp.	Quartz-Pebble	Volcanic	Intrusive	Vein	Metasomatite	Other	Total
Algeria	0	0	0	0	0	0	4	0	1	**5**
Argentina	0	4	0	0	0	0	2	0	1	**7**
Australia	21	19	7	0	5	4	1	3	11	**71**
Bolivia	0	1	0	0	0	0	0	0	0	**1**
Botswana	0	1	0	0	0	0	0	0	1	**2**
Brazil	0	2	0	1	1	0	1	3	2	**10**
Bulgaria	0	15	0	0	2	0	11	0	1	**29**
Cameroon	0	0	0	0	0	0	0	1	0	**1**
Canada	53	6	0	20	8	16	12	1	3	**119**
Central African Republic	0	0	0	0	0	0	0	0	1	**1**
Chile	0	0	0	0	0	0	0	2	2	**4**
China	0	11	0	0	4	2	4	0	4	**25**
Colombia	0	0	0	0	0	0	0	0	1	**1**
Czech Republic	0	6	0	0	0	0	15	0	2	**23**
Democratic Rep. of the Congo	0	0	0	0	0	0	7	0	1	**8**
Denmark	0	0	0	0	0	1	0	0	0	**1**
Finland	0	2	0	0	0	2	1	0	3	**8**
France	1	7	0	0	0	0	32	0	3	**43**
Gabon	0	9	0	0	0	0	0	0	0	**9**
Germany	0	3	0	0	0	0	11	0	2	**16**
Guinea	0	0	0	0	0	0	1	0	0	**1**
Guyana	0	0	0	0	0	0	1	0	0	**1**
Hungary	0	1	0	0	0	0	0	0	0	**1**
India	3	2	0	0	0	0	4	1	1	**11**
Indonesia	0	0	0	0	0	0	3	0	0	**3**
Iran, Islamic Republic of	0	0	0	0	0	0	0	1	0	**1**

Dep. Type Country	Unconformity	Sandstone	Hematite Breccia Comp.	Quartz-Pebble	Volcanic	Intrusive	Vein	Metasomatite	Other	Total
Italy	0	0	0	0	2	0	0	0	0	**2**
Japan	0	2	0	0	0	0	0	0	0	**2**
Jordan	0	0	0	0	0	0	0	0	5	**5**
Kazakhstan	0	25	0	0	6	0	27	0	9	**67**
Korea, Republic of	0	0	0	0	0	0	0	0	1	**1**
Kyrgyzstan	0	0	0	0	0	0	3	0	4	**7**
Madagascar	0	2	0	0	0	1	0	0	0	**3**
Malawi	0	1	0	0	0	1	0	0	0	**2**
Mali	0	1	0	0	0	0	0	0	0	**1**
Mauritania	0	0	0	0	0	0	1	0	0	**1**
Mexico	0	3	0	0	4	0	0	0	1	**8**
Mongolia	0	4	0	0	4	0	0	0	0	**8**
Morocco	0	0	0	0	0	0	0	0	4	**4**
Namibia	0	1	0	0	0	10	0	0	13	**24**
Niger	0	28	0	0	0	0	0	0	0	**28**
Pakistan	0	2	0	0	0	0	0	0	0	**2**
Paraguay	0	0	0	0	1	0	0	0	0	**1**
Peru	0	0	0	0	2	0	1	0	2	**5**
Poland	0	2	0	0	0	0	2	0	3	**7**
Portugal	0	0	0	0	0	0	11	0	0	**11**
Romania	0	8	0	0	1	0	10	0	0	**19**
Russian Federation	1	21	0	0	16	0	20	10	12	**80**
Saudi Arabia	0	0	0	0	0	1	0	0	0	**1**
Senegal	0	0	0	0	0	0	1	0	0	**1**
Serbia	0	3	0	0	0	0	4	0	0	**7**
Slovakia	0	0	0	0	2	0	0	0	0	**2**
Slovenia	0	1	0	0	0	0	0	0	1	**2**
Somalia	0	0	0	0	0	0	0	1	2	**3**
South Africa	0	2	0	26	0	1	0	0	1	**30**
Spain	0	1	0	0	0	0	10	2	6	**17**

Dep. Type / Country	Unconformity	Sandstone	Hematite Breccia Comp.	Quartz-Pebble	Volcanic	Intrusive	Vein	Metasomatite	Other	Total
Sweden	0	0	0	0	1	1	3	0	4	**11**
Tajikistan	0	0	0	0	0	0	2	0	0	**2**
Turkey	0	2	0	0	0	0	1	0	2	**5**
Turkmenistan	0	0	0	0	0	0	1	4	1	**2**
Ukraine	0	3	0	1	0	3	2	0	9	**22**
United Republic of Tanzania	0	1	0	0	0	0	0	0	2	**3**
USA	0	152	0	0	3	1	5	1	20	**182**
Uzbekistan	0	24	0	0	1	0	4	0	5	**34**
Vietnam	0	2	0	0	0	0	0	0	0	**2**
Zambia	0	3	0	0	0	0	0	0	3	**6**
Zimbabwe	0	1	0	0	0	0	1	0	0	**2**
Total	**79**	**384**	**7**	**48**	**63**	**44**	**219**	**30**	**150**	**1,024**

3.2.4. Deposit numbers by country and deposit status

Table 13. Deposit Numbers by Country and Deposit Status

Status / Country	Dormant	Feasibility	Exploration	Development	Operating	Standby	Closed	Depleted	Reclamation	Unknown	Total
Algeria	5	0	0	0	0	0	0	0	0	0	**5**
Argentina	5	0	0	0	0	0	0	2	0	0	**7**
Australia	39	0	19	3	3	0	0	7	0	0	**71**
Bolivia	1	0	0	0	0	0	0	0	0	0	**1**
Botswana	0	0	2	0	0	0	0	0	0	0	**2**
Brazil	4	1	0	1	1	0	1	0	1	1	**10**
Bulgaria	3	0	1	0	0	0	10	15	0	0	**29**
Cameroon	0	0	1	0	0	0	0	0	0	0	**1**
Canada	38	5	25	2	2	0	10	25	0	12	**119**
Central African Republic	0	0	0	1	0	0	0	0	0	0	**1**
Chile	0	0	0	0	0	0	0	0	0	4	**4**
China	3	0	10	0	5	0	0	7	0	0	**25**
Colombia	0	0	1	0	0	0	0	0	0	0	**1**
Czech Republic	5	0	0	0	2	0	0	16	0	0	**23**
Democratic Rep. of the Congo	5	0	0	0	0	0	0	3	0	0	**8**
Denmark	0	0	1	0	0	0	0	0	0	0	**1**
Finland	4	0	1	1	0	0	0	0	2	0	**8**
France	5	0	0	0	0	0	0	38	0	0	**43**
Gabon	1	0	0	0	0	0	0	8	0	0	**9**
Germany	4	0	0	0	0	0	3	8	0	1	**16**
Guinea	0	0	1	0	0	0	0	0	0	0	**1**
Guyana	0	0	1	0	0	0	0	0	0	0	**1**
Hungary	0	0	0	0	0	0	1	0	0	0	**1**
India	0	0	6	0	5	0	0	0	0	0	**11**
Indonesia	3	0	0	0	0	0	0	0	0	0	**3**

Status Country	Dormant	Feasibility	Exploration	Development	Operating	Standby	Closed	Depleted	Reclamation	Unknown	Total
Iran, Islamic Republic of	0	0	0	1	0	0	0	0	0	0	**1**
Italy	2	0	0	0	0	0	0	0	0	0	**2**
Japan	2	0	0	0	0	0	0	0	0	0	**2**
Jordan	5	0	0	0	0	0	0	0	0	0	**5**
Kazakhstan	39	0	1	5	8	1	0	12	0	1	**67**
Korea, Republic of	1	0	0	0	0	0	0	0	0	0	**1**
Kyrgyzstan	0	0	3	0	0	0	0	4	0	0	**7**
Madagascar	2	0	1	0	0	0	0	0	0	0	**3**
Malawi	0	0	1	1	0	0	0	0	0	0	**2**
Mali	0	0	1	0	0	0	0	0	0	0	**1**
Mauritania	0	0	1	0	0	0	0	0	0	0	**1**
Mexico	8	0	0	0	0	0	0	0	0	0	**8**
Mongolia	6	0	2	0	0	0	0	0	0	0	**8**
Morocco	4	0	0	0	0	0	0	0	0	0	**4**
Namibia	4	0	15	2	2	0	0	0	0	1	**24**
Niger	7	0	8	5	4	0	0	4	0	0	**28**
Pakistan	0	0	0	1	0	0	0	1	0	0	**2**
Paraguay	0	0	1	0	0	0	0	0	0	0	**1**
Peru	3	0	2	0	0	0	0	0	0	0	**5**
Poland	7	0	0	0	0	0	0	0	0	0	**7**
Portugal	5	0	0	0	0	0	0	6	0	0	**11**
Romania	8	0	1	0	3	0	5	2	0	0	**19**
Russian Federation	37	0	15	12	9	0	0	7	0	0	**80**
Saudi Arabia	0	0	1	0	0	0	0	0	0	0	**1**
Senegal	0	0	1	0	0	0	0	0	0	0	**1**
Serbia	0	0	0	0	0	0	0	0	0	7	**7**
Slovakia	0	0	2	0	0	0	0	0	0	0	**2**
Slovenia	1	0	0	0	0	0	0	0	0	1	**2**
Somalia	3	0	0	0	0	0	0	0	0	0	**3**

Status Country	Dormant	Feasibility	Exploration	Development	Operating	Standby	Closed	Depleted	Reclamation	Unknown	Total
South Africa	10	0	2	4	5	0	2	0	0	7	**30**
Spain	5	0	5	0	0	0	0	1	0	6	**17**
Sweden	9	0	2	0	0	0	0	0	0	0	**11**
Tajikistan	0	0	0	0	0	0	0	2	0	0	**2**
Turkey	5	0	0	0	0	0	0	0	0	0	**5**
Turkmenistan	1	0	0	0	0	0	0	1	0	0	**2**
Ukraine	15	0	0	0	3	0	0	4	0	0	**22**
United Republic of Tanzania	0	0	3	0	0	0	0	0	0	0	**3**
USA	91	0	10	7	7	0	7	55	0	5	**182**
Uzbekistan	12	0	0	0	16	0	0	5	0	1	**34**
Vietnam	0	0	2	0	0	0	0	0	0	0	**2**
Zambia	0	1	5	0	0	0	0	0	0	0	**6**
Zimbabwe	2	0	0	0	0	0	0	0	0	0	**2**
Total	**419**	**7**	**154**	**46**	**75**	**1**	**39**	**233**	**3**	**47**	**1,024**

3.2.5. Grade distribution by deposit type

TABLE 14. GRADE DISTRIBUTION BY DEPOSIT TYPE.

Grade Range Deposit Type	< 0.03	0.03–0.05	0.05–0.10	0.10–0.20	0.20–0.50	0.50–1.00	1.00–5.00	> 5.00	UNKNOWN	Total
Unconformity	0	2	4	9	15	10	17	1	10	79
Sandstone	13	57	112	97	65	1	1	0	24	384
Hematite Breccia Compl.	2	0	3	1	1	0	0	0	0	7
Quartz-pebble Congl.	18	5	13	4	0	0	0	0	3	48
Volcanic	0	6	16	28	8	1	0	0	0	63
Intrusive	14	7	11	3	1	2	0	0	2	44
Vein	3	9	47	76	50	4	6	0	11	219
Metasomatite	0	1	11	13	1	0	0	0	3	30
Other	28	27	24	16	7	9	1	0	5	124
Unknown	2	2	3	3	0	0	0	0	15	26
Total	**80**	**116**	**244**	**250**	**148**	**27**	**25**	**1**	**73**	**1024**
Percent (%)	**7.81**	**11.33**	**23.83**	**24.41**	**14.45**	**2.64**	**2.44**	**0.10**	**7.13**	**100.00**

3.2.6. InitialrResource distribution by deposit type

TABLE 15. INITIAL RESOURCE DISTRIBUTION BY DEPOSIT TYPE.

Resource Range DepositType	< 500	500–1,000	1,000–2,500	2,500–5,000	5,000–10,000	10,000–25,000	25,000–50,000	50,000–100,000	> 100,000	UNKNOWN	Total
Unconformity	2	14	14	9	7	14	5	0	4	10	79
Sandstone	16	56	73	78	50	68	22	6	2	12	384
Hematite Breccia Compl.	1	0	2	0	1	2	0	0	1	0	7
Quartz-pebble Congl.	0	1	3	7	10	5	4	5	1	11	48
Volcanic	3	13	12	16	7	9	2	1	0	0	63
Intrusive	4	8	8	9	6	3	4	0	1	1	44
Vein	16	54	41	48	22	16	5	0	1	15	219
Metasomatite	0	4	2	9	2	4	3	3	2	1	30
Other	1	20	26	26	14	8	13	3	4	9	124
Unknown	2	1	2	4	2	1	0	0	0	14	26
Total	**45**	**171**	**183**	**206**	**121**	**130**	**58**	**18**	**16**	**73**	**1024**
Percent (%)	**4.39**	**16.70**	**17.87**	**20.12**	**11.82**	**12.70**	**5.66**	**1.76**	**1.56**	**7.13**	**100.00**

3.2.7. Deposit status distribution by deposit type

TABLE 16. DEPOSIT STATUS DISTRIBUTION BY DEPOSIT TYPE

Status / Type	Dormant	Feasibility	Exploration	Development	Operating	Standby	Closed	Depleted	Reclamation	Unknown	Total
Unconformity	30	5	19	1	3	0	1	19	0	1	79
Sandstone	164	0	53	22	41	1	14	82	1	6	384
Hematite Breccia Complex	2	0	3	1	1	0	0	0	0	0	7
Quartz-pebble Conglomerate	17	1	2	4	5	0	7	3	0	9	48
Volcanic	36	0	11	2	6	0	1	6	1	0	63
Intrusive	10	0	21	0	1	0	4	3	0	5	44
Vein	69	0	14	4	12	0	8	107	0	5	219
Metasomatite	10	0	7	6	4	0	0	0	0	3	30
Other	77	0	19	6	2	0	4	13	1	2	124
Unknown	4	1	5	0	0	0	0	0	0	16	26
Total	**419**	**7**	**154**	**46**	**75**	**1**	**39**	**233**	**3**	**47**	**1024**
Percent (%)	**40.92**	**0.68**	**15.04**	**4.49**	**7.32**	**0.10**	**3.81**	**22.75**	**0.29**	**4.59**	**100.00**

In all summary tables, Other deposit type includes Metamorphic, Surficial, Collapse Breccia Pipe, Phosphorite, Lignite and Black Shales types. exploration status includes, exploration, partially explored and fully explored statuses. Feasibility status includes Feasibility Studies and Permitted statuses. Reclamation status includes Reclamation and Reclaimed statuses.

4. SUMMARY

The World Distribution of Uranium Deposits (UDEPO) database provides general, technical and geological information, including references, about the worlwide uranium deposits.

UDEPO has been published on the internet which allows the users to register freely and to work with datasets (http://www-nfcis.iaea.org). The web site provides filtering and navigation to the data from the database. It has also a statistical tool which provides summary information on number of deposits and uranium resources by type and status, and by country and status. In this respect and with regard to the data presented, the UDEPO database is a unique database which provides freely accessible information on worldwide uranium deposits.

Although a great effort is spent to have complete and accurate database, the users should take into consideration that there still might be missing or outdated data for individual deposits due to the rapid changes in the uranium industry due to the new exploration works which are ongoing everyday.

The feedback from the users of the database is very important and welcome to improve the usability and the usefulness of the database and its web site.

This document and its supplementary CD-ROM represent a snapshot of the status of the database as of the end of 2008. However, the database is being continuously updated and the latest updates and additions can be accessed from the database web site (http://www-nfcis.iaea.org).

REFERENCES

[1] INTERNATIONAL ATOMIC ENERGY AGENCY, World Distribution of Uranium Deposits (Map Rolled), IAEA, Vienna (1996).

[2] INTERNATIONAL ATOMIC ENERGY AGENCY, Guidebook to Accompany IAEA Map: World Distribution of Uranium Deposits, IAEA, Vienna (1996).

[3] INTERNATIONAL ATOMIC ENERGY AGENCY, Integrated Nuclear Fuel Cycle Information System (iNFCIS), IAEA, Vienna. http://www-nfcis.iaea.org/

[4] TradeTech Uranium.Info, NUEXCO Exchange Value, (www.uranium.info).

[5] The Ux Consulting Company, LLC Web Site, (www.uxc.com).

[6] OECD/NUCLEAR ENERGY AGENCY, INTERNATIONAL ATOMIC ENERGY AGENCY, Uranium 2007: Resources, Production and Demand, OECD/NEA, Paris (2008) [The '2007 Red Book'].

[7] CUNEY, M., PEYREL, J.Y., Origine des granïtoides fertiles, conséquences sur la définition de leurs caractéristiques spécifiques, unpubl CEE report (1984).

[8] HOEVE, J., QUIRT, D., Mineralization and host rock alteration in relation to clay mineral diagenesis and evolution of the Middle-Proterozoic Athabasca Basin, northern Saskatchewan, Canada, Saskatchewan Research Council, SRC Technical Report 187 (1984) 187.

[9] SIBBALD, T.I.I., Geology and genesis of the Athabasca Basin uranium deposits; in Summary of Investigations 1985, Saskatchewan Geological Survey, Saskatchewan Energy and Mines, Miscellaneous Report 84–4 (1985) 133–156.

[10] THOMAS, D.J., MATTHEWS, R.B., SOPUCK, V., 'Athabasca Basin (Canada) unconformity-type uranium deposits: Exploration model, current mine developments and exploration directions', Geology and Ore Deposits 2000: The Great Basin and Beyond, Proceedings of Geological Society of Nevada Symposium (CLUER, J.K., et al., Eds), May 15618 2000 **1** (2000) 103–126.

[11] KRUSE, P.D., et al., Katherine SD53-9, 1:250 000 Geological Map Series Explanatory Notes. Northern Territory Geological Survey and Australian Geological Survey Organization (1994) 69.

[12] RAWLINGS, D.J., PAGE R.W., Geology and geochronology and emplacement structures associated with the Jimbu Microgranite, McArthur Basin, Northern Territory, Precambrian Research 94: 225. 250. 194 (1999).

[13] RAINBIRD, R.H., STERN, R.A., RAYNER, N., JEFFERSON, C.W., Age, provenance and regional correlation of the Athabasca Group, Saskatchewan and Alberta, constrained by igneous and detrital zircon geochronology (JEFFERSON, C.W., DELANEY, G., Eds), EXTECH IV: Geology and Uranium EXploration TECHnology of the Proterozoic Athabasca Basin, Saskatchewan and Alberta, Geological Survey of Canada, Bulletin 588 (2005) 193–211.

[14] RAINBIRD, R., et al., Sequence stratigraphy and evolution of the Paleoproterozoic intracontinental Baker Lake and Thelon basins, western Churchill Province, Nunavut, Canada, Precambrian Research 125, Nos 1–2 (2003) 21–53.

[15] LUDWIG, K.R., et al., Age of uranium mineralization at the Jabiluka and Ranger uranium deposits, Northern Territory, Australia: new U-Pb isotope evidence, Economic Geology 82 (1987) 857–874.

[16] POLITO, P.A., et al., Re-evaluation of the Petrogenesis of the Proterozoic Jabiluka Unconformity-related Uranium Deposit, Northern Territory, Australia, Mineralium Deposita 40 (2005) 257–288.

[17] MAAS, R., Nd-Sr isotope constraints on the age and origin of unconformity-type uranium deposits in the Alligator River Uranium Field, Northern Territory, Australia, Econ. Geol. 84 (1989) 64–90.
[18] HEGGE, M.R., MOSHER, D.V., EUPENE, G.S. ANTHONY, P.J., 'Geologic setting of the East Alligator uranium deposits and prospects' (FERGUSON, J., GOLEBY, A.B., Eds), Uranium in the Pine Creek Geosyncline (Proc. Sydney, 4–8 June 1979), IAEA, Vienna (1980) 259–272.
[19] HANCOCK, M.C., MAAS, R., WILDE, A.R., Jabiluka uranium–gold deposits. In: Geology of the Mineral Deposits of Australia and Papua New Guinea (HUGHES, F.E., Ed.), The Australasian Institute of Mining & Metallurgy (1990) 785–793.
[20] BINNS, R.A., MCANDREW, J., SUN, S.S., 'Origin of uranium mineralization at Jabiluka' (FERGUSON, J., GOLEBY, A.B., Eds), Uranium in the Pine Creek Geosyncline (Proc. Sydney, 4–8 June 1979), IAEA, Vienna (1980) 543–562.
[21] HEGGE, M.R., Geologic setting and relevant exploration features of the Jabiluka uranium deposits, Proc. the Australasian Institute of Mining & Metallurgy **264** (1977) 19–32.
[22] Energy Resource of Australia Ltd., Annual Report 1992.
[23] EWERS, G.R., FERGUSON, J., NEEDHAM, R.S., DONNELLY, T.H., Pine Creek Geosyncline NT, in: Proterozoic unconformity and stratabound uranium deposits, IAEA-TECDOC-315, IAEA, Vienna (1984) 363-374.
[24] FOUQUES, J.P., FOWLER, M., KNIPPING, H.D., SCHIMANN, K., 'The Cigar Lake uranium deposit: discovery and general characteristics', Uranium deposits of Canada (Evans, E.L., Ed.), Canadian Institute of Mines and Metallurgy, Special **33** (1986) 218–229.
[25] BRUNETON, P., 'Geology of the Cigar Lake uranium deposit (Saskatchewan, Canada)', Economic minerals of Saskatchewan (GILBOY, C.E., VIGROSS, L.W., Eds), Saskatchewan Geological Society, Special Publication 8 (1987) 99–119.
[26] BRUNETON, P., Geological environment of the Cigar Lake uranium deposit (Saskatchewan, Canada), Can. J. Earth Sci. 30 (1993) 653–673.
[27] FAYEK, M., et al., O and Pb isotopic analysis of uranium minerals by ion microprobe and U-Pb ages from the Cigar Lake deposit, Chem. Geol. 185 (2002) 205–225.
[28] JEFFERSON, C.W., et al., 'Unconformity associated uranium deposits' (JEFFERSON, C.W., DELANEY, G., Eds), EXTECH IV: Geology and Uranium EXploration TECHnology of the Proterozoic Athabasca Basin, Saskatchewan and Alberta, Geological Survey of Canada, Bulletin 588 (2006) 23–68.
[29] HOEVE, J., SIBBALD, T., On the genesis of Rabbit Lake and other unconformity-type uranium deposits in northern Saskatchewan, Canada, Econ. Geol. 73 (1978) 1450–1473.
[30] HOEVE, J., SIBBALD, T., RAMAEKERS, P., LEWRY, J.F., 'Athabasca Basin unconformity-type uranium deposits: a special class of sandstone-type deposits ?' (FERGUSON, J., GOLEBY A.B., Eds), Uranium in the Pine Creek Geosyncline (Proc. Sydney, 4–8 June 1979), IAEA, Vienna (1980) 565–594.
[31] KOTZER, T., KYSER, T.K., Fluid history in the Athabasca Basin and its relation to diagenesis, uranium mineralization and paleohydrology, Chemical Geology 120 (1995) 45–89.
[32] FAYEK, M., KYSER, K., Characterisation of multiple fluid events and rare-earth element mobility associated with formation of unconformity-type uranium deposits in the Athabasca Basin, Saskatchewan, The Canadian Mineralogist 35 (1997) 627–658.

[33] TOURIGNY, G., et al., Descriptive geology and structures associated with the Sue C uranium deposit, eastern Athabasca Basin, Saskatchewan (JEFFERSON, C.W., DELANEY, G., Eds), EXTECH IV: Geology and Uranium EXploration TECHnology of the Proterozoic Athabasca Basin, Saskatchewan and Alberta, Geological Survey of Canada, Bulletin 588 (2005) 229–248.

[34] HOEVE, J., QUIRT, D., A stationary redox front as a critical factor in the formation of high-grade unconformity-type uranium ores in the Athabasca Basin, Saskatchewan, Canada, Bulletin de Mineralogie **110** (1987) 157–171.

[35] DEROME, D., et al., 'Mixing of sodic and calcic brines and uranium deposition at McArthur River, Saskatchewan, Canada', A raman and laser-induced breakdown spectroscopic study of fluid inclusions, Econ. Geol. 100 (2005) 1529–1545.

[36] LE CHEMINANT, A.N., HEAMAN, L.M., McKenzie igneous events, Canada: Middle Proterozoic hotspot magmatism associated with ocean opening, Earth and Planetary Science Letters **96** (1989) 38–48.

[37] Cuney, M. et al., 'What parameters control the high grade-large tonnage of the Proterozoic unconformity-related uranium deposits?', Proc. Uranium Geochemistry 2003, Int. Conf., April 13–16 2003 (CUNEY, M., Ed.), Unité Mixte de Recherche CNRS 7566 G2R, Université Henry Poincaré, Nancy, France (2003) 123–126.

[38] OZMIN Mineral Deposits Database, Australian Government, http://www.ga.gov.au/meta/ANZCW0703003393.html.

[39] Geoscience Australia for Australia, http://www.ga.gov.au.

[40] INTERNATIONAL ATOMIC ENERGY AGENCY, Geological Environments of Sandstone Type Uranium Deposits (Report of the Working Group on Uranium Geology), IAEA-TECDOC-328, IAEA, Vienna (1985).

[41] GRUTT, EW, Jr., Prospecting criteria for sandstone-type uranium deposits (BOWIE, SHU., DAVIS, M., OSTLE, D., Eds), Uranium prospecting handbook, IMM, London (1972) 47–77.

[42] FINCH, W.I., Geology of epigenetic uranium deposits in sandstone in the United States, US Geol Surv Prof Paper 538 (1967) 121.

[43] OECD/NUCLEAR ENERGY AGENCY, INTERNATIONAL ATOMIC ENERGY AGENCY, Uranium 2003: Resources, Production and Demand, OECD/NEA, Paris (2003) [The '2003 Red Book'].

[44] HOSTETLER, P.B., GARRELS, R.M., Transportations and precipitation of uranium and vanadium at low temperatures, with special reference to sandstone-type uranium deposits, Econ. Geol. **57** (1962) 139–167.

[45] ADAMS, S.S., SMITH, R.B. Geology and recognition criteria for sandstone uranium deposits in mixed fluvial-shallow marine sedimentary sequences, south Texas. Final report, US-DOE, GJBX-4(81), (1981), 145 p

[46] HARSHMAN, E.N., ADAMS, S.S., Geology and recognition critena for roll-type uranium deposits in continental sandstones. US-DOE, GJBX–1(81), (1981), 185 p

[47] TURNER-PETERSON, C.E., FISHMAN, N.S., Geologic Synthesis and Genetic Models for Uranium Mineralization in the Morrison Formation, Grants Mineral Region, New Mexico (TURNER-PETERSON, C.E., SANTOS, E.S., FISHMAN, N.S., Eds), A Basin Analysis Case Study: the Morrison Formation, Grants Uranium Region, New Mexico; American Association of Petroleum Geologists, Studies in Geology No. 22 (1986) 357–388.

[48] GAUTHIER-LAFAYE, F., WEBER, F., The Francevillian (Lower Proterozoic) uranium ore deposits of Gabon, Econ. Geol. **84** (1989) 2267–2268.

[49] OPENSHAW, R., PAGEL, M., POTY, B., Phases fluides contemporaines de la diagénèse des grès, des mouvements tectoniques et du fonctionnement des réacteurs nucléaires d'Oklo (Gabon). in: Les réacteurs de fission naturels. IAEA, Vienna (1978) 267–296

[50] BROS, R., et al., Sm-Nd isotopic dating of Proterozoic clay material. Example from Francevillian sedimentary series (Gabon): *Earth and Planetary Science Letter* **113** (1992) 207–218.

[51] GANCARZ, A.J., 'U-Pb age ($2.05.10^9$ years) of the Oklo uranium deposit', Les réacteurs de fission naturels, IAEA, Vienna (1978) 513–520.

[52] GAUTHIER-LAFAYE, F., HOLLIGER, P., BLANC, P.L., 'Natural fission reactors in the Franceville basin, gabon', A review of the conditions and results of a 'critcal event' in a geologic system, Geochimica et Cosmochimica Acta **60** (1996) 4831–4852.

[53] GAUTHIER-LAFAYE, F., 'Les gisements d'uranium du Gabon et les réacteurs nucléaires naturels d'Oklo', Modèle métallogénique de gîtes à fortes teneurs du Protérozoïque inférieur, Mem. Sci. Geol. n. 78 (1986) 206.

[54] MATHIEU, R., Paléocirculations fluides et migrations élémentaires dans l'environnement des réacteurs nucléaires naturels d'Oklo (Gabon) et des argilites de Touremire (France), Thesis INPL Nancy (1999) 519.

[55] CUNEY, M, MATHIEU, R., Extreme light rare earth element mobilization by diagenetic fluids in the geological environment of the Oklo natural reactor zones, Franceville basin, Gabon, Geology **28** 8 (2000) 743–746.

[56] MATHIEU, R., et al., Alteration of monazite and zircon and lead migration as geochemical tracers of fluid paleocirculations around the Oklo-Okélobondo and Bangombé natural nuclear reaction zones (Franceville basin, Gabon), Chem. Geol. No.171 (2001) 147–171.

[57] MATHIEU, R., CUNEY, M., CATHELINEAU, M., Geochemistry of fluid palaeo-circulations in the Franceville basin and around Oklo natural nuclear reaction zones (Gabon), J. Geochem. Exploration No. 69–70 (2000) 245–249.

[58] PFIFFELMANN, J-P, 'L'uranium dans le bassin de Franceville', The Oklo phenomenon, IAEA, Vienna (1975) 37–51.

[59] SQUYRES, J.B., Origin and Significance of Organic Matter in Uranium Deposits of Morrison Formation, San Juan Basin, New Mexico, in Geology and Mineral Technology of the Grants Uranium Region, New Mexico Bureau of Mines and Mineral Resources Memoir 38, Albuquerque, New Mexico, USA (1980).

[60] THAMM, J.K, KOVSCHAK, A.A., Jr., ADAMS, S.S., Geology and Recognition Criteria for Sandstone Uranium Deposits of the Salt Wash Type, Colorado Plateau Province, U.S. Department of Energy, GJBX-6(81), Grand Junction, Colorado, USA (1981).

[61] GRANGER, H.C., WARREN, C.G., Genetic implications of the geochemistry of vanadium-uranium deposits in the Colorado Plateau region. Amer Ass Petrol Geol, Albuquerque Meeting, New Mexico (1981), abstr w programs

[62] HAYNES, D.W., 'Iron oxide copper (–gold) deposits: their position in the ore deposit spectrum and modes of origin', Hydrothermal Iron Oxide Copper–Gold & Related Deposits: A Global Perspective (PORTER, T.M., Ed.), Australian Mineral Foundation, Adelaide (2000) 71–90.

[63] REEVE, J.S., CROSS, K.C., SMITH, R.N., ORESKES, N., 'Olympic Dam copper–uranium–gold deposit', Geology of the Mineral Deposits of Australia and Papua New Guinea (HUGHES, F.E., Ed.), The Australasian Institute of Mining & Metallurgy, Melbourne (1990) 1009–1035.

[64] Western Mining Corporation, ‘Olympic Dam Operations’,. Geology and Mining Technical Handbook, Issue 2, WMC, unpublished company brochure (1993).
[65] CROSS, K.C., DALY, S.J. FLINT, R.B., ‘Mineralisation associated with the GRV and Hiltaba Suite granitoids, Olympic Dam deposit’, The Geology of South Australia, Vol. 1, The Precambrian (DREXEL, J.F., PREISS, W.V., PARKER, A.J., Eds), Geological Survey of South Australia, Bulletin 54 (1993)132, 138.
[66] SKIRROW, R.G., et al., ‘Geological framework, distribution and controls of Fe-oxide Cu-Au deposits in the Gawler Craton’, Part II–Alteration and mineralization (PORTER, T.M., Ed.), Hydrothermal iron oxide copper-gold and related deposits, Volume 2, PGC Publishing, Adelaide (2002) 33–47.
[67] ORESKES, N., EINAUDI, M.T., Origin of rare earth element-enriched hematite breccias at the Olympic Dam Cu.U.Au.Ag deposit, Roxby Downs, South Australia, Econ. Geol. **85** (1990) 1–28.
[68] CREASER, R.A., COOPER, J.A., U–Pb geochronology of Middle Proterozoic felsic magmatism surrounding the Olympic Dam Cu–U–Au–Ag and Moonta Cu–Au–Ag deposits, South Australia, Econ. Geol. **88** (1993) 186–197.
[69] JOHNSON, J.P., CROSS, K.C., U–Pb Geochronological constraints on the genesis of the Olympic Dam Cu–U–Au–Ag deposit, South Australia, Economic Geology **90** (1995) 1046–1063.
[70] JAGODZINSKI, E.A., Compilation of SHRIMP U-Pb data, Olympic Dam Domain, Gawler Craton, South Australia, 2001–2003, Geoscience Australia, Record, 2005/20 (2005) 197.
[71] HAYNES, D.W., CROSS, K.C., BILLS, R.T., REED, M.H., Olympic Dam ore genesis: a fluid-mixing model, Economic Geology **90** (1995) 281–307.
[72] BASTRAKOV, E.N., SKIRROW, R.G., BAROVICH, K.M., ‘Towards discriminating Cu-Au mineralised from barren hydrothermal systems using fluid chemistry (FERRIS, G.M., compiler), Gawler Craton 2002*:* State of Play, Department of Primary Industries and Resources SA, Exploration Data Package 10 (2002).
[73] BHP Billiton, BHP Billiton Annual report for 2006.
[74] HITZMAN, M.W., VALENTA, R.K., Uranium in iron oxided-copper-gold (IOCG) systems, Econ. Geol. **100** (2005) 1657–1661.
[75] ROBERTSON, J.A., ‘The Blind River (Elliot Lake) uranium deposits’, Uranium resources and geology of North America, IAEA-TECDOC-500, IAEA, Vienna (1989) 111–147.
[76] RUZICKA, V., ‘Geology and genesis of uranium deposits in the Early Proterozoic Blind River-Elliot Lake Basin, Ontario, Canada’, Recognition of uranium provinces (Proc. TCM, London, 18–20 Sept. 1985), IAEA, Vienna (1988) 107–130.
[77] ANHAEUSSER, C.R., MASKE, S, (Eds), Mineral deposits of southern Africa. Geol Soc S Afr **1 2** (1986) 2340.
[78] BUTTON, A., ADAMS, S.S., Geology and recognition criteria for uranium deposits of the quartz-pebble conglomerate type, US-DOE, GJBX–3 (81) (1981) 390.
[79] HALLBAUER, D.K., The mineralogy and geochemistry of Witwatersrand pyrite, gold, uranium, and carbonaceous matter (ANHAEUSSER, C.R., MASKE, S, Eds), Mineral deposits of Southern Africa, Geol Soc S Afr **1** (1986) 731–752.
[80] INTERNATIONAL ATOMIC ENERGY ATENCY, ‘Uranium deposits in Morrison Formation (Upper Jurassic), Carrizo Mountains area, Arizona and New Mexico’ (PRETORIUS, D., Ed.), Proterozoic quartz-pebble conglomerates. IAEA-TECDOC-427, IAEA, Vienna (1987) 459.

[81] PRETORIUS, D.A., 'Gold in the Proterozoic sediments of South Africa: Systems, paradigms and models' (Wolf, K.H., Ed.), Handbook of strata-bound and stratiform ore deposits, Elsevier, Amsterdam **7** (1976a) 1–27.
[82] PRETORIUS, D.A., ibid., (1976b) 29–88.
[83] PRETORIUS, D.A., Gold and uranium in quartz-pebble conglomerates, Econ Geol, 75th Anniversary Vol (1981) 117–138.
[84] VON BACKSTRÖM, J.W., Uranium and the generation of power, South Africa perspective, Trans Geol Soc S Africa **78** (1975) 275–292.
[85] BUCK, S.G., MINTER, W.E.L, 'Paleocurrent and lithological facies control of uranium and gold mineralization in the Witwatersrand carbon leader placer, Carletonville Goldfield, South Africa', Uranium deposits in Proterozoic quartz-pebble conglomerates, IAEA-TECDOC-427, IAEA, Vienna (1987) 335–353.
[86] LEROY, J., Métallogénèse des gisements d'uranium de la Division de la Crouzille (COGEMA — Nord Limousin- France), Sci Terre, Nancy, Mém no. 36 (1978) 276.
[87] POTY, B, et al., 'Uranium deposits spatially related to granites in the French part of the Hercynian Orogen', Vein type uranium deposits, IAEA-TECDOC-361, IAEA, Vienna (1986) 215–246.
[88] TURPIN, L., Rb-Sr dating of hydrothermal alteration in the St Sylvestre leucogranite (French Massif Central), 3rd EUG Meeting Strasbourg, (abstr K 37) (1985).
[89] LEROY, J., HOLLIGER, P., Mineralogical, chemical and isotopic (U-Pb method) studies of Hercynian uraniferous mineralizations (Margnac and Fanay mines, Limousin, France), Chem Geol **45** (1984) 121–134.
[90] LEROY, J., The Margnac and Fanay uranium deposits of the La Crouzille district (western Massif Central, France): geologic and fluid inclusion studies, Econ Geol **73** (1978b) 1611–1634.
[91] LEROY, J., POTY, B., Recherches préliminaires sur les fluides associés à la genèse des minéralisations en uranium du Limousin (France), Mineral Deposita **4** (1969) 395–400.
[92] ZIEGLER, V., DARDEL, J., Uranium deposits in Europe (DE VIVO, F., et al., Eds), Uranium geochemistry, mineralogy, geology, exploration and resources, IMM, London (1984) 140–161.
[93] INTERNATIONAL ATOMIC ENERGY AGENCY, Uranium Resources and Geology of North America (Proc. Techn. Comm. Mtg, Saskatoon, Canada, 1–3 Sept. 1987), IAEA-TECDOC-500, IAEA, Vienna (1989).
[94] MAURICE, Y.T., (Ed.), Uranium in granites, Geol Surv Canada P 29 81–23 (1982) 173.
[95] INTERNATIONAL ATOMIC ENERGY AGENCY, Guidebook to Accompany the IAEA Map: World Distribution of Uranium Deposits, IAEA, Vienna (1996).
[96] BERNING, J., The Rössing uranium deposit, South West Africa/Namibia (ANHAEUSSER, C.R., MASKE, S., Eds), Mineral deposits of Southern Africa, Geol Soc S Afr **2** (1986) 1819–1832.
[97] BERNING, J., COOKE, R., HIEMSTRA, S.A., The Rössing uranium deposit, SWA, Econ Geol **71** (1976) 351–368.
[98] BRYNARD, H.J., ANDREOLI, M.A.G., 'The overview of the regional, geological and structural setting of the uraniferous granites of the Damara Orogen, Namibia', Recognition of Uranium Provinces (Proc. TCM, London, 18–20 Sept. 1985), IAEA, Vienna (1988) 195–212.

[99] MOUILLAC, J.L., et al., The Goanikontes uranium occurrence in South West Africa/Namibia (ANHAEUSSER, C.R., MASKE, S., Eds), Mineral deposits of Southern Africa, Geol Soc S Afr **2** (1986) 1833–1844.
[100] TOENS, P.D., CORNER, B., Uraniferous alaskitic granites with special reference to the Damara orogenic belt, S Afr Atomic Energy Board Res PER 55 (1980) 18.
[101] INTERNAIONAL ATOMIC ENERGY AGENCY, INTURGEO: The International Uranium Geology Information System, a world atlas of uranium occurrences and deposits, IAEA-TECDOC-471, IAEA, Vienna (1988) 493.
[102] SØRENSEN, H., et al., The uranium deposit at Kvanefeld, Ilimaussaq intrusion, South Greenland. Rapp Grønlands geol Unders 60 (1974) 54.
[103] OECD/NUCLEAR ENERGY AGENCY, INTERNATIONAL ATOMIC ENERGY AGENCY, International Uranium Resources Evaluation Project (IUREP)–Finland, 1981
[104] INTERNATIONAL ATOMIC ENERGY AGENCY, Vein Type Uranium Deposits (Report of a Working Group on Uranium Geology), IAEA-TECDOC–361, IAEA, Vienna (1986).
[105] CAMISANI-CALZOLARI, F.A.G.M., AINSLIE, L.C., VAN DER MERWE, P.J., Uranium in South Africa (1985), AEC-S Afr, Pretoria (1986) 27.
[106] ALEXANDER, R.L., Geology of Madawaska Mines Limited, Bancroft, Ontario, (EVANS, E.L., Ed.), Uranium deposits of Canada. CIM Spec **33** (1986) 62–69.
[107] TRÖGER, W.E., Spezielle Petrographie der Eruptivgesteine; ein Nomenklaturkompendium mit 1, Nachtrag Eruptivgesteinsnamen, (Nachdruck) Stuttgart (1969) 360 + 50 p
[108] MCKAY, A.D., MIEZITIS, Y., Australia's uranium resources, geology and development of deposits, AGSO — Geoscience Australia Resource Report 1 (2001).
[109] CAMERON, E., 'Yeelirrie Uranium Deposit', Geology of the Mineral Deposits of Australia and Papua New Guinea (HUGHES, F.E. Ed.), The Australasian Institute of Mining & Metallurgy (1990) 1625–1629.
[110] CAMERON, E., 'The Yeelirrie uranium deposit, Western Australia', Case Histories of Mineral Discoveries, Vol. 3: Porphyry Copper, Molybdenum, and Gold Deposits, Volcanogenic Deposits (Massive Sulphides), and Deposits in Layered Rock (HOLLISTER, V.F. Ed.), Society for Mining, Metallurgy & Exploration, Inc., Colorado (1991) 225–231.
[111] CAMERON, E., 'The Yeelirrie calcrete uranium deposit Western Australia', Surficial Uranium Deposits, IAEA-TECDOC-322, IAEA, Vienna (1984) 157–164.
[112] Western Mining Corporation, 'Yeelirrie Uranium Project, WA', Draft Environmental Impact Statement and Environmental Review and Management Programme, June 1978, Western Mining Corporation Ltd (1978) unpublished.
[113] BATTEY, G.C., MIEZITIS, Y., MCKAY, A.D., Australian Uranium Resources, Bureau of Mineral Resources, Resource Report No. 1, Australia Government Publishing Service, Canberra (1987).
[114] DAHLKAMP, F.J., Uranium Ore Deposits. Springer-Verlagm, Berlin Heidelberg (1993).
[115] HUNTOON, P.W, Large-Basin Ground Water Circulation and Paleo-Reconstruction of Circulation Leading to Uranium Mineralization in Grand Canyon Breccia Pipes, The Mountain Geologist, Rocky Mountain Association of Geologists, Denver, Colorado (1996).
[116] WENRICH, K.J., Mineralization of breccia pipes in northern Arizona, Economic Geology **80** 6 (1985).

[117] CHENOWITH, W.L., The Orphan Lode Mine, Grand Canyon, Arizona, a case history of a mineralized, collapse breccia pipe, U.S. Geological Survey Open File Report 86-510, Denver, Colorado (1986).
[118] GUILBERT, J.M., PARK, C.F., Jr., The Geology of Ore Deposits, W.H. Freeman and Company, New York (1975).
[119] BARTHEL, F.H., 'Thorium and Unconventional Resources', presented at IAEA Technical Meeting on Fissile Material Management Strategies for Sustainable Nuclear Energy, Vienna, Austria (September 2005).
[120] CARLSSON, D., NOJD, L.A., 'Uranium production from low-grade Swedish shale', Intern Conf Nuclear Power and its Fuel Cycle, Salzburg, Paper IAEA-CN 36/277, IAEA, Vienna (1977) 12.
[121] INTERNATIONAL ATOMIC ENERGY AGENCY, Analysis of Uranium Supply to 2050, IAEA, Vienna (2001).
[122] BLAKE, D.H., Geology of the Mount Isa Inlier and Environs, Queensland and Northern Territory, Bureau of Mineral Resources, Australia, Bulletin 225 (1987).
[123] HUTTON, L., Queensland Geological Survey, personal communication (2001).
[124] BROOKS, J.H., 'Uranium in the Mount Isa/Cloncurry District', Economic Geology of Australia and Papua New Guinea, 1. Metals (KNIGHT, C.L., Ed.), Australasian Institute of Mining & Metallurgy, Monograph 5 (1975) 396.398.
[125] SCOTT, A.K., SCOTT, A.G., Geology and genesis of uranium-rare-earth deposits at Mary Kathleen, northwest Queensland, AIMM Proc 290 (1985) 79–89.
[126] OLIVER, N.H.S., PEARSON, P.J., HOLCOMBE, R.J. ORD, A., Mary Kathleen metamorphic-hydrothermal uranium.rare earth element deposit, ore genesis and numerical model of coupled deformation and fluid flow, Australian J. Earth Sciences 46 (1999) 467.484.
[127] CRUIKSHANK, B.I., FERGUSON, J., DERRICK, G.M., 'The association of uranium and skarn development in the Mary Kathleen Area, Queensland', Uranium in the Pine Creek Geosyncline (Proc. Sydney, 4–8 June 1979), IAEA, Vienna (1980) 693–706.
[128] MAAS, R., MCCULLOCH, M.T., CAMPBELL, I.H., PAGE, R.W., Sm.Nd isotope systematics in uranium, Rare earth mineralisation at the Mary Kathleen uranium mine, Queensland, Economic Geology **82** (1987) 1805.1826.
[129] DERRICK, G.M., Metasomatic history and origin of uranium mineralization at Mary Kathleen, northwest Queensland, BMR, J. Austral **2** (1977) 123–130.
[130] PAGE, R.W., Chronology of magmatism, skarn formation, and uranium mineralization, Mary Kathleen, Queensland, Australia, Econ Geol **78** (1983) 838–853.
[131] OLIVER, N.H.S., WALL, V.J., PEARSON, P.J. HOLCOMBE, R.J., 'Unravelling more obscurities in the genesis of the Mary Kathleen U.REE orebody', Abstracts. Mount Isa Inlier Conference, Monash University, Melbourne (1990).
[132] Mary Kathleen Company Geologists, Mary Kathleen Uranium Ltd. Description of Operations (1981) (unpublished).
[133] HAWKINS, B.W., Mary Kathleen uranium deposit, Economic Geology of Australia and Papua New Guinea. 1. Metals (KNIGHT, C.L. Ed.), Australasian Institute of Mining & Metallurgy, Monograph 5 (1975) 398.402.
[134] MCLEMORE, V.T., and CHENOWETH, W.C., Uranium resources in New Mexico: New Mexico Bureau of Mines and Mineral Resources, Resource Map 18, 1989
[135] MCLEMORE, V.T., and CHENOWETH, W.C., Uranium mines and deposits in the Grants district, Cibola and McKinley Counties, New Mexico: New Mexico Bureau of Mines and Mineral Resources, Open File Report 353, 1991

[136] McLEMORE, V.T., DONAHUE, K., KRUEGER, C.B., ROWE, A., ULBRICHT, L., JACKSON, M.J., BREESE, M.R., JONES, G., WILS, M., Database of the uranium mines, prospects, occurrences, and mills in New Mexico: New Mexico Bureau of Geology and Mineral Resources, Open file Report 461, CD-ROM., 2002

[137] BERGLOF, W.R., Isotopic ages of uranium deposits in the Todilto Limestone, Grants district, and their relationship to the ages of other Colorado plateau deposits: New Mexico Geological Society, Guidebook 43, p. 351–358, 1989.

BIBLIOGRAPHY

Section 2.1 (Unconformity Related Deposits)

ALEXANDRE, P., KYSER, K., POLITO, P. Alteration mineralogy and stable isotope geochemistry of Paleoproterozoic basement-hosted unconformity-type uranium deposits in the Athabasca Basin, Canada, Economic Geology **100** (2005) 1547–1563.

CUMMING, G.L., KRSTIC, D., The age of unconformity-related uranium mineralization in the Athabasca Basin, northern Saskatchewan, Canadian Journal of Earth Sciences 29 (1992) 1623–1639.

EWERS, G.R., FERGUSON, J., NEEDHAM, R.S., DONNELLY, T.H., 'Pine Creek Geosyncline NT', Proterozoic Unconformity and Stratabound Uranium Deposits (FERGUSON, J., Ed.), IAEA-TECDOC-315, IAEA, Vienna; (1984) 135–206.

FAYEK, M., JANECZEK, J., EWING, P.C., 1997a. Mineral chemistry and oxygen isotopic analysis from uraninite, pichblende and uranium alteration minerals from the Cigar Lake deposit, Saskatchewan, Canada, Appl. Geochem. 12 (1997a) 549–565.

KYSER, K., et al., 'Diagenetic fluids in Paleo- and Mesoproterozoic sedimentary basins and their implications for long protracted fluid histories', Fluids and Basin Evolution (KYSER, K., Ed.), Mineralogical Association of Canada; Short Course V 28, Chapter 10, Calgary 2000 (Series Editor: Robert Raeside) (2000) 225–262.

MADORE, C., ANNESLEY, I., WHEATLEY, K., 'Petrogenesis, age and uranium fertility of peraluminous leucogranites and pegmatites of the McLean Lake / Sue and Key Lake / P-Patch deposit areas, Saskatchewan', Extended abstract in GeoCanada: the Millenium Geoscience Summit, Programme with Abstracts, v. 25, 1041.PDF (2000) 4.

NEEDHAM, R.S., Cahill Northern Territory (Sheet 5472). Bureau of Mineral Resources, Australia; 1:100 000 Geological Map Commentary (1982a).

NEEDHAM, R.S., Geology of the Alligator Rivers Uranium Field, Northern Territory. Bureau of Mineral Resources, Australia; Bulletin 224 (1988b).

Pancontinental Mining Ltd, Jabiluka Project — Environmental Impact Statement (July 1979).

PAGE, R.W., COMPSTON, W., NEEDHAM, R.S., 'Geochronology and evolution of the late Archean basement and Proterozoic rocks in the Alligator River uranium fields, Northern Territory, Australia' (FERGUSON, J., GOLEBY, A.B., Eds), Uranium in the Pine Creek Geosyncline (Proc. (Sydney, 4–8 June 1979**)**, IAEA, Vienna (1980) 36–68.

QUIRT, D., 'Athabasca unconformity-type uranium deposits : one deposit type with many variations; in Cuney M., ed., Uranium geochemistry 2003', Unité Mixte de Recherche CNRS 7566 G2R (Proc. Int. Conf., 13–16 April 2003), Université Henry Poincaré, Nancy, France (2003) 309–312.

REYX, J., RUHLMANN, F., Etude métallographique des différentes associations minérales et caractérisation chimique des minéraux uranifères du gisement de Cigar Lake, Saskatchewan, Canada.,Can. J. Earth Sci. 30 (1993) 705–719.

TREMBLAY, L.P., Geology of the uranium deposits related to the sub-Athabasca unconformity, Saskatchewan; Geological Survey of Canada, Paper 81–20 (1982) 56.

Section 2.2 (Sandstone Deposits)

INTERNAIONAL ATOMIC ENERGY AGENCY, Correlation of uranium geology between South America and Africa, Vienna, (1986), 475 p

INTERNAIONAL ATOMIC ENERGY AGENCY, Recognition of uranium provinces., Vienna, (1988), 459 p

INTERNAIONAL ATOMIC ENERGY AGENCY, Uranium deposits in Asia and the Pacific: geology and exploration. Vienna, (1988), 341 p

INTERNAIONAL ATOMIC ENERGY AGENCY, INTURGEO: The International Uranium Geology Information System, a world atlas of uranium occurrences and deposits, IAEA-TECDOC-471, Vienna, (1988), 493 p

INTERNAIONAL ATOMIC ENERGY AGENCY, Uranium deposits in magmatic and metamorphic rocks, Vienna, (1989), 253 p

INTERNAIONAL ATOMIC ENERGY AGENCY, Uranium resources and geology of North America, IAEA-TECDOC-500, Vienna, (1989), 529 p

INTERNAIONAL ATOMIC ENERGY AGENCY, Metallogenesis of uranium deposits,Vienna, (1989), 489 p

INTERNAIONAL ATOMIC ENERGY AGENCY, Innovations in uranium exploration, mining and processing techniques, and new exploration target areas. IAEA-TECDOC-868, Vienna, (1996), 148 p

DOLGUSHIN, P.S. et al., 'The Malinovskoye uranium deposit', Otechestvennaya Geologia No. 9 (1995)42–45 (in Russian).

LOUTCHININ, I.L., 'Uranium perspectives of Ural region', Otechestvennaya Geologia No. 9 (1995) 39–42 (in Russian).

LOUTCHININ, I.L., 'Valley-type of Uranium Deposits in Russia', Recent Developments in Uranium Resources and Supply, IAEA-IAEA-TECDOC-823, IAEA, Vienna (1995).

NAUMOV, S.S., TARKHANOV, A.V., BIRKA, G.I., 'Future Development of Russian Uranium Industry', Development in Uranium Resources, Production, Demand and the Environment (Proc. TCM, Vienna, 15–18 June 1999), IAEA-IAEA-TECDOC–1425, IAEA, Vienna (2005)43–49.

Section 2.3 (Hematite Breccia Complex Deposits)

GOW, P.A., WALL, V.J., OLIVER, N.H.S., VALENTA, R.K., Proterozoic iron oxide (Cu–U–Au–REE) deposits: further evidence of hydrothermal origins. Geology **22** (1994) 633–636.

DREXEL, J.F., MAJOR, R.B., Geology of the uraniferous breccias near Mount Painter, South Australia, and revision of rock nomenclature. Geological Survey of South Australia; Quarterly Geological Notes 104 (1987) 14–24.

IDNURM, M., HEINRICH, C.A., A palaeomagnetic study of hydrothermal activity and uranium mineralisation at Mount Painter, South Australia, Australian Journal of Earth Sciences 40 (1993) 87–101.

HITZMAN, M.W., ORESKES, N., EINAUDI, M.T., Geological characteristics and tectonic setting of Proterozoic iron oxide (Cu–U–Au–REE) deposits, Precambrian Research 58 (1992) 241–287.

Section 2.5 (Vein Type — Granite Related–Deposits)

BARBIER, J., Continental weathering as a possible origin of vein-type uranium deposits. Mineral Deposita, 9, (1974), pp 271–288

CUNEY, M., PEYREL, J.Y., Origine des granïtoides fertiles, conséquences sur la définition de leurs caractéristiques spécifiques. unpubl CEE report, (1984)

GEFFROY, J., SARCIA, J.A., Contribution à l'étude des pechblendes françaises. Rapp CEA no. 380, Sci Terre, 2, (1955), 157 p

KOLEKTIV, (ČSSR) Czechoslovakian uranium deposits. Nakl technicke literatury, Prague, (1984), 365 p (in Czech)

KOLEKTIV, Rudné a uranové hornictví České Republiky (Uranium mining industry, ed. J. Kafka). DIAMO/ANGRAM, (2003), 647 p (in Czech)

KOMÍNEK, J., VESELÝ, T., Uranium deposit of Jáchymov, ČSSR. *in:* Vein type uranium deposits. IAEA-TECDOC-361, IAEA, Vienna, (1986), pp 293–306

LEROY, J., Métallogénèse des gisements d'uranium de la Division de la Crouzille (COGEMA — Nord Limousin- France). Sci Terre, Nancy, Mém no. 36, (1978), 276 p

LEROY, J., The Margnac and Fanay uranium deposits of the La Crouzille district (western Massif Central, France): geologic and fluid inclusion studies. Econ Geol, v 73, (1978), pp 1611–1634

LEROY, J., HOLLIGER, P., Mineralogical, chemical and isotopic (U-Pb method) studies of Hercynian uraniferous mineralizations (Margnac and Fanay mines, Limousin, France), Chem Geol, 45, (1984), pp 121–134

LEROY, J., POTY, B., Recherches préliminaires sur les fluides associés à la genèse des minéralisations en uranium du Limousin (France). Mineral Deposita, 4, (1969), pp 395–400

MOREAU, M., POUGHON, A., PUYBARAUD, Y., SANSELME, H., L'uranium et les granites. Chron Mines Rech minière, 350, (1966), pp 47–50

PEINARDOR FERNANDES, A., JAMET, P., LE CAIGNEC, R., MOREAU, M., SERRANO, J.R., ZIEGLER, V,. Gisements d'uranium dans les schistes péribatholitiques (type ibérique) et dans les leucogranites (type Limousin) (Portugal, Espagne, France). Livret guide d'excursion, Sci Terre, Nancy XXIII, (1979), 47 p

POTY, B., LEROY, J., CATHELINEAU, M., CUNEY, M., FRIEDRICH, M., LESPINASSE, M., TURPIN, L., Uranium deposits spatially related to granites in the French part of the Hercynian Orogen. *in:* Vein type uranium deposits. IAEA-TECDOC-361, IAEA, Vienna, (1986), pp 215–246

ROUBAULT, M., COPPENS, R., Sur les relations entre certains gites filoniens d'uranium et la presence d'inclusions radioactives dans les roches encaissantes. CR Acad Sci Fr 240, (1955), pp 214–216

ROUBAULT, M., COPPENS, R. Observation de deplacements de l'uranium dans les roches cristallines relations possibles de ce phénomène avec la genèse de certains gisements. UN 2nd Intern Conf Peaceful Uses Atomic Energy, Proc, v 2, Genève, (1958), pp 335–337

ZIEGLER, V., DARDEL, J., Uranium deposits in Europe. *in:* de Vivo F et al., eds., Uranium geochemistry, mineralogy, geology, exploration and resources. IMM, London, (1984), pp 140–161

Section 2.6 (Intrusive Deposits)

ALEXANDER, R.L., Geology of Madawaska Mines Limited, Bancroft, Ontario. *in:* Evans EL, ed., Uranium deposits of Canada. CIM Spec Vol. 33, (1986), pp 62–69

BERNING, J., The Rössing uranium deposit, South West Africa/Namibia. *in:* Anhaeusser CR, Maske S, eds., Mineral deposits of Southern Africa. Geol Soc S Afr, v 2, (1986), pp 1819–1832

BERNING, J., COOKE, R., HIEMSTRA, S.A., The Rössing uranium deposit, SWA. Econ Geol, v 71, (1976), pp 351–368

BRYNARD, H.J., ANDREOLI, M.A.G., The overview of the regional, geological and structural setting of the uraniferous granites of the Damara Orogen, Namibia. *in:* Recognition of uranium provinces. IAEA, Vienna, (1988), pp 195–212

CUNEY, M., Preliminary results on the petrology and fluid inclusions of the Rössing uraniferous alakites. Trans Geol Soc S Afr, 83, (1980), pp 39–45

JACOB, R.E., The radioactive mineralization in part of the central Damara belt, South West Africa, and its possible origin. S Afr Atomic Energy Board Rep PIN 234(B/R), (1974), 17 p

JACOB, R.E., CORNER, B., BRYNARD, H.J., The regional geological and structural setting of the uraniferous granitic provinces of southern Africa. *in:* Anhaeusser CR, Maske S, eds., Mineral deposits of southern Africa. Geol Soc S Afr, v 2, (1986), pp 1807–1818

MAURICE, Y.T., ed. Uranium in granites. Geol Surv Canada P 29 81–23, (1982), 173 p

MOUILLAC, J.L., VALOIS, J-P., WALGENWITZ, The Goanikontes uranium occurrence in South West Africa/Namibia. *in:* Anhaeusser CR, Maske S, Mineral deposits of Southern Africa. Geol Soc S Afr, v 2, (1986), pp 1833–1844

SMITH, D.A.M., The geology of the area around the Khan and Swakop Rivers in South West Africa. Mem Geol Surv S Afr, 3 (SWA Series), (1965), 113 p

TOENS, P.D., CORNER, B., Uraniferous alaskitic granites with special reference to the Damara orogenic belt. S Afr Atomic Energy Board Res PER 55, (1980), 18 p

TOENS, P.D., HAMBLETON-JONES, B.B., Uraniferous surficial deposits. S Afr Atomic Energy Board Rep PER 57, (1980), 16 p

TRÖGER, W.E., Spezielle Petrographie der Eruptivgesteine; ein Nomenklaturkompendium mit 1. Nachtrag Eruptivgesteinsnamen. (Nachdruck) Stuttgart, (1969), 360 + 50 p

VON BACKSTRÖM, J.W., JACOB, R.E., Uranium in South Africa and South West Africa (Namibia). Phil Trans Royal Soc, London, A291, (1979), pp 307–319

WINKLER, H.G.F., in: MARTIN, H., EDER, F.W., eds., Intracontinental fold belts. Springer-Verlag, Berlin ff, (1983), 945 p

Section 2.8 (Metasomatic Deposits)

BELEVTSEV, Y.N., KOVAL, V.B., eds. Genetic types and regularities of the location of uranium deposits in Ukraine. Navkova, Dumka, Kiev, (1995), 395 p (in Russian)

BOITSOV, V.E., Geology of uranium deposits. NEDRA, Moscow, (1989), 302 p (in Russian)

MIGUTA, A.K., Uranium deposits of the Elkon ore district in the Aldan shield. Geol Ore Deposits, v 43, no. 2, (2001), pp 117–135

Section 2.10 (Collapse Breccia Pipe Deposits)

BREED, W.J., ROUT, E.C. (Eds), Geology of the Grand Canyon, Museum of Northern Arizona (1976) 186.

Section 2.12 (Black Shale Deposits)

BELL, R.T., Uranium in black shales: a review. *in:* Kimberley MM, ed., Short course in uranium deposits: their mineralogy and origin. Miner Ass Can, Short Course Handbook no. 3, (1978), pp 207–329

KIM, J.H., Uranium geology of the Republic of Korea. *in* Uranium deposits in Asia and the Pacific: geology and exploration. IAEA, Vienna, (1988), pp 141–154

MUTSCHLER, P.H., HILL, J.J., WILLIAMS, B.B., Uranium from the Chattanooga Shale. US Bur Mines Inform Circ 8700, (1976), 85 p

CONTRIBUTORS TO DRAFTING AND REVIEW

Blaise, J.R.,	International Atomic Energy Agency
Boitsov, S.,	TVEL/Russian Federation
Bruneton, P.,	AREVA/France
Ceyhan, M.,	International Atomic Energy Agency
Dahlkamp, F.,	Consultant/Germany
Mathieu, R.,	AREVA/France
McKay, A.,	Geoscience Australia/Australia
McMurray, J.,	Consultant/USA
Slezak, J.,	International Atomic Energy Agency
Subhash, J.,	Geoscience Australia/Australia

Consultants Meetings

Vienna, Austria: 16–18 March 2005, 1–3 March 2006, 14–16 March 2007.